R. & M. No. 3791

R. & M. No. 3791

PROCUREMENT EXECUTIVE MINISTRY OF DEFENCE

AERONAUTICAL RESEARCH COUNCIL

REPORTS AND MEMORANDA

Prediction of Turbulent Boundary Layers and Wakes in Compressible Flow by a Lag-Entrainment Method

By J. E. GREEN, D. J. WEEKS AND J. W. F. BROOMAN

Aerodynamics Dept., R.A.E., Farnborough

LONDON: HER MAJESTY'S STATIONERY OFFICE

1977

£6 net

HMSO

LIST OF CONTENTS

1. Introduction

This Report describes an integral method for predicting the behaviour of turbulent boundary layers in two-dimensional and axisymmetric, compressible flows. It is believed to be a significant improvement upon, and was developed as a replacement for, the version[1] of Head's[2] entrainment method which has been in use in R.A.E. for some years. At the cost of a fractional increase in computing time—three simultaneous ordinary differential equations have to be integrated, as compared with two in Head's method—the new method is consistently the more accurate, particularly in its predictions of the test cases of the Stanford Conference[3] on Computation of Turbulent Boundary Layers.

In fact, it was largely in the aftermath of the Stanford Conference that the present method was developed. The Conference had convincingly demonstrated that a number of methods existed which were generally more accurate than the original entrainment method. It had also provided a fairly clear indication that the future lay with methods in which the turbulence stresses were treated as independent of the local mean velocity profile—so called 'historical' methods. On the other hand, for the flows to which it was restricted—that is two-dimensional, thin, attached boundary layers in incompressible flow—the Conference had not shown that there was any one class of method which was uniquely successful and, in particular, had not shown finite-difference methods to be significantly more accurate than integral methods, or *vice versa.*

The virtues of Head's original method and its R.A.E. counterpart were:

(1) its well established[3] adaptability which derived from use of the entrainment equation—compressible flows, three-dimensional flows, flows with boundary layer control, flows with heat transfer, wake flows had all been treated successfully;

(2) its speed, which derived from it being an integral method, and which enabled its extension to treat general three-dimensional boundary layers[4], and its incorporation in iterative schemes for calculating the weak viscous/inviscid interaction in flow about a two-dimensional aerofoil[5], without computing times becoming unduly large.

The combination of speed and adaptability held, in particular, the prospect that a general, three-dimensional version of the method could be nested within an iterative scheme for calculating three-dimensional inviscid flow to produce a method for predicting, at an acceptable computing cost, the fully three-dimensional flow over a swept wing.

To some of those familiar with these virtues of Head's method, the Stanford Conference brought to a focus the feeling that there was a place for a new method which retained the adaptability of the original entrainment method but which was 'historical'. Already, at Stanford, Hirst and Reynolds had presented one such method which the Evaluation Committee had placed in either the first or second classes (depending on how its starting conditions were specified) and, shortly after the Conference, Head and Patel[6] and then Horton[7] also put forward new methods. Impressed by the simplicity and accuracy of the method developed by Head and Patel, we decided that, extended to compressible flows, it would make a suitable replacement for our version of the original entrainment method.

Head and Patel calculated boundary-layer development using only two differential equations, momentum-integral and entrainment, with the entrainment coefficient determined from an algebraic expression in which 'history' was allowed for by incorporation of a measure of the local departure of the boundary layer from an equilibrium state. The present method emerged from a somewhat light-hearted attempt to show a formal equivalence, for small sustained departures from equilibrium, between the relationships developed by Head and Patel and the model of turbulence proposed by Bradshaw, Ferriss and Atwell[8] in their highly successful finite-difference method. The attempt was unsuccessful—the two methods do not seem to be formally related—but it did yield an ordinary differential equation for peak shear stress, derived from the form of the turbulent kinetic energy equation put forward by Bradshaw *et al.*, which invited conversion into a differential equation for entrainment coefficient.

The end result was a 'lag-entrainment' integral method involving three differential equations, momentum-integral, entrainment, and a rate equation for the entrainment coefficient. Because this last equation represented explicitly the balance between the production, advection, diffusion and dissipation of turbulent energy, and because its coefficients could be determined directly from the work of Bradshaw *et al.*, it was preferred to the simpler but more empirical algebraic relation of Head and Patel. Even so, the way in which the method as a whole is built around the concept of 'equilibrium' flows, as discussed by Rotta[9] for example, follows closely the path trodden by Head and Patel. Also, the differential equation for shear stress was partly anticipated by McDonald[10] though, as observed in Section 2.2, there is a significant difference between his equation and ours.

The method is derived primarily from the model of the turbulence structure proposed by Bradshaw *et al.*, and the analysis of 'equilibrium' boundary layers by Mellor and Gibson[11]. It has evolved from these

antecedents without the introduction of any important new empiricism; i.e. no disposable constants have been adjusted to provide an optimum fit to the available experimental data. Nevertheless, its predictions of the Stanford test cases appear at least to match those of the methods placed in the first class by the Conference Evaluation Committee.

The directness of the physical reasoning behind the method is an advantage when considering secondary effects. For example, Bradshaw's[13] proposed allowance for the influence of longitudinal curvature on the turbulence structure has been incorporated in a simple and logical fashion. Allowances for the effect of flow divergence on the turbulence structure, and for the change of turbulence structure in a wake have been introduced in a very similar way. The effect of lack of two-dimensionality on the development of momentum and displacement thicknesses has also been taken into account to provide a firmer base for comparisons between prediction and experiment.

The extension of the method to compressible flow is based primarily on the interpretation by Bradshaw and Ferriss[14] of Morkovin's[15] hypothesis that the turbulence structure is essentially unaffected by compressibility. No coordinate transformations are invoked, though the integral parameters used to specify the compressible boundary layer, the same as were used in the method's predecessor[1], necessitate the introduction of an empirical factor to account for their variation with Mach number in 'equilibrium' flows. As described here, the method is restricted to compressible adiabatic flows, although its extension to treat flows with heat transfer along the lines tentatively proposed in Ref. 1 is straightforward. In the section on compressible flow, a very recent and somewhat speculative proposition by Bradshaw[16] that the turbulence structure is influenced by flow dilatation is noted, and an allowance for this effect is introduced into the method for illustrative purposes.

The Report sets out the derivation of the method, first for incompressible flow, then for compressible flow. Although the derivations are not short, and the lag equation in its final form looks rather long, the method is essentially straightforward and its algebra simple. As the equations are predominantly algebraic, with a minimum of empirical exponential or logarithmic functions, their integration on a computer is in fact a very rapid process. The predictions of the method are compared with a wide range of experimental data, including a representative sample from the Stanford Conference, to demonstrate both its significant improvement on the earlier entrainment method and its accuracy in absolute terms. For compressible flows, the limited data available, and the uncertainty as to their validity as test cases, undermine any firm assessment of the method in flows other than at constant pressure.

2. The Prediction Method for Incompressible Flow

2.1. Outline

The boundary layer is defined by three independent parameters, momentum thickness θ, shape parameter $H(=\delta^*/\theta)$ and entrainment coefficient C_E. The development of these in a given pressure distribution, with their initial values known, is predicted by the forward integration of three simultaneous ordinary differential equations. Two of these, the momentum-integral and entrainment equations, are those used in Head's[2] original method; the third, a rate equation for entrainment coefficient (the 'lag' equation), is derived from the turbulent kinetic energy equation. This third equation is written explicitly in terms of the factors tending to drive the overall turbulence structure away from, and those tending to restore, a state of equilibrium.

The derivation of the lag equation is given later. The other two equations, in incompressible, two-dimensional (i.e. planar or axisymmetric) flow may be written: the momentum integral equation,

$$\frac{1}{U_e}\frac{d}{dx}(rU_e\theta) = r\frac{C_f}{2} - (H+1)\frac{r\theta}{U_e}\frac{dU_e}{dx}, \tag{1}$$

where suffix e denotes conditions at the edge of the boundary layer and r, the body radius in axisymmetric flow, may be set to unity in planar flow; the entrainment equation,

$$r\theta\frac{dH}{dx} = \frac{dH}{dH_1}\left(rC_E - H_1\frac{1}{U_e}\frac{d}{dx}(rU_e\theta)\right), \tag{2}$$

where H_1 is the mass-flow shape parameter $(\delta-\delta^*)/\theta$ first proposed by Head. The grouping of the terms in these equations differs slightly from that used previously[1], eliminating terms in dr/dx and hence avoiding unnecessary differentiation of the input data.

As in Head's method, relations are needed between H_1 and H, and to determine skin friction coefficient. In addition, a relation for the variation of shape parameter with pressure gradient in equilibrium flows is required in order to specify some of the terms in the lag equation, which here replaces the empirical relation between C_E and H_1 used by Head. Use of the properties of equilibrium flows is also made to take the final steps in the process of deriving the lag equation from the turbulent energy equation.

The form of the lag equation makes it possible to represent extraneous influences on the turbulence structure, such as that of longitudinal curvature, in a logical and straightforward manner. This feature of the method is also employed in extending the method to calculate wakes. Finally, a set of first-order corrections is obtained for use when testing the method against imperfectly two-dimensional experimental data.

2.2. The Lag Equation in Embryo

The turbulent kinetic energy equation, an exact equation derived from the Navier–Stokes equations, may for two-dimensional flow be written

$$\frac{1}{2}\rho\left(U\frac{\overline{\partial q^2}}{\partial x}+V\frac{\overline{\partial q^2}}{\partial y}\right)- \quad \tau\frac{\partial U}{\partial y} \quad +\frac{\partial}{\partial y}\left(\overline{pv}+\frac{1}{2}\rho\overline{q^2v}\right)+ \quad \rho\varepsilon \quad =0. \tag{3}$$

advection production diffusion dissipation

Bradshaw, Ferriss and Atwell[8] defined parameters

$$a_1\equiv\tau/\rho\overline{q^2} \qquad L\equiv(\tau/\rho)^{\frac{3}{2}}/\varepsilon$$
$$G=\left(\frac{\overline{pv}}{\rho}+\frac{1}{2}\overline{q^2v}\right)\Big/\left(\frac{\tau_{\max}}{\rho}\right)^{\frac{1}{2}}\frac{\tau}{\rho} \tag{4}$$

such that this could be written, still as an exact equation,

$$U\frac{\partial}{\partial x}\left(\frac{\tau}{2a_1\rho}\right)+V\frac{\partial}{\partial y}\left(\frac{\tau}{2a_1\rho}\right)-\frac{\tau}{\rho}\frac{\partial U}{\partial y}+\left(\frac{\tau_{\max}}{\rho}\right)^{\frac{1}{2}}\frac{\partial}{\partial y}\left(G\frac{\tau}{\rho}\right)+\frac{(\tau/\rho)^{\frac{3}{2}}}{L}=0. \tag{5}$$

adv adv prod diff diss

Their prediction method was then derived by postulating that L and $G/(\tau_{\max}/\rho U_e^2)^{\frac{1}{2}}$ could be taken as functions only of y/δ and that a_1 was effectively a constant, so that equation (5) became an approximate, empirical, partial differential equation for shear stress.

In flows with adverse pressure gradients, profiles of shear stress against y have a maximum in τ/ρ at which, if G, L and a_1 behave as Bradshaw and his colleagues postulated, equation (5) reduces to an ordinary differential equation for maximum shear stress. Noting that, if

$$\frac{G}{(\tau_{\max}/\rho U_e^2)^{\frac{1}{2}}}=\zeta=f\left(\frac{y}{\delta}\right),$$

we have, at a maximum in τ/ρ in incompressible flow,

$$\left(\frac{\tau_{\max}}{\rho}\right)^{\frac{1}{2}}\frac{\partial}{\partial y}\left(G\frac{\tau}{\rho}\right)=\frac{1}{\delta U_e}\left(\frac{\tau_{\max}}{\rho}\right)^2\zeta'$$

where $\zeta'=d\zeta/d(y/\delta)$, and equation (5) becomes

$$\frac{U}{2a_1}\frac{d}{dx}\left(\frac{\tau}{\rho}\right)_{\max}-\left(\frac{\tau}{\rho}\right)_{\max}\frac{\partial U}{\partial y}+\frac{1}{\delta U_e}\left(\frac{\tau}{\rho}\right)^2_{\max}\zeta'+\frac{(\tau/\rho)^{\frac{3}{2}}_{\max}}{L}=0. \tag{6}$$

adv prod diff diss

If we write $\tau_{max}/\rho U_e^2 = C_{\tau m}$, multiply equation (6) by $2a_1\delta$ and divide it by $UU_e^2 C_{\tau m}$, it becomes, after some rearrangement,

$$\underset{\text{adv}}{\frac{\delta}{C_{\tau m}}\frac{dC_{\tau m}}{dx}} = 2a_1\frac{U_e}{U}\left[\underset{\text{prod}}{\frac{\delta}{U_e}\frac{\partial U}{\partial y}} - \underset{\text{diss}}{\frac{\delta}{L}C_{\tau m}^{\frac{1}{2}}} - \underset{\text{diff}}{C_{\tau m}\zeta'}\right] - \underset{\text{adv}}{\frac{2\delta}{U_e}\frac{dU_e}{dx}}. \tag{7}$$

Anticipating Section 2.3, we define 'equilibrium' flows as those in which $C_{\tau m}$ and the shapes of the shear–stress and velocity profiles do not vary with x. Assuming that the dissipation length scale L can be equated to the conventional mixing length $l(=\sqrt{\tau/\rho}/\partial U/\partial y)$ at the position of τ_{max} in these flows, we may write equation (7)

$$\underset{\text{adv}}{\frac{\delta}{C_{\tau m}}\frac{dC_{\tau m}}{dx}} = 2a_1\frac{U_e}{U}\frac{\delta}{L}\underset{\text{prod}}{\{C_{\tau m_{EQ}}^{\frac{1}{2}} - \underset{\text{diss}}{C_{\tau m}^{\frac{1}{2}}}\}} + \underset{\text{diff}}{\left(\frac{2\delta}{U_e}\frac{dU_e}{dx}\right)_{EQ}} - \underset{\text{adv}}{\frac{2\delta}{U_e}\frac{dU_e}{dx}}, \tag{8}$$

where, by virtue of the condition that the right-hand side of this equation should be zero in equilibrium flows, we have been able to replace the diffusion term of equation (7) by $2((\delta/U_e)(dU_e/dx))_{EQ}$.

Equation (8) is the basis of the lag equation of the present method. It differs from earlier, wholly empirical equations, such as that employed by Nash and Hicks[3], in containing a pressure gradient term (the right-hand side of the early empirical equations was typically of the form $(C_{\tau EQ}/C_\tau - 1) \times$ constant) and, though similar to the equation derived by McDonald[10], differs from it in containing a term explicitly representing diffusion.

As written above, equation (8) was derived independently by B. G. J. Thompson and the first author of this Report, and both explored simple ways of converting it into a differential equation for entrainment coefficient. The procedure finally adopted by the present authors is given in Section 2.6.

2.3. Equilibrium Flows

Equilibrium flows are here defined as flows in which the shape of the velocity and shear–stress profiles in the boundary layer do not vary with x. Throughout the flow, dH/dx and $dC_{\tau m}/dx$ are both zero. As Rotta[9] has observed, such flows are in general strictly possible only on surfaces with an appropriate streamwise distribution of roughness. This does not, however, restrict their usefulness as a foundation for a boundary-layer method.

The physical reasoning underlying the concept of such flows is set out by Rotta. The parameters which characterise them are the shape parameter of the velocity-defect profile,

$$G = \frac{H-1}{H}\sqrt{\frac{2}{C_f}}, \tag{9}$$

and the pressure-gradient parameter

$$\Pi = \frac{\delta^*}{\tau_w}\frac{dp}{dx}. \tag{10}$$

Various empirical correlations of Π as a function of G have been proposed. In the present method, we have adopted the relation

$$G = 6{\cdot}432(1 + 0{\cdot}8\Pi)^{\frac{1}{2}} \tag{11}$$

which is shown in Fig. 1 compared with experimental data from a range of flows in near equilibrium and with the analytical results of Mellor and Gibson[11].

Although perceptibly different from the $G(\Pi)$ locus of Mellor and Gibson equation (11) lies very close to the empirical $G(\Pi)$ locus proposed by Nash and MacDonald[12], differing primarily in being slightly offset from the observed behaviour on smooth surfaces. For example, in flow at constant pressure over a smooth surface, the method does not predict the value of G given by equation (11) with Π zero because this flow is not an

equilibrium flow by our definition: the constants in equation (11) have therefore been chosen so that the zero-pressure-gradient value of G *as given by a calculation* using the method is close to 6·55, in agreement with the flat-plate skin-friction law of Winter and Gaudet[17].

The final form of the lag equation involves equilibrium values of C_E and of $(\delta/U_e)(dU_e/dx)$. These are obtained straightforwardly given that dH/dx is zero in equilibrium. Thus, writing the equilibrium locus, equation (11),

$$\frac{H-1}{H}=6{\cdot}432\left(\frac{C_f}{2}-0.8H\frac{\theta}{U_e}\frac{dU_e}{dx}\right)^{\frac{1}{2}}, \tag{12}$$

we have immediately

$$\left(\frac{\theta}{U_e}\frac{dU_e}{dx}\right)_{EQ}=\frac{1{\cdot}25}{H}\left\{\frac{C_f}{2}-\left(\frac{H-1}{6{\cdot}432H}\right)^2\right\} \tag{13}$$

and, by definition,

$$\left(\frac{\delta}{U_e}\frac{dU_e}{dx}\right)_{EQ}=(H+H_1)\left(\frac{\theta}{U_e}\frac{dU_e}{dx}\right)_{EQ}. \tag{14}$$

Finally, from equations (1) and (2) we obtain

$$(C_E)_{EQ}=H_1\left\{\frac{C_f}{2}-(H+1)\left(\frac{\theta}{U_e}\frac{dU_e}{dx}\right)_{EQ}\right\}, \tag{15}$$

so that the two required parameters are determined as functions of H, H_1 and C_f.

2.4. Shape Parameter Relation

In Head's original entrainment method[2] and the later development of it at R.A.E.[1], C_E and H were assumed to be uniquely related to H_1. These relationships in fact determined the effective equilibrium locus of the method, and in the R.A.E. version of the method some care was taken to match the two relationships to achieve a particular value of G in zero pressure gradient.

In the present method, the equilibrium locus is explicitly specified and as a result, given equations (13) to (15), the performance of the method does not depend very critically on the assumed relationship between H_1 and H. Although some previous workers have sought to improve the entrainment method by introducing a more elaborate relationship between H, H_1 and Reynolds number based on momentum thickness R_θ, derived from a two-parameter velocity profile family such as Cole's[18], we do not think there is anything worthwhile to be gained in this. In reality, H_1 is a somewhat arbitrary parameter whose value depends on how we define boundary-layer thickness. If we take the purpose of the method to be solely to predict R_θ and H accurately (in the knowledge that any other properties of the velocity profile can then be determined readily from a profile family), its performance is not perceptibly impaired by the use of a unique relation between H and H_1: in effect, this amounts to making our definition of the edge of the boundary layer weakly dependent on Reynolds number.

The particular form of relation adopted here is shown in Fig. 2 where it is compared with a trajectory from Thompson's[19] two-parameter profile family and with some experimental measurements by East and Hoxey[20] of the boundary layer on the plane of symmetry ahead of a bluff obstacle.

The divergence between Thompson's line and the experimental results is attributed to the very severe adverse pressure gradient in the flow studied by East and Hoxey. Seddon[21] has found that velocity profiles are appreciably distorted away from the simple 'log-law plus wake' shapes of Coles[18] and Thompson if pressure gradients are sufficiently severe, and East[22] has confirmed that Seddon's type of distortion was clearly in evidence in the experiments by Hoxey and himself.

The line drawn in Fig. 2 is

$$H_1=3{\cdot}15+\frac{1{\cdot}72}{H-1}-0{\cdot}01(H-1)^2. \tag{16}$$

It has been biased away from the well-established profile family towards the particular experimental results shown because it is in severe pressure gradients that the $H(H_1)$ curve, particularly its shape, has its greatest influence on the performance of the method. If streamwise variations are gentle, the method will track along close to the equilibrium locus and the precise shape of the $H(H_1)$ curve is of minor importance. For values of H less than 2·35, equation (16) lies close to the results generated by Mellor and Gibson[11] in their analytical treatment of equilibrium boundary layers.

The third term in the equation is of little significance in attached flows but, by ensuring finite dH/dH_1 for all positive H_1 (see inset in Fig. 2), it avoids the possibility of singular behaviour in integrations into regions of rising pressure. It is merely a device to simplify programming the method so that, given a set of input data, it will continue its computation to the end without the need for special subroutines to identify a breakdown in the computation and then seek out the start of a new set of data. The credibility of predicted values of H greater than, say, 2·5 is somewhat doubtful, but there are some situations (for example, a sudden pressure rise followed by a plateau, as in a shock and boundary layer interaction) in which the excursion of H to high values is of relatively short duration. It is possible that the method will still be useful to an engineer in these situations, but we have not explored this aspect of its behaviour to any extent, and each user will need to judge the accuracy of the method from his experience with it in his own particular context.

2.5. Skin Friction Relation

Skin friction coefficient is determined as a function of H and R_θ. Following Ref. 1, skin friction in a general flow is related to skin friction on a flat plate by the empirical expression

$$\left(\frac{C_f}{C_{f_0}}+0{\cdot}5\right)\left(\frac{H}{H_0}-0{\cdot}4\right)=0{\cdot}9, \tag{17}$$

where suffix zero indicates values in zero pressure gradient. Flat-plate skin friction is then obtained from the correlation of Winter and Gaudet[17] (in the earlier entrainment method, the correlation of Spalding and Chi[23] was used). For our purposes this correlation, which does not give C_f explicitly, has been approximated by the expression

$$C_{f_0}=\frac{0{\cdot}01013}{\log_{10} R_\theta-1{\cdot}02}-0{\cdot}00075, \tag{18}$$

which fits the correlation to within 0·04 per cent for values of R_θ between 5×10^3 and 5×10^5. At values of R_θ below 5000, C_f given by equation (18) rises above that of the Winter and Gaudet correlation, being slightly more than 7 per cent high at $R_\theta=320$. This is in qualitative agreement with the observed behaviour at low Reynolds number although, according to Coles[24], the increase in C_{f_0} above that given by logarithmic 'high Reynolds number' formulae is rather greater than 7 per cent at a value of R_θ as low as this. Whilst it should be possible to correct the method for the anomalous behaviour of C_{f_0} and of the $G(\Pi)$ locus at low Reynolds number, this would require a more careful study of the available experimental data than we have yet made, and no such corrections are at present included.

To complete the skin-friction relation, we write

$$1-\frac{1}{H_0}=6{\cdot}55\sqrt{\frac{C_{f_0}}{2}} \tag{19}$$

where, following Winter and Gaudet, we take G in zero pressure gradient to be 6·55.

2.6. Completion of the Lag Equation

To complete the prediction method, equation (8) needs to be converted from a differential equation for maximum shear stress into a differential equation for entrainment coefficient.

As it stands, equation (8) applies only to flows with a maximum stress away from the wall, and contains the grouping $2a_1U_e\delta/UL$ which is a strong function of the position of τ_{max} if this is at a value of y/δ less than 0.2

approximately. The first approximation we therefore make is to delete the suffix m, writing the equation

$$\frac{\delta}{C_\tau}\frac{dC_\tau}{dx}=2a_1\frac{U_e}{U}\frac{\delta}{L}\{(C_\tau)_{EQ}^{\frac{1}{2}}-C_\tau^{\frac{1}{2}}\}+2\left(\frac{\delta}{U_e}\frac{dU}{dx}\right)_{EQ}-2\frac{\delta}{U_e}\frac{dU}{dx}, \tag{20}$$

where C_τ is now $C_{\tau m}$ if the maximum shear stress occurs at $y/\delta \geqslant 0{\cdot}2$, but is otherwise the value of $\tau/\rho_e U_e^2$ at $y/\delta = 0{\cdot}2$.

Referring back to equation (5) we see that the only terms simplified by applying the equation at a maximum in τ are the advective term involving $V\partial\tau/\partial y$ and the diffusion term involving $\partial(G\tau)/\partial y$. We must therefore assess how important are the terms in $\partial/\partial y$ which have implicitly been omitted in regarding equation (20) as a transformation of equation (5) into a differential equation for τ at $y/\delta =$ constant.

In all adverse pressure gradients except the mildest, maximum τ occurs at $y/\delta > 0{\cdot}2$; it is therefore only in strong favourable pressure gradients that we might expect the omitted terms in $\partial\tau/\partial y$ to be important. However, for two-dimensional sink flow, which has the strongest favourable pressure gradient for which an equilibrium flow is possible, lines of $y/\delta =$ constant are also streamlines. In this flow, the terms representing advection along a streamline are identical with those in equation (20), the production and dissipation terms are also identical and, since $\tau/\rho U_e^2$ is constant along streamlines in sink flows, the diffusion term must also be given correctly by equation (20). On the basis that, if equation (20) is applicable to virtually all adverse pressure gradient flows and also to sink flows it is not likely to be appreciably in error for flows intermediate between these, we assume therefore that it is a valid approximation for all flows of practical interest.

The second approximation we make is to replace the group $2a_1U_e\delta/UL$ by a constant. Bradshaw *et al.*[8] have suggested that a_1 is effectively constant at 0·15, and their function L/δ is very nearly constant at 0·09 for values of y/δ between 0·2 and, say 0·5, which is the range of application of equation (20). The velocity ratio U_e/U at the point of application of equation (20) is a function of velocity profile shape, but not a strong one (in adverse pressure gradients, the influence of the velocity profile becoming less full is to some extent compensated by the outward movement of the position of maximum τ). From the work of Mellor and Gibson[11], we have taken an approximate mean value of U_e/U at the position of τ_{max} in flows with adverse pressure gradients to be 1·5. We have also adopted a value of 0·08 rather than 0·09 for L/δ, to allow for the fact that the shape-parameter relation of equation (16) gives values of boundary-layer thickness typically 10 per cent greater than those determined from the value of y at $U/U_e = 0{\cdot}995$.

Replacing a_1, L/δ and U_e/U by these constants, equation (20) becomes

$$\frac{\delta}{C_\tau}\frac{dC_\tau}{dx}=5{\cdot}6\{(C_\tau)_{EQ}^{\frac{1}{2}}-C_\tau^{\frac{1}{2}}\}+2\left(\frac{\delta}{U_e}\frac{dU_e}{dx}\right)_{EQ}-\frac{2\delta}{U_e}\frac{dU_e}{dx}, \tag{21}$$

and all that remains is replace the terms in C_τ by corresponding terms in C_E. At first it might be thought that the assumption $C_E =$ constant $\times C_\tau$, as is employed by Bradshaw *et al.*[8] in evaluating their diffusion term, would be an adequate approximation. This has proved, however, to be an oversimplification which leads to highly unrealistic behaviour of the method in certain circumstances.

We have derived a more realistic relationship between C_E and C_τ from the analytical study of equilibrium boundary layers by Mellor and Gibson[11], using equation (16) to determine H_1 as a function of H and hence, for our purposes, to define the edge of the boundary layer and thus C_E.

Fig. 3a shows the calculated variation of C_E with C_τ for Reynolds numbers R_{δ^*} of 10^3 and 10^5. The division between flows with maximum shear stress at $y/\delta > 0{\cdot}2$ and those in which C_τ is based on τ at $y/\delta = 0{\cdot}2$ is indicated. The fact that C_τ remains finite when C_E goes to zero in sink flows is an important feature which it is essential to incorporate into the lag equation if it is to be physically realistic.

Fig. 3b shows the analytic approximation that we have adopted for the curves in Fig. 3a. It may be written

$$C_\tau = 0{\cdot}024C_E + 1{\cdot}2C_E^2 + 0{\cdot}32C_{f_0}, \tag{22}$$

where C_{f_0} is the flat plate skin-friction coefficient given by equation (18). The accuracy of this is consistent with the approximation made in going from equation (20) to equation (21). Differentiating equation (22) with respect to x, we obtain

$$\frac{dC_\tau}{dx}=(0.024+2{\cdot}4C_E)\frac{dC_E}{dx}+0{\cdot}32\frac{dC_{f_0}}{dx}. \tag{23}$$

Since C_{f_0} (not C_f, note) is a weak function solely of R_θ, its streamwise variation will always be slow and so, given that equations (21) and (22) both already include a degree of approximation, the neglect of dC_{f_0}/dx in equation (23) is thought justified. Omitting this term, and making the assumption that the relationship between C_τ and C_E derived for equilibrium boundary layers also holds good in flows which are out of equilibrium, so that the above derivation of equation (23) from equation (22) is justified, we combine equation (21) with equation (23) to obtain, after a little manipulation,

$$\theta(H_1+H)\frac{dC_E}{dx}=\frac{C_E(C_E+0{\cdot}02)+0{\cdot}2667C_{f_0}}{C_E+0{\cdot}01}\Big[\underbrace{2{\cdot}8\{(0{\cdot}32C_{f_0}+0{\cdot}024(C_E)_{EQ}+1{\cdot}2(C_E)_{EQ}^2)^{\frac{1}{2}}}_{\text{prod}}$$

$$\underbrace{-(0{\cdot}32C_{f_0}+0{\cdot}024C_E+1{\cdot}2C_E^2)^{\frac{1}{2}}\}}_{\text{diss}}+\underbrace{\left(\frac{\delta}{U_e}\frac{dU_e}{dx}\right)_{EQ}}_{\text{diff}}-\underbrace{\frac{\delta}{U_e}\frac{dU_e}{dx}}_{\text{adv}}\Big]. \tag{24}$$

This equation completes the method, in its basic form, for incompressible flows. In some circumstances, it allows negative values of C_E to be generated. Negative entrainment is physically possible in strongly accelerated flows (though in such a situation equation (24) is of uncertain accuracy) and in programming the method the only constraint imposed on C_E has been that it shall not fall below $-0{\cdot}009$. This quite arbitrary limit ensures that we avoid singular behaviour due to the denominator in equation (24) becoming zero.

2.7. Extraneous Influences on the Turbulence Structure

There are a number of extraneous influences which can modify the turbulence structure in a boundary layer—longitudinal surface curvature is one such, freestream turbulence another, flow convergence or divergence apparently a third. The mechanisms underlying these influences are not well established, and are probably quite different from case to case. Nevertheless, for engineering purposes, a first-order correction for each may plausibly be made by suitable adjustment of the dissipation length scale L/δ.

Bradshaw[13], considering longitudinal surface curvature, developed an analogy between its influence on the turbulence structure and that of buoyancy. Then, on the basis of correlations derived in meteorology, he proposed that the only change needed to the method of Ref. 8 to allow for longitudinal curvature was to write his dissipation length scale

$$\frac{L}{\delta}=\left(\frac{L}{\delta}\right)_0(1+\beta Ri)^{-1}, \tag{25}$$

where suffix zero indicates a flat surface, Ri is Richardson number (more correctly, the analogue in curved flows for Richardson number in buoyant flows) and β, an empirical constant, has a value of 7 for flows over convex surfaces (Ri positive) and 4·5 for flows over concave surfaces (Ri negative).

Richardson number, written

$$Ri=\frac{2U}{R}\Big/\frac{\partial U}{\partial y}, \tag{26}$$

where R is the longitudinal streamline curvature, varies from point to point across the boundary layer. To incorporate Bradshaw's argument into an integral method, therefore, an average value of Ri must be determined. We have taken the average to be the value at $y/\delta=0{\cdot}5$, and have used the tabulated results of Mellor and Gibson[11] for equilibrium boundary layers to arrive at this. In round numbers, we find from Mellor and Gibson that we may write

$$\left.\begin{aligned} U_{0{\cdot}5}&=U_e\left(1-0{\cdot}7\frac{\delta^*}{\delta}\right)\\ \text{and}\qquad \left(\frac{\partial U}{\partial y}\right)_{0{\cdot}5}&=\frac{3U_e\delta^*}{\delta^2}, \end{aligned}\right\} \tag{27}$$

whence we have

$$Ri = \frac{2}{3}\frac{\theta}{R}\left(\frac{H+H_1}{H}\right)^2\left(1-\frac{0{\cdot}7H}{H+H_1}\right) = \frac{2\theta}{3R}(H+H_1)\left(\frac{H_1}{H}+0{\cdot}3\right). \tag{28}$$

Another influence on the turbulence structure which may be treated similarly is that of flow convergence or divergence. Bradshaw[25] has suggested that, as a general rule of thumb, the effect on the turbulence of small extra rates of strain may be represented by multiplying eddy viscosity—say—by a factor

$$1+\frac{K\times\text{extra rate of strain}}{\partial U/\partial y}$$

where K is an empirical constant which appears to be of order ± 10. If, for consistency with equation (25), we write an analogous expression*,

$$\frac{L}{\delta} = \left(\frac{L}{\delta}\right)_0\left\{1-K\frac{U\,dr}{r\,dx}\Big/\frac{\partial U}{\partial y}\right\}^{-1}, \tag{29}$$

we should expect the empirical constant K to be of order ± 5 (since, by definition, $\tau \propto$ eddy viscosity $\propto$ (mixing length)^2 for a given shape of velocity profile). In the case of longitudinal curvature, however, where the ratio of the two rates of strain is $0{\cdot}5Ri$, we have assigned this constant a value of 9 for unstable flows and 14 for stable flows. Here, for laterally strained flows, we tentatively and rather arbitrarily adopt a value of 7 for K. Then, taking the ratio of the two rates of strain at $y/\delta = 0{\cdot}5$ as the appropriate average value for the outer part of the boundary layer, we may substitute equation (27) in equation (29) to obtain

$$\frac{L}{\delta} = \left(\frac{L}{\delta}\right)_0\left(1-\frac{7}{3}(H+H_1)\left(\frac{H_1}{H}+0{\cdot}3\right)\frac{\theta}{r}\frac{dr}{dx}\right)^{-1}. \tag{30}$$

Considering how we incorporate these effects into the boundary-layer method, let us first propose that they be lumped together into a single overall scaling factor λ such that

$$\frac{L}{\delta} = \left(\frac{L}{\delta}\right)_0\lambda^{-1}, \tag{31}$$

where

$$\lambda = (1+\beta Ri)\left(1-\frac{K}{3}\left(\frac{H_1}{H}+0{\cdot}3\right)\frac{\delta}{r}\frac{dr}{dx}\right)(\ldots\text{etc.}). \tag{32}$$

Then, in the presence of secondary effects, we can write equation (7)

$$\frac{\delta}{C_{\tau m}}\frac{dC_{\tau m}}{dx} = 2a_1\frac{U_e}{U}\left[\frac{\delta}{U_e}\frac{\partial U}{\partial y}-\left(\frac{\delta}{L}\right)_0\lambda C_{\tau m}^{\frac{1}{2}}-C_{\tau m}\zeta'\right]-\frac{2\delta}{U_e}\frac{dU_e}{dx}, \tag{33}$$

adv — shear prod — diss + extra strain effects — diff — adv

* Since this form of correction is assumed valid only if the correction is small, the factors $(1+K\sigma)$ and $(1-K\sigma)^{-1}$, where σ is the ratio of secondary strain to the main shear, are usually treated as equal under the binomial theorem. Throughout this Report, we use only the form in equation (29). In the computer program a limit of $0{\cdot}6 > K\sigma > -1{\cdot}5$ is arbitrarily set so that L/δ and $(L/\delta)_0$ never differ by more than a factor of 2·5.

where, in effect, we are representing the influence of secondary strain by the addition of the term

$$-2a_1\frac{U_e}{U}\left(\frac{\delta}{L}\right)_0(\lambda-1)C_{\tau m}^{\frac{1}{2}}$$

to the right hand side of the equation. Although it is convenient algebraically to group this term with the viscous dissipation term, it should be remembered that it is an engineering approximation, derived by multiplying a small physical quanity by a large empirical constant. Without a better understanding of why such a term arises, we cannot classify it in physical terms in the way that the other components of the equation, derived from the Navier–Stokes equations, have been classified.

Equation (33) is recast in a form similar to equation (21),

$$\frac{\delta}{C_\tau}\frac{dC_\tau}{dx}=5{\cdot}6\{(C_\tau)_{EQ_0}^{\frac{1}{2}}-\lambda C_\tau^{\frac{1}{2}}\}+2\left(\frac{\delta}{U_e}\frac{dU_e}{dx}\right)_{EQ}-2\frac{\delta}{U_e}\frac{dU_e}{dx}. \tag{34}$$

The points to note about this equation are:

(1) The coefficient of the shear production term, which is a function only of the shape of the velocity profile, is unchanged from its form in flows free from secondary influences, and hence is written with suffix EQ_0.

(2) The coefficient of the 'dissipation' term is simply scaled by λ, and this will carry over directly to the more complicated dissipation term of equation (24).

(3) The diffusion term is written without suffix zero, indicating that this term has to be modified to allow for secondary influences*.

The diffusion term is evaluated by making the assumption that mixing length and dissipation length become effectively equal in an equilibrium situation, so that the production and dissipation terms and the two pressure gradient terms in equation (34) separately balance each other when $dC_\tau/dx = 0$. From the definition of mixing length, it follows that, for the same shape of velocity profile,

$$C_{\tau_{EQ}}=C_{\tau_{EQ_0}}\lambda^{-2}. \tag{35}$$

We may therefore, from equation (22), write for equilibrium flows

$$(0{\cdot}024C_E+1{\cdot}2C_E^2+0{\cdot}32C_{f_0})\lambda^2=(0{\cdot}024C_{E_0}+1{\cdot}2C_{E_0}^2+0{\cdot}32C_{f_0}) \tag{36}$$

where suffix EQ has been omitted from C_E for clarity. Knowing $(C_E)_{EQ_0}$ and λ, it is a simple matter to solve this quadratic for $(C_E)_{EQ}$.

The value of $(C_E)_{EQ_0}$ is determined from equations (13) and (15) as a function of H, H_1 and C_f. Having then, from equation (36), evaluated $(C_E)_{EQ}$, we invert equation (15) to obtain

$$\left(\frac{\delta}{U_e}\frac{dU_e}{dx}\right)_{EQ}=\frac{H+H_1}{H+1}\left(\frac{C_f}{2}-\frac{(C_E)_{EQ}}{H_1}\right). \tag{37}$$

This may seem, in all, a slightly involved procedure to deal with influences which are secondary in nature. On a computer, however, it increases the total calculation time by at most fifty per cent, and it has the virtue of providing a flexible means of handling potentially a wide range of effects without introducing any problems of keeping the method internally consistent.

2.8. Wakes

The entrainment method of Ref. 1 was extended to treat two-dimensional wakes and was applied with some success to the prediction of wakes downstream of lifting aerofoils. A similar extension of the present method has been made. Taking as background the discussion in the earlier Report[1] of the approximations implied in applying the method to wakes, particularly to the asymmetrical wakes of lifting aerofoils, we shall only outline here how the present method is used, offering justification for assumptions only if they are new.

---

* Bradshaw does not modify his diffusion function to allow for these influences, but our diffusion term approximates the product of his function and $C_{\tau m}$, so the two approaches are not necessarily inconsistent.

The computation of boundary layer growth over one surface of an aerofoil is taken beyond a *sharp* trailing edge, to treat the development of the part wake on one side of the streamline originating at the trailing edge, by continuing the integration of the three governing differential equations. Downstream of the trailing edge, the only changes to the method are:

(1) C_f and C_{f_0} are set to zero in all equations in which they occur;

(2) the dissipation length scale is doubled.

The first implies: no friction contribution in the momentum integral and entrainment equations (1) and (2); a change in equilibrium pressure gradient and equilibrium entrainment coefficient for a given H (equations (13) and (15)); an alteration to the lag equation (24)†.

The second change is made in order to match the observed asymptotic behaviour of far wakes. In the earlier treatment[1] of wakes, entrainment in the far wake was empirically increased so as to reproduce the behaviour observed by Townsend[26] in a wake of small velocity defect at constant pressure:

$$\theta\frac{dH}{dx} = -0{\cdot}234(H-1)^3, \tag{38}$$

where θ is the momentum thickness of the half-wake. In the limit $H \to 1$, $H_1 \to \infty$, C_E, $C_\tau \to 0$, with $C_f = 0$, the present method can readily be shown to give

$$\theta\frac{dH}{dx} \to -0{\cdot}060(H-1)^3 \qquad \text{if} \quad \lambda = 1,$$

but

$$\theta\frac{dH}{dx} \to -0{\cdot}242(H-1)^3 \qquad \text{if} \quad \lambda = 0.5.$$

Corroboration for setting $\lambda = 0{\cdot}5$ in the far wake comes from Narasimha and Prabhu[27], who tabulate some properties for wakes in equilibrium from which we can write eddy viscosity

$$\nu_T = 0{\cdot}0634 U_e \delta^*.$$

This is almost exactly four times the value

$$\nu_T = 0{\cdot}016 U_e \delta^*$$

used by Mellor and Gibson[11] in their studies on equilibrium boundary layers. A fourfold increase in ν_τ corresponds to a doubling of L/δ; it is reassuring that this change in the dissipation scale corresponds, in a symmetrical flow at least, to the change in the scale of the large eddies between flow over a surface and flow in a wake.

In general, the change in L/δ associated with the wake should be compounded with other secondary influences by writing equation (32)

$$\lambda = \tfrac{1}{2}(1 + \beta Ri)(\ldots etc.), \tag{39}$$

but it is not clear in what situations other secondary influences will be significant. For example, if there is longitudinal curvature in the wake, its sign will be opposite for the two sides of the wake and the effects will

† To justify this change to the lag equation in physical terms, compare boundary layers and wakes passing from a region of strong favourable pressure gradient (but not so strong as to cause relaminarisation) to a region of constant pressure. In the boundary layer, entrainment falls to a very low value but skin friction is high; when the pressure gradient relaxes, the boundary layer starts to grow fairly rapidly due to the high C_f and entrainment quickly builds up; the term in C_{f_0} in equation (24) is needed to provide for this. In contrast, in a wake, whilst a strong favourable pressure gradient will almost destroy the velocity defect and will lead to a very low value of C_E, relaxation of the pressure gradient will not cause the wake to grow again; the C_{f_0} term in equation (24), which is in effect a regenerative term, is inappropriate.

tend to cancel. Given that the treatment of asymmetrical wakes[1] is already approximate, it is doubtful whether this particular influence is worth including.

2.9. Corrections in Comparisons with Experiment

Many of the available experimental data for nominally two-dimensional flow are impaired by the flow not having been perfectly two-dimensional. With some experiments, there is the additional difficulty that the boundary layer was far from a state of equilibrium at the first measuring station so that, if measurements of turbulent shear stress were not made, problems arise in determining starting values for 'historical' calculation methods which treat shear stress or entrainment as an independent variable. This section describes some modifications to the method which are intended to put comparisons between calculation and experiment on as sound a footing as is practicable.

The conclusion that the boundary layer in any particular experiment was not two-dimensional is usually based on the failure of the momentum integral equation to balance when all the terms in it are evaluated from the experimental data, (see, for example, the analysis of test cases for the Stanford Conference[3]). Not necessarily all the imbalance in the momentum equation is due to three-dimensionality; there can also be a contribution from the growth of the Reynolds normal stresses. However, when the imbalance is sufficient to have a serious effect on comparisons between measurement and prediction, it is usually so gross that the major part of it has to be attributed to three-dimensionality.

For comparison with experiment, the present method can be programmed to accept the experimental distribution of momentum thickness as part of the input data. Then, assuming that the entire experimental imbalance in the momentum equation is due to three-dimensionality, a distribution of free-stream convergence or divergence can be computed such that the predicted and measured distributions of momentum thickness are in precise agreement. If this is achieved, the comparison between experiment and the predicted value of H and C_f provides a rather more realistic test of the method than does a comparison with predictions for wholly two-dimensional flow.

The assumption we make is that departures from two-dimensionality—(planar or axisymmetric) take the form of the plane-of-symmetry flow studied by Johnston[28]. Relative to the nominal flow, this involves a local convergence or divergence of the free stream which is amplified within the boundary layer. We define w as the velocity component within the boundary layer at right angles to the flow direction at the edge of the layer and take ϕ as this flow direction. Then, following Johnston[28], for a small rate of divergence suddenly applied we write

$$\frac{\partial w}{\partial z} = 2(U_e - U)\frac{\partial \phi}{\partial z} \tag{40}$$

as a description of the crossflow within the boundary layer. The experiments of East and Hoxey[20] confirm Johnston's findings that equation (40) is a good approximation for all the boundary layer outside a narrow region close to the wall; for simplicity, however, we assume that equation (40) applies to the entire boundary layer.

With the assumption that a local rate of divergence $\partial\phi/\partial z$ of the free stream generates crossflows given by equation (40) within the boundary layer, it may be shown, from the equations for three-dimensional boundary layers[29], that the momentum integral and entrainment equations (1) and (2) have to be rewritten:

$$\frac{1}{U_e}\frac{d}{dx}(rU_e\theta) = r\frac{C_f}{2} - (H+1)\frac{r\theta}{U_e}\frac{dU_e}{dx} \underbrace{- r\theta\frac{\partial \phi}{\partial z}}_{\text{divergence}} \underbrace{- 2r\theta(H-1)\frac{\partial \phi}{\partial z}}_{\text{crossflow}}; \tag{41}$$

$$r\theta\frac{dH}{dx} = \frac{dH}{dH_1}\left\{rC_E - H_1\frac{1}{U_e}\frac{d}{dx}(rU_e\theta) \underbrace{- r\theta H_1\frac{\partial \phi}{\partial z}}_{\text{divergence}} \underbrace{- 2r\theta H\frac{\partial \phi}{\partial z}}_{\text{crossflow}}\right\}. \tag{42}$$

The lag equation remains unchanged, as do the various auxiliary relations. In a calculation using these equations, equation (41) is solved for $\partial\phi/\partial z$ with the left-hand side evaluated from the input data.

The more usually employed correction for momentum imbalance assumes coplanar velocity profiles so that w is zero, only the divergence terms in equation (41) and equation (42) appear, and the result of substituting the momentum equation into the entrainment equation is that the divergence terms cancel leaving dH/dx locally unaffected by flow divergence. The present treatment differs in leaving a residual term $2r\theta[H_1(H-1)-H]\partial\phi/\partial z$ in the entrainment equation after substitution of the momentum equation.

Whilst it has not been demonstrated that Johnston's flow model is universally more accurate than assuming co-planar flow, there is strong experimental evidence to support it in flows in which convergence or divergence occurs relatively suddenly over a short streamwise distance. Since the crossflow terms in equation (42) are likely to be significant only in these circumstances—in flows with a more gradual but sustained divergence the other terms in equation (42) will dominate—we have felt fully justified in applying equation (41) and equation (42) generally.

The second problem which has to be faced in making comparisons with experiment is the choice of starting values. If measurements of turbulent shear stress were available at the station of the first velocity profile measurement, it would be possible to evaluate C_τ and hence, from equation (22), obtain an initial value of C_E. So far, however, we have chosen either to take initial C_E as $(C_E)_{EQ}$, as indeed we generally must for all calculations performed in the abstract, or else we have evaluated an initial C_E from the experimental velocity profile measurements. In the latter case, values of $d\theta/dx$ and dH/dx at the starting point are estimated from the experimental data, equation (41) is solved for $\partial\phi/\partial z$ and this enables equation (42) to be solved for C_E. For some experiments, the general level of agreement between measurement and prediction has been found to depend quite significantly on the initial value of entrainment coefficient.

3. The Method for Compressible Flows

3.1. Outline

In this section we describe the application of the method to adiabatic compressible flows. The method has, in fact, also been programmed to treat compressible flows with heat transfer by including a fourth differential equation, the total energy equation, as proposed in Appendix A of Ref. 1: this aspect of the method is not, however, sufficiently developed to justify further discussion here.

The extension to compressible flows is fairly straightforward and does not involve any coordinate transformations. For the lag equation, we follow the reasoning applied to the turbulent kinetic energy equation by Bradshaw and Ferriss[14], and which is their interpretation of Morkovin's[15] hypothesis that the turbulence structure is unaffected by compressibility. The other two differential equations are changed to include density terms, and some of the empirical relations are modified to account for compressibility. The concept of equilibrium flows as used in Section 2 is not entirely applicable in compressible flows, but it has been possible to derive adequate working relationships by considering flows which are locally in equilibrium in a more restricted sense. In deriving these relations, we have relied on the observation of previous workers[30] that distributions of mixing length and eddy viscosity, suitably scaled, are insensitive to Mach number.

In compressible flow, the three independent parameters used to specify the boundary layer are momentum thickness θ, entrainment coefficient C_E, and the shape parameter

$$\bar{H}=\frac{\int_0^\infty \frac{\rho}{\rho_e}\left(1-\frac{U}{U_e}\right)dy}{\int_0^\infty \frac{\rho U}{\rho_e U_e}\left(1-\frac{U}{U_e}\right)dy}. \tag{43}$$

The momentum integral and entrainment equations, with density terms included and with some rearrangement from equation (1) and equation (2), are written

$$\frac{d}{dx}(r\theta)=r\frac{C_f}{2}-(H+2-M^2)\frac{r\theta}{U_e}\frac{dU_e}{dx} \tag{44}$$

and

$$r\theta\frac{d\bar{H}}{dx}=\frac{d\bar{H}}{dH_1}\left[rC_E-H_1\left\{r\frac{C_f}{2}-(H+1)\frac{r\theta}{U_e}\frac{dU_e}{dx}\right\}\right], \tag{45}$$

where M is Mach number at the edge of the boundary layer. Fuller derivations are given in earlier work[1,31]. Implicit in equation (45) is the assumption made below that $\bar{H}$ is a unique function of H_1.

The lag equation, written in the form of equation (21), is unchanged. Its derivation for compressible flow and conversion to a differential equation for C_E are given in Section 3.2.

For the shape-parameter and skin-friction relationships, we make assumptions similar to those used in extending Head's method to compressible flow[1]. Thus, taking $\bar{H}$ as the analogue in compressible flows for H at low speeds, we now write equation (16)

$$H_1 = 3{\cdot}15 + \frac{1{\cdot}72}{\bar{H}-1} - 0{\cdot}01(\bar{H}-1)^2, \tag{46}$$

and equation (17) becomes

$$\left(\frac{C_f}{C_{f_0}} + 0{\cdot}5\right)\left(\frac{\bar{H}}{\bar{H}_0} - 0{\cdot}4\right) = 0{\cdot}9 \tag{47}$$

where suffix 0 indicates values in zero pressure gradient. Following Winter and Gaudet[17], for compressible flow we write equation (18)

$$F_c C_{f_0} = \frac{0{\cdot}01013}{\log_{10}(F_R R_\theta) - 1{\cdot}02} - 0{\cdot}00075 \tag{48}$$

where

$$F_c = (1 + 0{\cdot}2M^2)^{\frac{1}{2}} \tag{49}$$

and

$$F_R = 1 + 0{\cdot}056M^2. \tag{50}$$

For zero pressure gradient equation (19), extended empirically as shown below, becomes

$$1 - \frac{1}{\bar{H}_0} = 6{\cdot}55\sqrt{\frac{C_{f_0}}{2}(1 + 0{\cdot}04M^2)} \tag{51}$$

and, finally, the shape parameters $H(=\delta^*/\theta)$ and $\bar{H}$ are related by

$$H + 1 = (\bar{H} + 1)\left(1 + \frac{rM^2}{5}\right) \tag{52}$$

where r is temperature recovery factor.

The last of these equations (52) is the well known result for flows with a parabolic relation between velocity and temperature. Equation (51) differs from that used with the previous method[1] in containing the empirical term in M which is derived in Section 3.2. Equations (48)–(50) have been demonstrated by Winter and Gaudet[17] to be in good agreement with experiment at Mach numbers up to 3. The general forms of equations (46) and (47) have also been shown previously[1] to be in agreement with experiment. To complete the method, we need now only the differential equation for C_E, and auxiliary relations for any new unknowns in this equation.

3.2. Lag Equation and Equilibrium Flows

Bradshaw and Ferriss[14], to whom the reader is referred for a more detailed discussion, derive for compressible flows a differential equation involving shear stress, their equation (19), which at a maximum in τ/ρ can be written*

$$\frac{U}{2a_1}\frac{d}{dx}\left(\frac{\tau}{\rho}\right)_m = \left(\frac{\tau}{\rho}\right)_m \frac{\partial U}{\partial y} - \frac{(\tau/\rho)_m^{\frac{3}{2}}}{L} - \left(\frac{\tau}{\rho}\right)_m^{\frac{3}{2}}\left[\frac{\partial G}{\partial y} - Gr(\gamma - 1)\frac{M^2}{U}\frac{\partial U}{\partial y}\right]. \tag{53}$$

* In this particular equation, M denotes local Mach number; elsewhere, it denotes Mach number at the edge of the boundary layer.

It should be noted that the important variable in this equation is not shear stress itself but the quantity τ/ρ, which has the dimensions of (velocity)^2 and is assumed by Bradshaw and Ferriss to be directly proportional to the local mean square fluctuating velocity. Making the definition

$$C_\tau = \frac{1}{U_e^2}\left(\frac{\tau}{\rho}\right) \tag{54}$$

(not $\tau/\rho_e U_e^2$, note), we now follow Section 2.6 in assuming equation (53) to apply at a maximum in (τ/ρ)if this occurs at $y/\delta \geq 0{\cdot}2$, and otherwise to be a good approximation for $y/\delta = 0{\cdot}2$. Equation (53) is then written

$$\frac{\delta}{C_\tau}\frac{dC_\tau}{dx} = 2a_1\frac{U_e}{U}\frac{\delta}{L}\{(C_\tau)_{EQ}^{\frac{1}{2}} - C_\tau^{\frac{1}{2}}\} + 2\left(\frac{\delta}{U_e}\frac{dU_e}{dx}\right\}_{EQ} - 2\frac{\delta}{U_e}\frac{dU_e}{dx} =$$

$$= 5{\cdot}6\{(C_\tau)_{EQ}^{\frac{1}{2}} - C_\tau^{\frac{1}{2}}\} + 2\left(\frac{\delta}{U_e}\frac{dU_e}{dx}\right)_{EQ} - 2\frac{\delta}{U_e}\frac{dU_e}{dx}. \tag{55}$$

In making this step, we have followed Bradshaw and Ferriss in assuming that the dissipation length scale L/δ is independent of Mach number; we have also assumed that mixing length and dissipation length are equal at $(\tau/\rho)_{max}$ in an 'equilibrium' flow, which is defined at this stage as a flow in which the shape of the velocity profile, i.e. its kinematic shape parameter

$$H_k = \frac{\int_0^\infty \left(1-\frac{U}{U_e}\right)dy}{\int_0^\infty \frac{U}{U_e}\left(1-\frac{U}{U_e}\right)dy}, \tag{56}$$

does not vary with streamwise distance. The experiments of Winter and Gaudet[17] have demonstrated the very closely similar shapes of velocity profiles in compressible and incompressible flow, so we have good reason to postulate that a flow in which the H_k is constant, even if Mach number is varying, will have velocity profiles which outside the viscous sub-layer will remain virtually identical in shape. The work of Maise and McDonald[30] confirms that the mixing length scale l/δ, and the kinematic eddy viscosity scaled on the kinematic displacement thickness, are both effectively independent of Mach number in flows at constant pressure. Hence, we argue that a flow in which the shape of the velocity profiles does not vary with distance will also have unvarying profiles of $(\tau/\rho)/U_e^2$ and dC_τ/dx will be zero.

Now the ratio $H_k/\bar{H}$, though always fairly close to unity, is a weak function of Mach number. Hence, if H_k is constant in a flow with pressure gradient, $\bar{H}$ will slowly vary. Because it is convenient to use the entrainment relation to evaluate the 'equilibrium' value of C_E, we have chosen to define equilibrium flows as those with $\bar{H}$ rather than H_k constant. Although C_τ will not be constant in these flows, we assume that its variation will be sufficiently slow for mixing length and dissipation length to be effectively equal: for a given H, R_θ and M, this assumption implies that values of C_τ and C_E will be the same in the two kinds of equilibrium flow, although the pressure gradients necessary to give zero $d\bar{H}/dx$ and dH_k/dx will differ.

For compressible flow, the parameters of Section 2.3 are defined

and

$$\left.\begin{aligned} G &= \frac{\bar{H}-1}{\bar{H}}\sqrt{\frac{2}{C_f}} \\ \Pi &= -\frac{2\delta^*}{C_f}\frac{1}{U_e}\frac{dU_e}{dx}. \end{aligned}\right\} \tag{57}$$

The dependence of the $G(\Pi)$ locus on Mach number has been estimated by considering two particular cases: (1) zero pressure gradient flow, $\Pi = 0$, for which experimental data of high quality exist, and (2) flow on the verge of separation, $\Pi = \infty$, $C_f = 0$, which we have treated analytically using the results of Mellor and Gibson[11]

for equilibrium boundary layers in incompressible flow. Rearranging the equilibrium locus for incompressible flow, equation (11),

$$6{\cdot}432 = \frac{H-1}{H}\left(\frac{C_f}{2} - 0{\cdot}8\frac{\delta^*}{U_e}\frac{dU_e}{dx}\right)^{-\frac{1}{2}},$$

and with G and Π as defined in equations (57), we write for these two cases in compressible flow

$$\left.\begin{aligned} A &= \frac{\bar{H}-1}{\bar{H}}\left(\frac{C_f}{2}\right)^{-\frac{1}{2}} \qquad \text{for} \quad \Pi = 0 \\ \text{and} \qquad A &= \frac{\bar{H}-1}{\bar{H}}\left(-0{\cdot}8\frac{\delta^*}{U_e}\frac{dU_e}{dx}\right)^{-\frac{1}{2}} \qquad \text{for} \quad \Pi = \infty, \end{aligned}\right\} \tag{58}$$

where A is a function of M (and possibly of Π) which becomes the constant 6·432 written A_i, in incompressible flow. Fig. 4 shows the estimated variation of A/A_i with Mach number.

For the flow on the verge of separation, assuming mixing length l/δ to be independent of M, we have considered boundary layers with profiles of velocity and (τ/ρ) identical to those computed by Mellor and Gibson for $\Pi = \infty$. Over a range of Mach numbers, with total temperature taken as constant through the boundary layer, the appropriate integral quantities have been evaluated from the velocity and shear stress profiles to enable us to solve the mean kinetic energy equation which, for $C_f = 0$, can be written

$$\theta\frac{dH_\varepsilon}{dx} = C_D + H_\varepsilon\left[H - 1 - \frac{2M^2}{5}\right]\frac{\theta}{U_e}\frac{dU_e}{dx} \tag{59}$$

where

$$\left.\begin{aligned} H_\varepsilon &= \frac{1}{\theta}\int_0^\infty \frac{\rho U}{\rho_e U_e}\left(1 - \frac{U}{U_e}\right)^2 dy \\ \text{and} \qquad C_D &= \int_0^\infty \frac{\tau}{\rho_e U_e^3}\frac{\partial U}{\partial y}\,dy. \end{aligned}\right\} \tag{60}$$

By analogy with equation (46), we assume H_ε and $\bar{H}$ to be so related that when dH_ε/dx is zero $d\bar{H}/dx$ is zero also; from equation (59) it is then possible to evaluate the equilibrium pressure gradient and hence to determine A from equation (58).

For the case $\Pi = 0$, we have adopted the simpler course of assuming A/A_i to vary with M in the same way as G/G_i (remembering that A and G are nearly, but not exactly, equal in zero pressure gradient). In Fig. 4, the points shown are in fact experimental values of G/G_i obtained by Winter and Gaudet[17] and Hastings and Sawyer[32].

The curve drawn in Fig. 4,

$$\frac{A}{A_i} = (1 + 0{\cdot}04M^2)^{\frac{1}{2}}, \tag{61}$$

is thought sufficiently close to the two cases $\Pi = 0$ and $\Pi = \infty$ to justify the assumption that it applies at all values of Π. Hence, for compressible flow, the equilibrium locus becomes

$$G = 6{\cdot}432((1 + 0.8\Pi)(1 + 0{\cdot}04M^2))^{\frac{1}{2}} \tag{62}$$

or

$$\frac{\bar{H}-1}{\bar{H}} = 6{\cdot}432\left\{\left(\frac{C_f}{2} - 0{\cdot}8\frac{H\theta}{U_e}\frac{dU_e}{dx}\right)(1 + 0.04M^2)\right\}^{\frac{1}{2}}. \tag{63}$$

From this we obtain

$$\left(\frac{\theta}{U_e}\frac{dU_e}{dx}\right)_{EQ}=\frac{1{\cdot}25}{H}\left\{\frac{C_f}{2}-\left(\frac{\bar{H}-1}{6{\cdot}432\bar{H}}\right)^2(1+0{\cdot}04M^2)^{-1}\right\} \tag{64}$$

and

$$\left(\frac{\delta}{U_e}\frac{dU_e}{dx}\right)_{EQ}=(H+H_1)\left(\frac{\theta}{U_e}\frac{dU_e}{dx}\right)_{EQ}, \tag{65}$$

while from equation (45) we have

$$(C_E)_{EQ}=H_1\left\{\frac{C_f}{2}-(H+1)\left(\frac{\theta}{U_e}\frac{dU_e}{dx}\right)_{EQ}\right\}, \tag{66}$$

where equations (65) and (66) are identical to equations (14) and (15).

To convert equation (55) into a differential equation for C_E, we consider first the behaviour of C_τ in flows in which $d\bar{H}/dx$ is zero. In such flows we have assumed mixing length to have its equilibrium value so that (τ/ρ) depends only on the shape of the velocity profile and we may write

$$C_\tau=\text{const}\times\left(\frac{H_k-1}{H_k}\right)^2 \tag{67}$$

(this is nominally exact for τ/ρ at constant y/δ, and a close approximation if $(\tau/\rho)_{\max}$ occurs at $y/\delta>0{\cdot}2$).

For a flow with $\bar{H}$ constant and H_k varying, we can differentiate equation (67) to obtain

$$\frac{1}{C_\tau}\frac{dC_\tau}{dx}=\frac{2}{H_k(H_k-1)}\frac{dH_k}{dx}. \tag{68}$$

In Ref. 31, an analysis is given of adiabatic boundary layers with power-law velocity profiles which leads to an expression of the form

$$\frac{H_k}{\bar{H}}=1+\frac{F_1(\bar{H})M^2}{1+F_2(\bar{H})M^2}. \tag{69}$$

For $\bar{H}$ constant, this may be differentiated to give

$$\frac{dH_k}{dM}=\frac{2\bar{H}}{M}\frac{F_1(\bar{H})M^2}{(1+F_2(\bar{H})M^2)^2}, \tag{70}$$

which combines with equation (68) to produce

$$\left(\frac{1}{C_\tau}\frac{dC_\tau}{dx}\right)_{EQ}=\frac{4\bar{H}}{H_k(H_k-1)}\frac{F_1(\bar{H})M^2}{(1+F_2(\bar{H})M^2)^2}\frac{1}{M}\frac{dM}{dx} \tag{71}$$

and we may now write the differential equation for C_τ

$$\frac{\delta}{C_\tau}\frac{dC_\tau}{dx}=5{\cdot}6\{(C_\tau)_{EQ}^{\frac{1}{2}}-C_\tau^{\frac{1}{2}}\}+2\left(\frac{\delta}{U_e}\frac{dU_e}{dx}\right)_{EQ}-\frac{2\delta}{U_e}\frac{dU_e}{dx}+\left(\frac{\delta}{C_\tau}\frac{dC_\tau}{dx}\right)_{EQ} \tag{72}$$

which contains one term more than equation (55) as a result of defining equilibrium as $\bar{H}$ constant.

The relationship between C_E and C_τ in equilibrium flows has been estimated from the same data as were used in Fig. 4. From our own analysis of flows with $\Pi=\infty$ and $C_\tau=$ constant, and from the analysis of Winter

and Gaudet of flows with $\Pi = 0$ which allows us to treat the case of H_k and therefore C_τ constant, we have determined $(C_E)_{EQ}$, as defined by equation (66), as a function of Mach number. We find that the fall in C_E as M increases with C_τ constant is fairly well approximated by

$$C_\tau = (0{\cdot}024C_E + 1{\cdot}2C_E^2 + 0{\cdot}32C_{f_0})(1 + 0{\cdot}1M^2) \tag{73}$$

which, on differentiation with respect to x, gives

$$\frac{1}{C_\tau}\frac{dC_\tau}{dx} = \frac{(0{\cdot}024 + 2{\cdot}4C_E)(dC_E/dx) + 0{\cdot}32(dC_{f_0}/dx)}{(0{\cdot}024C_E + 1{\cdot}2C_E^2 + 0{\cdot}32C_{f_0})} + \frac{0{\cdot}2M^2}{1 + 0{\cdot}1M^2}\frac{1}{M}\frac{dM}{dx} \tag{74}$$

where, following the derivation of equation (24) for incompressible flow, we have assumed that equation (73) applies equally to equilibrium and non-equilibrium flows. If, also following equation (24), we neglect dC_{f_0}/dx, we may combine equations (74), (71) and (72) to obtain

$$\frac{(0{\cdot}01 + C_E)}{(0{\cdot}02C_E + C_E^2 + 0{\cdot}2667C_{f_0})}\delta\frac{dC_E}{dx} = 2{\cdot}8\{(C_\tau)_{EQ}^{\frac{1}{2}} - (C_\tau)^{\frac{1}{2}}\} + \left(\frac{\delta}{U_e}\frac{dU_e}{dx}\right)_{EQ} - \frac{\delta}{U_e}\frac{dU_e}{dx} + \left[\frac{2\bar{H}}{H_k(H_k - 1)}\frac{F_1(\bar{H})M^2}{(1 + F_2(\bar{H})M^2)^2} - \frac{0{\cdot}1M^2}{1 + 0{\cdot}1M^2}\right]\frac{\delta}{M}\frac{dM}{dx} \tag{75}$$

where C_τ and $(C_\tau)_{EQ}$ are evaluated from C_E and $(C_E)_{EQ}$ using equation (73).

The two terms in the square brackets are of similar order, but their difference is not in general negligible. Although expressions for $F_1(\bar{H})$ and $F_2(\bar{H})$ are given in Ref. 31, the labour involved in using them in equation (75) is not thought justified. Instead, the contents of the square brackets are approximated by $-0{\cdot}075M^2/(1 + 0{\cdot}1M^2)$ so that, replacing $(dM)/M$ by $(1 + 0{\cdot}2M^2)(dU_e/U_e)$, equation (75) finally becomes

$$\frac{(0{\cdot}01 + C_E)}{(0{\cdot}02C_E + C_E^2 + 0{\cdot}2667C_{f_0})}\delta\frac{dC_E}{dx} = 2{\cdot}8\{(C_\tau)_{EQ}^{\frac{1}{2}} - C_\tau^{\frac{1}{2}}\} + \left(\frac{\delta}{U_e}\frac{dU_e}{dx}\right)_{EQ} - \frac{\delta}{U_e}\frac{dU_e}{dx}\left\{1 + 0{\cdot}075M^2\frac{(1 + 0{\cdot}2M^2)}{(1 + 0{\cdot}1M^2)}\right\}. \tag{76}$$

At $M = 3$, the approximation to the square brackets of equation (75) is accurate to within 15 per cent for $\bar{H} < 2$, the term in M is $\doteq 1$, so the pressure-gradient term in equation (76) agrees with that in equation (75) to within 8 per cent. Given that the lag equation is approximate in every respect, this level of agreement is acceptable.

3.3. Wakes, Other Factors Affecting the Turbulence Structure, and Momentum Imbalance

In compressible flow, the method of allowing for extraneous influences on the turbulence structure is exactly the same as at low speeds: the dissipation length scale is written

$$\frac{L}{\delta} = \left(\frac{L}{\delta}\right)_0 \lambda^{-1} \tag{77}$$

where suffix 0 denotes a flow free from such influences and λ is a scaling factor obtained by compounding the various secondary influences as in equation (32).

From the derivation of the lag equation in Section 3.2, it is clear that the alterations to the equation to account for variations in L/δ are identical in compressible and incompressible flow. Thus equation (34) is applicable to compressible flow with only the addition of the term $(\delta/C_\tau)(dC_\tau/dx)_{EQ}$, which was introduced in equation (72) as a consequence of our adopted definition of equilibrium flows. The notes following equation (34) apply, and equations (35), (36) and (37) may be used without alteration.

In applying this technique of scaling L/δ to compressible flows, we have even less empirical information on which to base our corrections than we had at low speeds. Nevertheless, the following effects have so far been tentatively incorporated into the computer programme.

Wakes. As in low-speed flow, we write $\lambda = \frac{1}{2}$. The main justification for carrying over this assumption lies in the observed[30] insensitivity to Mach number of mixing length and kinematic eddy viscosity in the flat plate boundary layer. The calculation procedure for wakes is the same as described in Section 2.8.

Longitudinal curvature. With the same definition of 'Richardson number' as in incompressible flow,

$$Ri = \frac{\delta U}{R} \Big/ \frac{\partial U}{\partial y},$$

we follow Bradshaw and Ferriss[14] in assuming that the effects of longitudinal curvature are amplified by a factor $1+M^2/5$ in compressible flow, giving

$$\lambda = 1+\beta\left(1+\frac{M^2}{5}\right)Ri. \tag{78}$$

Denoting kinematic integrals by suffix k, we may repeat the arguments used in Section 2.7 to obtain the relations

$$\left.\begin{aligned} U_{0\cdot5} &= U_e\left(1-0\cdot7\frac{\delta_k^*}{\delta}\right) \\ \text{and} \qquad \left(\frac{\partial U}{\partial y}\right)_{0\cdot5} &= \frac{3U_e}{\delta^2}\delta_k^*, \end{aligned}\right\} \tag{79}$$

whence

$$Ri = \frac{2}{3}\frac{\delta}{R}\left(\frac{\delta}{\delta_k^*}-0\cdot7\right). \tag{80}$$

The inconvenience of having a kinematic integral in this expression may be circumvented by noting that

$$\frac{\delta}{\delta_k^*} \simeq 1+\frac{H_1}{\bar{H}}, \tag{81}$$

which allows us finally to write

$$Ri = \frac{2}{3}\frac{\delta}{R}\left(\frac{H_1}{\bar{H}}+0\cdot3\right). \tag{82}$$

As in incompressible flow, β is taken as 7 on a convex wall (Ri positive) and 4·5 on a concave wall.

Lateral strain. For this effect we assume that, as in incompressible flow, we may write

$$\lambda = 1-K\frac{U}{r}\frac{dr}{dx}\Big/\frac{\partial U}{\partial y}$$

whence, making the same approximations as in the derivation of Ri above, and with K taken as 7, we have

$$\lambda = 1-\frac{7}{3}\left(\frac{H_1}{\bar{H}}+0\cdot3\right)\frac{\delta}{r}\frac{dr}{dx}. \tag{83}$$

Dilatation. Bradshaw has very recently[16] suggested that an additional and previously unexpected effect arises as a result to dilatation of the stream in compressible flow. A similar effect appears to have been incorporated into the turbulence model of Wilcox and Alber[33]. Taking

$$1+\frac{K\times\text{extra rate of strain}}{\partial U/\partial y} = 1-K\frac{\text{div } U}{\partial U/\partial y}$$

as the multiplying factor on mixing or dissipation length (i.e., for near equilibrium flows, on $\sqrt{\tau/\rho}$ rather than on τ/ρ), Bradshaw estimated K by trial and error, comparing recent experimental results with calculations for a range of K. Finally, he concluded that optimum agreement was obtained by taking $K = 10$ in equilibrium, but allowing it to lag behind equilibrium with a 'time constant' of 10δ. Physical reasons can be put forward to justify this procedure and, indeed, to suggest that all components of λ should lag behind their local equilibrium values. However, Bradshaw found that predictions with K assigned the constant value of 7 gave results comparable with, though not quite as accurate as, those obtained with K lagging behind a value of 10. For simplicity, we have adopted the relation

$$\lambda = 1 + 7\frac{\text{div } U}{\partial U/\partial y}, \tag{84}$$

noting that, because stream dilatation in two-dimensional flow and lateral strain in incompressible flow have a similar influence on transverse vorticity (*see* Bradshaw[16]), it is appropriate that K should have the same values in equations (83) and (84). We evaluate λ at $y/\delta = 0{\cdot}5$, recalling equations (79) and (81) but noting that the value of div U at $y/\delta = 0{\cdot}5$, in equilibrium flows at least, is close to that at the edge of the boundary layer, and may consequently be written

$$\text{div } U = -\frac{U_e}{\rho_e}\frac{d\rho_e}{dx} = M^2\frac{dU_e}{dx}. \tag{85}$$

Thus

$$\lambda = 1 + \frac{7}{3}M^2\left(1 + \frac{H_1}{\bar{H}}\right)\frac{\delta}{U_e}\frac{dU_e}{dx}. \tag{86}$$

Although the evidence for this effect is at present rather indirect, as indeed is the evidence for the other secondary effects we have discussed, we present this treatment of them to illustrate the relative ease with which phenomena of this kind can be brought within the framework of the method and also to show that, in some experiments, their influence might well be appreciable.

Momentum imbalance and initial C_E. When the method is being checked against experiment, corrections for departure from two-dimensional flow in the experiment may be made in the way described in Section 2.9. We have assumed, though with uncertain justification, that Johnson's relation for the cross flow velocity, equation (40), remains a good approximation in compressible flow;

$$\frac{1}{U_e}\frac{\partial w}{\partial z} = 2\left(1 - \frac{U}{U_e}\right)\frac{\partial \phi}{\partial z}.$$

The corrected versions of the momentum integral and entrainment equations can then be written

$$\frac{d}{dx}(r\theta) = \frac{rC_f}{2} - (H + 2 - M^2)\frac{r\theta}{U_e}\frac{dU_e}{dx} - r\theta\frac{\partial \phi}{\partial z} - 2r\theta(\bar{H} - 1)\frac{\partial \phi}{\partial z} \tag{87}$$

divergence crossflow

and

$$r\theta\frac{d\bar{H}}{dx} = \frac{d\bar{H}}{dH_1}\left[rC_E - H_1\left\{\frac{rC_f}{2} - (H+1)\frac{r\theta}{U_e}\frac{dU_e}{dx}\right\} + 2r\theta(H_1(\bar{H} - 1) - \bar{H})\frac{\partial \phi}{\partial z}\right], \tag{88}$$

crossflow

where the divergence terms in the entrainment equation have been cancelled on substitution of the momentum equation.

To determine a starting value of C_E, as an alternative to taking it as $(C_E)_{EQ}$, the procedure of Section 2.9 is followed. Given experimental values of $d\theta/dx$ and $d\bar{H}/dx$, equation (87) is solved to obtain $\partial\phi/\partial z$ and C_E is then determined from equation (88).

4. Performance of the Method

To assess the performance of the method, we have tested its predictions against a wide range of experiments, including those used as test cases at the Stanford Conference[3], and have also performed a number of calculations for hypothetical flows with analytic pressure distributions. The results presented in this section are typical but not of course exhaustive. Our aim is to illustrate the general accuracy of the method both in absolute terms and in comparison with other methods. Particular among these are the method of Head, which the present method was developed to replace, and the more successful methods at the Stanford Conference (including Bradshaw and Ferriss, our source), which the present method must at least match to justify its existence.

4.1. Abstract Test Cases

Fig. 5 shows the computed variation of the shape parameter G with R_θ in incompressible flow at constant pressure. The calculation was started with an initial value of G chosen by trial and error to give a slow initial variation of G, and an initial value of entrainment coefficient equal to its equilibrium value. Although G does not remain constant, the enlarged scale of Fig. 5 may give a false impression of its variation; in fact, the value of H corresponding to the G of Fig. 5 is everywhere within 0·2 per cent of that given by the correlation of Winter and Gaudet with $G = 6{\cdot}55$.

Fig. 6 shows another calculation for incompressible flow at constant pressure, but this time with initial conditions far from equilibrium. The horizontal scale and initial boundary layer thickness for this calculation match those in the experimental investigation by Bradshaw and Wong[34] of flow reattachment downstream of a two-dimensional step. The ordinate is the reciprocal of G. The calculation was started at the reattachment point ($C_f = 0$, $G = \infty$) at $x/h = 6$, with an initial value for C_E of 0·12 characteristic of the free shear layer before reattachment. This illustration is intended primarily not to show the method tested against experiment—no attempt was made to satisfy in any detail the boundary conditions of the Bradshaw and Wong experiment—but rather to demonstrate the predicted overshoot of the equilibrium condition when starting from such severely perturbed initial conditions. As a guide to the extent of this overshoot, equilibrium values of $1/G$ are shown for zero pressure gradient, $\Pi = 0$, and for the most severely accelerated flow studied by Mellor and Gibson, $\Pi = -0{\cdot}5$ (the latter giving a value of $1/G$ which is probably close to the maximum attainable). Although Bradshaw and Wong have argued that this particular type of flow is too severely perturbed for current boundary layer methods to be applicable, it is worth noting that the present method does show at least qualitatively the correct behaviour. In contrast, methods which implicitly or explicitly treat the turbulent stresses as a function only of the local velocity profile (Head's is shown as an example) will, for the flow of Fig. 6, predict a monotonic return to equilibrium $\Pi = 0$.

Fig. 7 shows the calculated variation of G with R_x in compressible adiabatic flow over a range of Mach numbers. At any particular R_x, the variation of G with M does not follow the form of equation (61) precisely. Again, however, the resulting discrepancies in H are of order 0·2 per cent or less. On the other hand, at $M = 5$, the value of $H\ (=\delta^*/\theta)$ corresponding to the G shown in Fig. 7 is roughly 5 per cent greater than that given by the assumption that G remains independent of M (made in the previous extension[1] of Head's method to compressible flow).

Fig. 8 shows calculations, for two arbitrary pressure distributions in incompressible flow, by the present method and by the methods of Head and of Bradshaw, Ferriss and Atwell. In flow A, which is derived from the flow over the upper surface of one of a family of high lift aerofoils proposed by Weeks[35], the boundary layer passes abruptly from an initial region of constant pressure to a region of sustained adverse pressure gradient. The form of the pressure distribution in this second region is such that the boundary layer tends ultimately to an equilibrium state with $H \sim 1{\cdot}6$. In flow B, the boundary layer is allowed to approach its equilibrium retarded state and then the pressure gradient is suddenly removed, allowing the boundary layer to relax back to a flat plate condition. The calculations by the methods of Head and of Bradshaw *et al.* were started at the point of application of the adverse pressure gradient, $x/L = 0{\cdot}17$, with the values of H and R_θ predicted at that point by the present method.

We see from the figure that very similar responses to the sudden changes in pressure gradient are predicted by the method of Bradshaw *et al.* and the present method, even though the final levels of H and C_f predicted by the two methods differ slightly. The similarity of response to sudden perturbations is particularly significant, since it is primarily when conditions change rapidly over a distance of a few boundary-layer thicknesses that we may expect an integral method (because of the limitations imposed by its use of simple shape-parameter and skin friction relationships) to suffer in comparison with a finite difference method. The agreement in Fig. 8, on the boundary-layer behaviour in conditions far from equilibrium, suggests that the salient features of the method of Bradshaw and Ferriss have been satisfactorily approximated in the present method.

Where the disagreement between the two methods is most pronounced, the boundary layer is close to a state of equilibrium; consequently, the discrepancies are primarily attributable to differences between the equilibrium and skin friction relations used or implied in the methods, rather than to a failure of the integral method to reproduce satisfactorily some particular characteristic of the finite difference method. The predictions of Head's method differ appreciably from those of the other two, particularly in the region of sustained adverse pressure gradient. Fig. 8 thus illustrates, on the one hand, an appreciable difference between the present and the earlier entrainment methods and, on the other, a perceptible difference between the two more highly developed methods arising out of the spread of the experimental results from which the empirical content of the methods has been drawn.

4.2. Comparisons with Experiment in Incompressible Flow

Figs. 9a to 9g show predictions by the present method and by Head's method of a representative sample of test cases from the Stanford Conference[3]. Also shown inset in each figure is the appropriate summary figure from the proceedings of the Conference showing, for that particular test case, the predictions of all the contending methods. The seven methods which were ranked in the first category by the Evaluation Committee are marked with an asterisk.

Although many of the experiments used as test cases were marred by appreciable departures from two-dimensionality—revealed by a substantial momentum imbalance in the data—most of the comparisons made at the Conference were limited to predictions for two-dimensional flow. As a result, the major part of the divergence between prediction and experiment could in many cases be attributed to three-dimensionality in the experiment.

Figs. 9a to 9c show predictions for three flows which had fairly satisfactory momentum balance and with which the better methods should therefore show reasonable agreement. In Fig. 9a, the equilibrium retarded flow studied by Bradshaw, the present method is seen to be in good agreement with the experiment, being substantially more accurate than Head's method and apparently slightly more accurate, for H and C_f judged together, than any of the methods at the Stanford Conference.

In Fig. 9b, the severely retarded non-equilibrium flow of Schubauer and Spangenberg, the difference between the present method and Head's is not so pronounced, although the present method is still marginally the more accurate. In this type of flow, in which the severity of the pressure gradient increases with x as occurs typically on the upper surface of a lifting aerofoil, Head's method is well known to be fairly accurate. Because this was not a mandatory test case at Stanford, only a few of the contenders attempted it; of those that did, the most successful achieve an accuracy very similar to the present method.

Fig. 9c shows the flow studied by Bradshaw and Ferriss in which the boundary layer passes from a region of sustained adverse pressure gradient to one of zero pressure gradient. Although this flow had a significant momentum imbalance in its early stages, the calculations shown assume two-dimensional flow. The present method is significantly more accurate than Head's method, although their differences are not great, and is again on a par with the best of the Stanford contenders.

In Fig. 9d we show prediction of the flow of Schubauer and Klebanoff made assuming the boundary layer to be two-dimensional. This flow is somewhat similar in character to that of Schubauer and Spangenberg shown in Fig. 9b, and is one of the test cases for which Head's method is known to be fairly accurate. As we see, Head's method appears in fact to be marginally more accurate than the present method, and both are in as good agreement with the experiment as are the seven methods of the top classification at Stanford.

However, as the boundary layer approaches separation in this experiment, the imbalance of the momentum equation becomes considerable and we can infer that there was appreciable convergence over the final few feet of the measured flow. Fig. 9e shows the effect of allowing for this flow convergence, as described in Section 2.9, by forcing the calculated distribution of momentum thickness to match the experiment. The result of making this allowance is roughly to halve the discrepancy between calculated and measured values of H and C_f in the later stages of the flow. A further expected effect in this experiment, to which Bradshaw[13] has drawn attention, is inhibition of the turbulence in the later stages of the flow due to convex longitudinal curvature of the wall. When allowance for longitudinal curvature, as proposed in Section 2.7, is combined with an allowance for flow convergence, the agreement with experiment is seen to be very satisfactory right up to the predicted point of separation.

Fig. 9f shows predictions for the boundary layer measured by Tillman downstream of reattachment aft of a ledge. The calculations are by: Head's method for two-dimensional flow; the present method for two-dimensional flow, with initial C_E equal to its equilibrium value; and the present method with a correction for flow divergence and with initial C_E chosen to give agreement with the initial dH/dx as described in Section 2.9.

Two sets of experimental values of C_f are shown. The higher set are the values against which methods were tested by the evaluation committee at Stanford; the second set, also given in the Conference proceedings, come from Cole's reappraisal of the data and are thought to be the more accurate. With initial C_E and flow divergence matched to the experimental data, the present method is in excellent agreement with the experiment. Without these corrections, its predictions are comparable with those of the better methods at Stanford, and lie rather closer to the data than do those of Head's method.

The final test case from Stanford, shown in Fig. 9g, is the nominally axisymmetric boundary layer studied by Moses. The boundary layer is brought close to separation by a severe adverse pressure gradient which then abruptly falls to zero allowing the boundary layer to relax back to its flat plate condition. The same three types of calculation as in the previous figure are shown. The R.A.E. version of Head's method predicts separation at the end of the region of adverse pressure gradient—more precisely, the method breaks down when H reaches 2·85 and dH/dH_1 becomes infinite—whereas the original version of Head's method (*HE* in inset) predicts a maximum value of roughly 2·8 for H, after which the boundary layer recovers. The recovery is, however, not very accurately predicted. The two-dimensional calculation by the present method is in fairly close agreement with the experimental values of H and C_f, giving results very similar to the best of the Stanford methods (the predictions of which were also for two-dimensional flow). When the prediction by the present method is corrected for the flow convergence indicated by the imbalance of the momentum equation, and an independent estimate of initial C_E is made, the agreement with experiment is less satisfactory. However, since the thickness of the boundary layer in this experiment was not strictly small compared with the radius of the cylinder along which it developed (boundary-layer thicknesses were evaluated by integration with respect to $(r+y)^2/r$ rather than to y), we do not know what accuracy to require, for this test case, of a prediction method developed for thin boundary layers.

As a final test of the method in incompressible flow, Fig. 10 shows it applied to a symmetrical two-dimensional wake subject to a sudden deceleration, one of the nonequilibrium flows studied by Prabhu and Narasimha[36]. To give some indication of the influence of entrainment in a flow of this type, with its characteristically low values of H, we also show the calculated behaviour of an inviscid rotational flow with the same initial velocity profile. Agreement with experiment is fairly satisfactory and it is clear that the method represents entrainment accurately over the major part of the flow, the errors becoming significant only in the region of severe deceleration. At its greatest, the discrepancy between prediction and experiment amounts to an error of 1 per cent in displacement thickness.

4.3. Comparisons with Experiment in Compressible Flow

Fig. 11 shows predictions of boundary layer development in the experiments by Cook on a lifting aerofoil at high subsonic speeds. The calculations are by the R.A.E. version of Head's method and the present method both for two-dimensional flow, and by the present method with a correction for momentum imbalance. The distributions of $\bar{H}$ and C_f on the upper and lower surfaces of the aerofoil are seen to be quite well predicted by all three methods. A point worth noting is that, on the upper surface of the aerofoil where the severity of the adverse pressure gradient steadily increases, predictions of $\bar{H}$ by the original entrainment method are in fairly good agreement with both the present method and the experimental data. Over the rearward part of the lower surface, however, where the adverse pressure gradient diminishes and eventually changes sign, the original method appreciably overestimates $\bar{H}$ whilst the present one predicts it fairly accurately. Thus the pattern we have noted previously for incompressible flow is repeated.

Although we may also note that agreement between the present method and the measurements is improved by allowing for lack of two-dimensionality in the experiment, not too much weight should be given to the absolute levels of agreement. On the one hand, the measured values of integral parameters were subject to appreciable corrections for interference from the traverse gear, and the values of skin friction shown in Figs. 11d and 11e, measured by surface razor blades, were significantly lower than values deduced from Preston tube readings and Clauser plots; on the other hand, certain secondary effects which might be significant—longitudinal curvature and perhaps dilatation—have not been included in the calculations.

In Fig. 11f, a prediction of wake development is compared with Cook's measurements. The asymmetry of the wake of a lifting aerofoil no doubt complicates the flow structure appreciably. Nevertheless, the assumption (discussed in Ref. 1) that the two halves of the wake can be predicted separately, and their integral parameters added to give integrals across the whole wake, has already been shown[1,37] to give results adequate for engineering purposes. Fig. 11f confirms that this remains true for the present method.

Measurements by Winter, Rotta and Smith[38] of the boundary layer on a waisted body of revolution in subsonic and supersonic flow are shown in Fig. 12. In this experiment, all the secondary influences on

turbulence structure treated in this Report—longitudinal curvature, lateral strain, dilatation—are thought to have had a significant effect on the flow. In the figures we compare: first, the R.A.E. version of Head's method, the basic lag method with no allowance for secondary influences, and the lag method with all three of the above named influences allowed for as outlined in Section 3.3 and with C_E chosen to match the initial value of dH/dx (Figs. 9b and 9d); second, the basic lag method, and versions of the lag method with an allowance for each secondary influence on its own (Figs. 9c and 9e). Because the momentum balance in the experiment is reasonably good, all calculations are for axisymmetric flow.

Figs. 12c and 12e show the predicted influence of the secondary effects to be appreciable, particularly on C_f. At $M = 0{\cdot}6$, the effect of lateral strain is considerable, that of longitudinal curvature is significant though not large, and that of dilatation small. At $M = 2{\cdot}0$, all three influences are considerable, though longitudinal curvature has less effect than the other two. The body geometry is such that at a high rate of lateral strain is sustained for a considerable fraction of the length shown in Figs. 12b to 12e, whereas the longitudinal curvature is high only for a relatively short distance near the waist. The occurrence of the factor $(1 + M^2/5)$ in the allowance for longitudinal curvature is of course responsible for the greater predicted influence of this effect at $M = 2$.

In Figs. 12b and 12d, the basic version of the lag method is shown to be on balance perhaps less successful than the R.A.E. version of Head's method. With all secondary influences allowed for, however, the lag method is the most accurate of the three, particularly if compared with values of C_f deduced from the Clauser plots by Winter *et al.* of their velocity profiles, rather than from their surface-razor-blade readings. Over the rear flare of the body at $M = 2$, this version of the method predicts velocity profiles appreciably fuller and skin friction higher than for zero pressure gradient at the same R_θ, in agreement with the experimental results. The simpler methods in Fig. 12d predict the boundary layer at the base of the body still to be recovering towards the flat-plate condition after its passage through the adverse pressure gradients between $x/h = 0{\cdot}4$ and $0{\cdot}75$ (Fig. 12a).

Although we may take some encouragement from the results of the fully corrected calculations in Figs. 12b and 12d, it is in our view unrealistic to look for really close agreement between current prediction methods and this particular experiment. Leaving aside questions of interpreting the measurements—skin friction deduced by surface razor blade did not agree with that derived from Clauser plots, and the Clauser plots themselves were sometimes anomalous in form—it seems likely that the secondary influences in this experiment were too powerful to lie within the scope of the rudimentary first-order allowances which are possible with our present, very limited understanding of these influences. For example, the term $\beta(1 + M^2/5)Ri$ which occurs in the allowance for longitudinal curvature attains a value of around unity at the waist of the body at $M = 2$, whereas the allowance was initially assumed valid only if this term was of order less than unity. The corresponding lateral strain and (at $M = 2$) dilatation terms are also of similar order to unity. Finally, although the experimental results give no indication of such an effect, it would not be surprising to find that over the concave part of the surface a system of longitudinal vortices developed, similar to those noted by other workers in both low speed[39] and hypersonic[40] flow.

Fig. 13 shows predictions of boundary layer recovery[31] downstream of a small region of separation induced by an incident-reflected shock of 8 degrees deflection; the Mach number downstream of the shock system was approximately 2. The calculation by the present method with C_E initially taken at its equilibrium value is appreciably more accurate than that by the previous R.A.E. entrainment method, and choosing an initial C_E to match the initial $d\bar{H}/dx$ improves agreement further still. Although this agreement with experiment is very satisfactory, the rather violent history of the boundary layer in the immediately upstream region must nevertheless cast some doubt on the value of making close comparisons with data of this kind.

Finally, in Fig. 14, we show some predictions of the supersonic flow studied by Lewis, Gran and Kubota[41] in which the boundary layer along the inside wall of a cylinder was severely decelerated and then reaccelerated by a system of waves generated by a spiked centrebody. The three calculations shown are by the original entrainment method, the present method in its simplest form, and the present method with an allowance for dilatation as outlined in Section 3.3. Although Lewis *et al.* do not present experimental values of H or $\bar{H}$, the values of $\bar{H}$ calculated by the three methods are shown in Fig. 14 for comparative purposes.

These particular experimental results, and some earlier ones[42,43] obtained in qualitatively similar flows, were cited by Bradshaw[16] as the chief evidence that dilatation has an important effect on the turbulence structure. They were also used by him to determine the empirical constant in his formula correcting for this effect. Calculations by the present method, with and without a correction for dilatation, agree fairly closely with corresponding calculations by Bradshaw, and the calculation allowing for dilatation is in reasonable agreement with experiment. This last result is hardly surprising, in view of the use of these data in the derivation of the correction term in the prediction method, and we should, on the basis of Bradshaw's results,

expect similarly good agreement with the other experiments of this kind[42,43] (though no predictions of these by the present method with an allowance for dilatation have been made).

It must be observed, however, that the allowance for dilatation in the calculation shown in Fig. 14 becomes a dominant effect rather than a mere first-order correction. The result of making the allowance is roughly to double the predicted values of C_E in the region of strong deceleration and, conversely, to reduce C_E to virtually zero over the second half of the region of reacceleration. Until we have a more detailed understanding of the turbulence structure in flows such as these, therefore, it would seem premature to interpret the results shown in Fig. 14 as indicating that our flow model is generally adequate in strongly perturbed compressible flows.

5. Conclusions

The prediction method described in this Report, applicable to turbulent boundary layers and wakes in two-dimensional and axisymmetric, adiabatic, compressible flow, is, in our view, a worthwhile improvement on the original entrainment method of Head and its variants. Whilst retaining the potential of the original method for extension to a range of more complicated flows, the new method, at the cost of only a fractional increase in computing time, gives significantly greater all-round accuracy than its predecessor. Tested against the data compiled for the Stanford Conference on Computation of Turbulent Boundary Layers, it has shown a general accuracy fully comparable with that of the methods most highly rated by the Evaluation Committee of the Conference.

The chief distinguishing characteristic of the method is the 'lag' equation for entrainment coefficient, developed, with as little additional empiricism as possible, from the differential equation for shear stress derived by Bradshaw, Ferriss and Atwell from the turbulent kinetic energy equation. These origins of the present lag equation are grounds for expecting it to represent the turbulence behaviour more realistically than earlier and more empirical lag equations; they may also account for the success of the method when tested (without any empirical 'tuning') against the data of the Stanford Conference; they certainly make it possible to introduce first-order corrections for secondary influences on the turbulence structure, such as longitudinal surface curvature, in a logical and straightforward manner.

The dominant influence on the predictions of the method is, however, the equilibrium locus rather than the lag equation. Although the empirical locus employed in the present method lies very close to those used in other methods, the scatter of the experimental data for equilibrium flows is such that some element of uncertainty must remain as to the absolute accuracy of the method in flows with strong, sustained pressure gradients. In compressible flow, the concept of equilibrium flows is not as useful as at low speeds, there are few if any experiments (except in zero pressure gradient) which we can be satisfied are free from significant secondary influences on the turbulence structure, and uncertainty as to the absolute accuracy of the method in compressible flows with strong pressure gradients is therefore somewhat greater than at low speeds. These uncertainties must of course afflict all prediction methods to a similar degree, and will only be diminished as and when more extensive, more detailed and better understood experimental data become available.

In the meantime, the present method provides accurate predictions over a range of flow conditions perhaps as wide as we may realistically hope to cover, with understanding of turbulence as it stands at present. Given this accuracy, the main virtue of the method is its speed, and the potential this provides for applying the method, or developments of it, to those problems (for example, fully three-dimensional boundary-layer calculations nested within an iterative calculation of the overall flow field) for which finite-difference methods may well prove too costly to use on a routine basis.

LIST OF SYMBOLS

a_1	Ratio of turbulent shear stress to kinetic energy (equation (4))
A	Parameter in equilibrium locus (equation (58))
C	Function of C_E and C_{f_0} (equation (A-31))
C_D	Shear work integral (equation (60))
C_E	Entrainment coefficient (equation (A-7))
C_f	Skin-friction coefficient (equation (A-6))
C_{f_0}	Skin-friction coefficient in equilibrium flow in zero pressure gradient
C_τ	Shear stress coefficient (equation (54))
F	Function of C_E and C_{f_0} (equation (A-21))
F_1, F_2	Functions of $\bar{H}$ (equation (69))
F_c, F_R	Scaling functions in skin-friction law (equations (49) and (50))
G	Clauser shape parameter $= (\bar{H}-1)/\bar{H}\sqrt{C_f/2}$
G	Diffusion function in turbulent kinetic energy equation (equations (4), (5), (53))
H	(Equation (A-3)) — velocity-profile shape parameters
H_k	(Equation (56)) — velocity-profile shape parameters
H_ε	(Equation (60)) — velocity-profile shape parameters
H_1	(Equation (A-5)) — velocity-profile shape parameters
$\bar{H}$	(Equation (A-4)) — velocity-profile shape parameters
$\bar{H}_0$, H_0	Values of $\bar{H}$ and H in equilibrium flows at constant pressure
K	Empirical constant (equation (29))
L	Dissipation length scale (equation (4))
l	Mixing length $= \sqrt{\tau/\rho}/(\partial u/\partial y)$
M	Mach number at the edge of the boundary layer
p	Pressure
$\overline{q^2}$	Mean fluctuating velocity
R	Radius of longitudinal curvature
Ri	'Richardson number' (equations (26), (A-22))
R_θ	Reynolds number based on momentum thickness (equation (A-11))
R_x	Reynolds number based on x
r	Transverse radius of axisymmetric body
r	Temperature recovery factor (equations (52), (53), (A-17))
T	Temperature
u	Fluctuating component of streamwise velocity
U	Mean component of streamwise velocity
v	Fluctuating component of velocity normal to surface

LIST OF SYMBOLS (continued)

V	Mean component of velocity normal to surface
w	Mean velocity component parallel to surface and *normal to external streamline*
x	Coordinate along surface
y	Coordinate normal to surface
z	Coordinate parallel to surface and perpendicular to external streamlines
β	Empirical constant (equations (25), (A-23))
δ	Boundary-layer thickness (Section 2.4)
δ^*	Displacement thickness (equation (A-1))
ε	Dissipation of turbulent energy (equation (3))
ζ	Diffusion function (equation (6))
ζ'	$= d(\zeta)/d(y/\delta)$
θ	Momentum thickness (equation (A-2))
λ	Scaling factor on dissipation length (equations (31), (A-27))
μ	Absolute viscosity
ν_T	Kinematic eddy viscosity
Π	Pressure gradient parameter for equilibrium flows (equations (10) and (57))
ρ	Density
τ	Shear stress
ϕ	External streamline deviation *relative to nominal flow direction*

Subscripts

e	Denotes conditions at edge of boundary layer
EQ	Denotes equilibrium conditions
EQ_0	Denotes equilibrium conditions in absence of secondary influences on turbulence structure
i	Denotes values in incompressible flow
$m, \max$	Denotes conditions at the maximum in (τ/ρ)
O	Sometimes denotes freedom from secondary influences on turbulence structure, sometimes denotes stagnation conditions: which is always obvious from the context
TE	Denotes the trailing edge
w	Denotes conditions at the wall
$2D$	Denotes conditions in two-dimensional flow

REFERENCES

No.	*Author(s)*	*Title, etc.*
1	J. E. Green	Application of Head's entrainment method to the prediction of turbulent boundary layers and wakes in compressible flow. A.R.C. R. & M. 3788, 1972.
2	M. R. Head	Entrainment in the turbulent boundary layer. A.R.C. R. & M. 3152, 1958.
3	S. J. Kline *et al.*	Computation of turbulent boundary layers. AFOSR-IFP-Stanford Conference Proceedings, 1968.
4	P. D. Smith	An integral prediction method for three-dimensional compressible turbulent boundary layers. A.R.C. R. & M. 3739, 1972.
5	M. C. P. Firmin	Calculations of the pressure distribution, lift and drag on single aerofoils at sub-critical speeds, including an allowance for the effects of boundary layer and wake. R.A.E. Technical Report 72235, 1972.
6	M. R. Head and V. C. Patel	An improved entrainment method for calculating turbulent boundary-layer development. A.R.C. R. & M. 3643, 1969.
7	H. P. Horton	Entrainment in equilibrium and non-equilibrium turbulent boundary layers. H.S.A. (Hatfield)/Research/1094/HPH, 1969.
8	P. Bradshaw, D. H. Ferriss and N. P. Atwell	Calculation of turbulent boundary layer development using the turbulent energy equation. *J. Fluid Mech.*, Vol. 28, pp. 593–616, 1967.
9	J. C. Rotta	Turbulent boundary layers in incompressible flow. *Prog. Aeronaut. Sci.*, Vol. 2, pp. 1–219, Pergamon Press, 1962.
10	H. McDonald	The departure from equilibrium of turbulent boundary layers. *Aero. Quart.*, Vol. 19, Part 1, pp. 1–19, 1968.
11	G. L. Mellor and D. M. Gibson	Equilibrium turbulent boundary layers. *J. Fluid Mech.*, Vol. 24, Part 2, pp. 225–254, 1966.
12	J. F. Nash and A. G. J. McDonald ...	The calculation of momentum thickness in turbulent boundary layers at Mach numbers up to unity. A.R.C. C.P. No. 963, 1966.
13	P. Bradshaw	The analogy between streamline curvature and buoyancy in turbulent shear flow. *J. Fluid Mech.*, Vol. 36, pp. 177–191, 1969.

REFERENCES

No.	*Author(s)*	*Title, etc.*
14	P. Bradshaw and D. H. Ferriss	Calculation of boundary layer development using the turbulent energy equation; compressible flow on adiabatic walls. *J. Fluid Mech.*, Vol. 46, pp. 83–110, 1971.
15	M. V. Morkovin	Effects of compressibility on turbulent flows (1964). *The mechanics of turbulence,* Gordon and Breach (French edition published by Editions du CNRS, 1962).
16	P. Bradshaw	Anomalous effects of pressure gradient on supersonic turbulent boundary layers. Imperial College Aero Report 72-21, 1972.
17	K. G. Winter and L. Gaudet	Turbulent boundary-layer studies at high Reynolds numbers at Mach Numbers between 0·2 and 2·8. A.R.C. R. & M. 3712, 1970.
18	D. E. Coles	The law of the wake in the turbulent boundary layer. *J. Fluid Mech.*, Vol. 1, pp. 191–226, 1956.
19	B. G. J. Thompson	A new two-parameter family of mean velocity profiles for incompressible turbulent boundary layers on smooth walls. A.R.C. R. & M. 3463, 1967.
20	L. F. East and R. P. Hoxey	Low-speed three-dimensional turbulent boundary layer data. A.R.C. R. & M. 3653, 1969.
21	J. Seddon	The flow produced by interaction of a turbulent boundary layer with a normal shock wave of strength sufficient to cause separation. A.R.C. R. & M. 3502, 1960.
22	L. F. East	Private communication.
23	D. B. Spalding and S. W. Chi	The drag of a compressible turbulent boundary layer on a smooth flat plate with and without heat transfer. *J. Fluid Mech.*, Vol. 18, Part 1, pp. 117–143, 1964.
24	D. E. Coles	The turbulent boundary layer in a compressible fluid. Project Rand Report R-403-PR, 1962.
25	P. Bradshaw	Variations on a theme of Prandtl. A.G.A.R.D.-CP-93, 1972.
26	A. A. Townsend	The structure of turbulent shear flows. Cambridge University Press, 1956.
27	R. Narasimha and A. Prabhu	Equilibrium and relaxation in turbulent wakes. *J. Fluid Mech.*, Vol. 54, Part 1, pp. 1–18, 1972.

REFERENCES

No.	*Author(s)*	*Title, etc.*
28	J. P. Johnston	On the three-dimensional turbulent boundary layer generated by secondary flow. *J. bas. Engng.*, Trans. A.S.M.E. Series D, Vol. 82, 1960.
29	J. C. Cooke and M. G. Hall	Boundary layers in three dimensions. *Prog. Aeronaut. Sci.*, Vol. 2, pp. 221–282, 1962.
30	G. Maise and H. McDonald	Mixing length and kinematic eddy viscosity in a compressible boundary layer. AIAA Vol. 6, pp. 73–80, 1968.
31	J. E. Green	The prediction of turbulent boundary layer development in compressible flow. *J. Fluid Mech.*, Vol. 31, Part 4, pp. 753–778, 1968.
32	R. C. Hastings and W. G. Sawyer ...	Turbulent boundary layers on a large flat plate at $M = 4$. A.R.C. R. & M. 3678, 1970.
33	D. C. Wilcox and I. E. Alber	A turbulence model for high speed flows. Proc. 1972 Heat Transfer and Fluid Mechanics Institute, 1972.
34	P. Bradshaw and F. Y. F. Wong	The relaxation of a turbulent shear layer after reattachment. *J. Fluid Mech.*, Vol. 52, Part 1, pp. 113–135, 1972.
35	D. J. Weeks	Some applications of boundary layer theory in the design of aerofoil sections for high lift. Unpublished M.O.D. (P.E.) work.
36	A. Prabhu and R. Narashimha	Turbulent non-equilibrium wakes. *J. Fluid Mech.*, Vol. 54, Part 1, pp. 19–38, 1972.
37	T. A. Cook	Measurements of the boundary layer and wake of two aerofoil sections at high Reynolds numbers and high subsonic Mach numbers. A.R.C. R. & M. 3722, 1971.
38	K. G. Winter, J. C. Rotta and K. G. Smith	Studies of the turbulent boundary layer on a waisted body of revolution in subsonic and supersonic flow. A.R.C. R. & M. 3633, 1968.
39	R. M. C. So and G. L. Mellor	An experimental investigation of turbulent boundary layers along curved surfaces. NASA CR-1940, 1972.
40	V. Zakkay and W. Calarese	An experimental investigation of vortex generation in a turbulent boundary layer undergoing adverse pressure gradient. NASA CR-2037, 1972.

REFERENCES

No.	*Author(s)*	*Title, etc.*
41	J. E. Lewis, R. L. Gran and T. Kubota	An experiment on the adiabatic compressible turbulent boundary layer in adverse and favourable pressure gradients. *J. Fluid Mech.,* Vol. 51, Part 4, pp. 657–672, 1972.
42	D. J. Peake, G. Brakmann and J. M. Romeskie	Comparisons between some high Reynolds number turbulent boundary layer experiments and various recent calculation procedures at Mach 4. AGARD-CP-93, 1972.
43	F. J. Zwarts	Ph.D. Thesis. McGill University, 1970.

APPENDIX A

Summary of the Method

A.1. Definition of Main Parameters

In compressible flow, the parameters which occur in the present method are defined as: boundary-layer thickness $\delta = y$ at $U/U_e \sim 0{\cdot}995$, but with the precise value depending on Mach number and Reynolds number (see Section 2.4).

Displacement thickness
$$\delta^* = \int_0^\infty \left(1 - \frac{\rho U}{\rho_e U_e}\right) dy \tag{A-1}$$

momentum thickness
$$\theta = \int_0^\infty \frac{\rho U}{\rho_e U_e}\left(1 - \frac{U}{U_e}\right) dy \tag{A-2}$$

shape parameters
$$H = \delta^*/\theta \tag{A-3}$$

$$\bar{H} = \frac{1}{\theta}\int_0^\infty \frac{\rho}{\rho_e}\left(1 - \frac{U}{U_e}\right) dy \tag{A-4}$$

$$\left.\begin{aligned} H_1 &= \frac{1}{\theta}\int_0^\delta \frac{\rho U}{\rho_e U_e}\, dy \\ &= \frac{\delta - \delta^*}{\theta} \end{aligned}\right\} \tag{A-5}$$

skin-friction coefficient
$$C_f = \frac{\tau_w}{\frac{1}{2}\rho_e U_e^2} \tag{A-6}$$

entrainment coefficient
$$\left.\begin{aligned} C_E &= \frac{1}{r\rho_e U_e}\frac{d}{dx}\left(r\int_0^\delta \rho U\, dy\right) \\ &= \frac{1}{r\rho_e U_e}\frac{d}{dx}(r\rho_e U_e H_1 \theta). \end{aligned}\right\} \tag{A-7}$$

A.2. Compressible Flow over Solid Surfaces

Boundary-layer development, specified by the three independent parameters θ, $\bar{H}$ and C_E, is predicted by the numerical integration of the three simultaneous ordinary differential equations:

$$\frac{d}{dx}(r\theta) = \frac{rC_f}{2} - (H + 2 - M^2)\frac{r\theta}{U_e}\frac{dU_e}{dx}. \tag{A-8}$$

$$\frac{\theta\, d\bar{H}}{dx} = \frac{d\bar{H}}{dH_1}\left[C_E - H_1\left\{\frac{C_f}{2} - (H+1)\frac{\theta}{U_e}\frac{dU_e}{dx}\right\}\right], \tag{A-9}$$

$$\frac{\theta\, dC_E}{dx} = F\left[\frac{2{\cdot}8}{H + H_1}\left\{(C_\tau)^{\frac{1}{2}}_{EQ_0} - \lambda C_\tau^{\frac{1}{2}}\right\} + \left(\frac{\theta}{U_e}\frac{dU_e}{dx}\right)_{EQ} - \frac{\theta}{U_e}\frac{dU_e}{dx}\left\{1 + 0{\cdot}075M^2\frac{(1+0{\cdot}2M^2)}{(1+0{\cdot}1M^2)}\right\}\right]. \tag{A-10}$$

In these equations, r is the body radius in axisymmetric flow, set to unity for two-dimensional flow. The various dependent variables and functions in the equations are evaluated from the following relationships:

For C_f: from the known surface-pressure distribution the local free-stream properties M, U_e, ρ_e are evaluated from gas-dynamic relations and the absolute viscosity μ_e from an appropriate relation such as Sutherland's.

Then we write:

$$R_\theta = \frac{\rho_e U_e \theta}{\mu_e}, \tag{A-11}$$

$$F_c = (1 + 0{\cdot}2M^2)^{\frac{1}{2}}, \tag{A-12}$$

$$F_R = 1 + 0{\cdot}056M^2, \tag{A-13}$$

$$F_c C_{f_0} = \frac{0{\cdot}01013}{\log_{10}(F_R R_\theta) - 1{\cdot}02} - 0{\cdot}00075, \tag{A-14}$$

$$1 - \frac{1}{\bar{H}_0} = 6{\cdot}55\left\{\frac{C_{f_0}}{2}(1 + 0{\cdot}04M^2)\right\}^{\frac{1}{2}}, \tag{A-15}$$

$$C_f = C_{f_0}\left\{0{\cdot}9\left(\frac{\bar{H}}{\bar{H}_0} - 0{\cdot}4\right)^{-1} - 0{\cdot}5\right\}. \tag{A-16}$$

For H:

$$H = (\bar{H} + 1)\left(1 + \frac{rM^2}{5}\right) - 1, \tag{A-17}$$

where, in this particular equation, r is the temperature recovery factor in adiabatic flow. A value of unity is recommended for r when calculating integral quantities involving density (*see* Ref. 17 for example).

For H_1 and $d\bar{H}/dH_1$:

$$H_1 = 3{\cdot}15 + \frac{1{\cdot}72}{\bar{H} - 1} - 0{\cdot}01(\bar{H} - 1)^2; \tag{A-18}$$

$$\frac{d\bar{H}}{dH_1} = -\frac{(\bar{H} - 1)^2}{1{\cdot}72 + 0{\cdot}02(\bar{H} - 1)^3}. \tag{A-19}$$

For C_τ and F:

$$C_\tau = (0{\cdot}024C_E + 1{\cdot}2C_E^2 + 0{\cdot}32C_{f_0})(1 + 0{\cdot}1M^2); \tag{A-20}$$

$$F = \frac{(0{\cdot}02C_E + C_E^2 + 0{\cdot}8C_{f_0}/3)}{(0{\cdot}01 + C_E)}. \tag{A-21}$$

For secondary influences:

If R is radius of longitudinal curvature, positive on a convex wall, we write

$$Ri = \frac{2}{3}\frac{\theta}{R}(H + H_1)\left(\frac{H_1}{\bar{H}} + 0{\cdot}3\right), \tag{A-22}$$

$$\beta = 7 \quad \text{for} \quad Ri > 0, \qquad 4{\cdot}5 \quad \text{for} \quad Ri < 0, \tag{A-23}$$

and

$$\lambda_1 = 1 + \beta\left(1 + \frac{M^2}{5}\right)Ri. \tag{A-24}$$

Also,

$$\lambda_2 = 1 - \frac{7}{3}\left(\frac{H_1}{\bar{H}} + 0{\cdot}3\right)(H + H_1)\frac{\theta}{r}\frac{dr}{dx}, \tag{A-25}$$

$$\lambda_3 = 1 + \frac{7}{3}M^2(H + H_1)\left(\frac{H_1}{\bar{H}} + 1\right)\frac{\theta}{U_e}\frac{dU_e}{dx}, \tag{A-26}$$

and any other extraneous influences (free-stream turbulence, perhaps?) which can be represented by further terms in the form $\lambda_r = 1 + \ldots$. Finally, we have

$$\lambda = \lambda_1\lambda_2\lambda_3 \ldots \text{etc.} \tag{A-27}$$

It should be borne in mind that these correction formulae are of a provisional nature, and are best programmed as an optional subroutine. As they are believed to be justified only when secondary influences are small to moderate, we have arbitrarily imposed the limit

$$0{\cdot}4 \leqslant \lambda \leqslant 2{\cdot}5$$

in the computer program, with any value of λ outside either of these limits reset equal to the limit.

For equilibrium quantities:

$$\left(\frac{\theta}{U_e}\frac{dU_e}{dx}\right)_{EQ_0} = \frac{1{\cdot}25}{H}\left\{\frac{C_f}{2} - \left(\frac{\bar{H} - 1}{6{\cdot}432\bar{H}}\right)^2(1 + 0{\cdot}04M^2)^{-1}\right\}, \tag{A-28}$$

$$(C_E)_{EQ_0} = H_1\left\{\frac{C_f}{2} - (H+1)\left(\frac{\theta}{U_e}\frac{dU_e}{dx}\right)_{EQ_0}\right\}, \tag{A-29}$$

and

$$(C_\tau)_{EQ_0} = (0{\cdot}024(C_E)_{EQ_0} + 1{\cdot}2(C_E)^2_{EQ_0} + 0{\cdot}32C_{f_0})(1 + 0{\cdot}1M^2). \tag{A-30}$$

Also, from equation (36) of the main text, writing

$$\left.\begin{aligned} C &= (0{\cdot}024(C_E)_{EQ_0} + 1{\cdot}2(C_E)^2_{EQ_0} + 0{\cdot}32C_{f_0})\lambda^{-2} - 0{\cdot}32C_{f_0} \\ &= (C_\tau)_{EQ_0}(1 + 0{\cdot}1M^2)^{-1}\lambda^{-2} - 0{\cdot}32C_{f_0}, \end{aligned}\right\} \tag{A-31}$$

we have

$$(C_E)_{EQ} = (C/1{\cdot}2 + 0{\cdot}0001)^{\frac{1}{2}} - 0{\cdot}01, \tag{A-32}$$

whence

$$\left(\frac{\theta}{U_e}\frac{dU_e}{dx}\right)_{EQ} = \left(\frac{C_f}{2} - (C_E)_{EQ}/H_1\right)/(H+1). \tag{A-33}$$

Equations (A-11) to (A-33), arranged in a subroutine in the computer program in the order presented here, provide the dependent variables needed to evaluate equations (A-8), (A-9) and (A-10) at each stage of the numerical integration.

A.3. Wake Flows

To continue a boundary layer calculation past a trailing edge, so that one side of the wake is calculated at a time, for $x > x_{TE}$:

(1) by-pass equations (A-11) to (A-16) and set

$$C_f = C_{f_0} = 0; \tag{A-34}$$

(2) replace equation (A-27) by

$$\lambda = \tfrac{1}{2}\lambda_1\lambda_2\lambda_3 \ldots \text{etc.} \tag{A-35}$$

A.4. Boundary Conditions

To specify the problem, free-stream stagnation properties p_O and T_O and streamwise distributions of $M(x)$ and $r(x)$, or some equivalent information must be given. Sometimes longitudinal curvature of the surface $R(x)$ will also be required. Ideally, initial values of θ, $\bar{H}$ and C_E should also be given, but these will usually be known only when making comparisons with experiment. The minimum practicable information is an initial value of θ; frequently calculations are started at an assumed transition point, and the initial θ is estimated by applying a simple, approximate method to the laminar boundary-layer development from its origin to the transition point. Initial $\bar{H}$ may then be estimated either from equation (A-15), i.e. assuming a flat-plate velocity profile at the starting point, or else by assuming the flow is locally in equilibrium and using equations (A-28) to (A-33) to evaluate $\bar{H}$ given $(\theta/U_e)(dU_e/dx)$. In this case, it is simplest to assume $\lambda = 1$ and determine $\bar{H}$ from equation (A-28), but even to do this a process of iteration is required. With θ and $\bar{H}$ known, the initial value of C_E may be taken as its equilibrium value. In this case, whether or not we assume $\lambda = 1$, C_E may be determined directly as $(C_E)_{EQ}$ from equation (A-32) (if $\lambda = 1$, equation (A-29) will do) and the preceding equations.

A.5. Comparisons with Experiment

For comparisons against experimental data which do not fully satisfy the two-dimensional or axisymmetric momentum integral equation, and for which the model of flow three-dimensionality of Section 2.9 is thought justified, the streamwise distribution of momentum thickness $\theta(x)$ measured in the experiment is specified as part of the input data. Differentiating this data numerically to obtain $(d(r\theta)/dx)_{\text{EXP}}$, and using equations (A-11) to (A-33) as before to determine the other dependent variables, we then write

$$r\theta(2\bar{H}-1)\frac{\partial\phi}{\partial Z} = r\frac{C_f}{2} - (H+2-M^2)r\frac{\theta}{U_e}\frac{dU_e}{dx} - \left(\frac{d}{dx}(r\theta)\right)_{\text{EXP}}, \tag{A-36}$$

from which $\theta(\partial\phi/\partial Z)$ is determined. The three equations then to be integrated (assuming the method is to be programmed with a common format and common use of library routines for both this and the straightforward type of calculation) are:

$$\frac{d}{dx}(r\theta) = \left(\frac{d}{dx}(r\theta)\right)_{\text{EXP}} \tag{A-37}$$

$$\theta\frac{d\bar{H}}{dx} = \frac{d\bar{H}}{dH_1}\left\{C_E - H_1\left(\frac{C_f}{2} - (H+1)\frac{\theta}{U_e}\frac{dU_e}{dx}\right) + 2(H_1(\bar{H}-1) - \bar{H})\theta\frac{\partial\phi}{\partial Z}\right\} \tag{A-38}$$

and equation (A-10) unchanged.

Knowing initial values of θ and $\bar{H}$ in the experiment, the starting value of C_E may be determined either by assuming equilibrium conditions initially, and using equations (A-29) or (A-32), or by specifying the experimental value of $d\bar{H}/dx$ at the starting point as part of the input data. In the latter case, C_E may be determined by inverting equation (A-38), evaluating the other terms in the equation from equations (A-11) to (A-33) and (A-36).

A.6. Incompressible Flow and Other Simplifications

The equations of the method do not involve division by M at any point, so there is not lower limit to the value of M for which the method in its above form will work. However, if the method is to be used exclusively for incompressible flows, the computer program may be somewhat simplified by striking out all terms in M in the equations of this Appendix and by-passing some of the equations altogether. For example, H and $\bar{H}$ become identical, and equations (A-12), (A-13), (A-17), (A-26) become redundant.

Similarly, if extraneous effects are to be ignored and the method is not to be used for wake calculations, λ may be equal to 1 and equations (A-22) to (A-27) and (A-31) to (A-33) become redundant.

Finally, two points are worth making. First, the method is fast enough for simplifications in order to save computing time to be hardly worth making. Second, the method is so straightforward that, given a Runge–Kutta library routine for integrating the differential equations, with a control on step-length to ensure numerical accuracy, a major part of the programming effort is spent on handling the input and output data and, for example, determining the streamwise distributions of M, ρ_e, U_e, μ_e and dU_e/dx from the given pressure distributions. As a result, the main bonus of simplification comes from savings on the input/output programming, which is effectively common to all boundary layer methods, rather than from simplifying the internals of the computation.

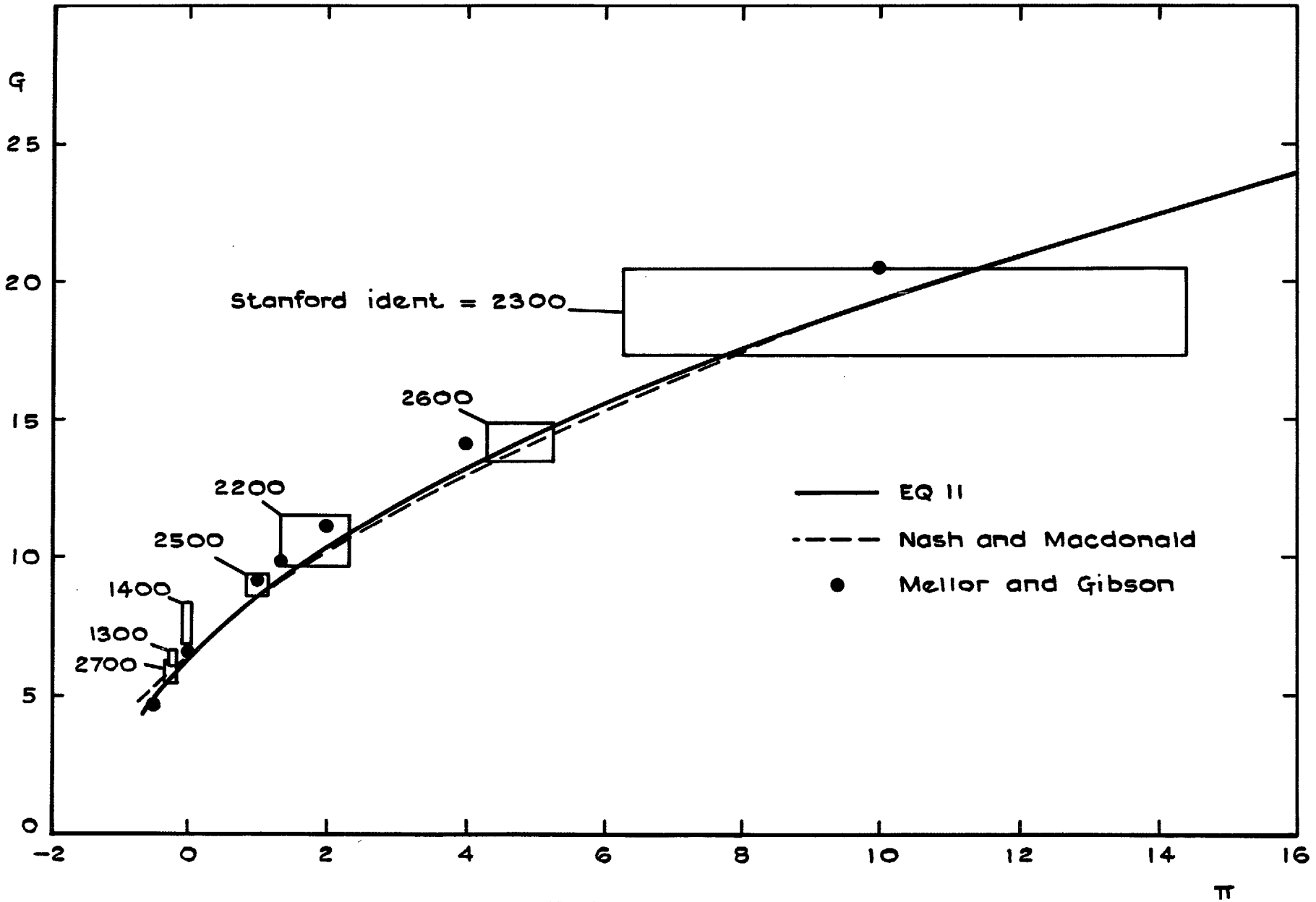

FIG. 1. Equilibrium locus.

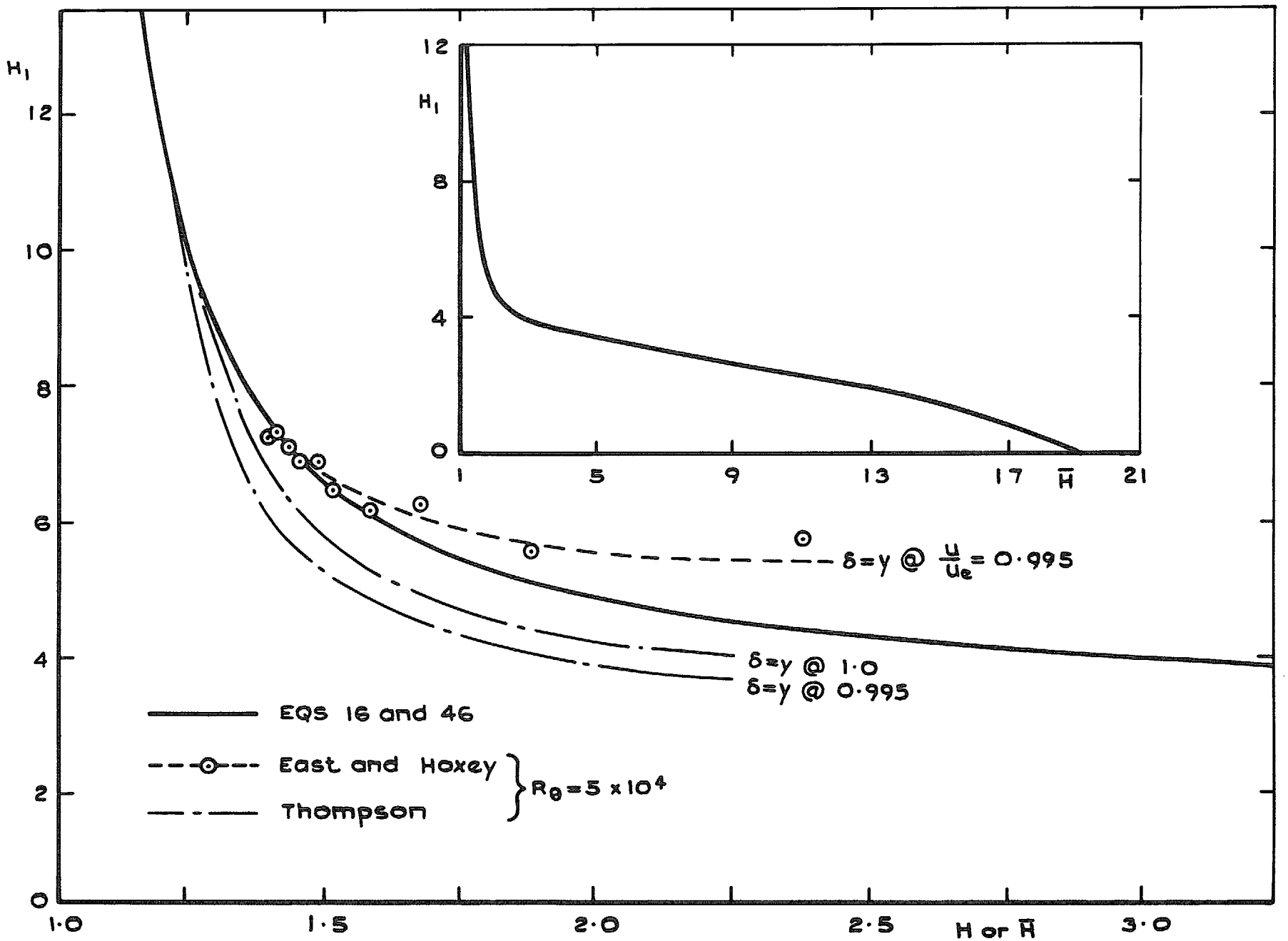

FIG. 2. Shape parameter relation.

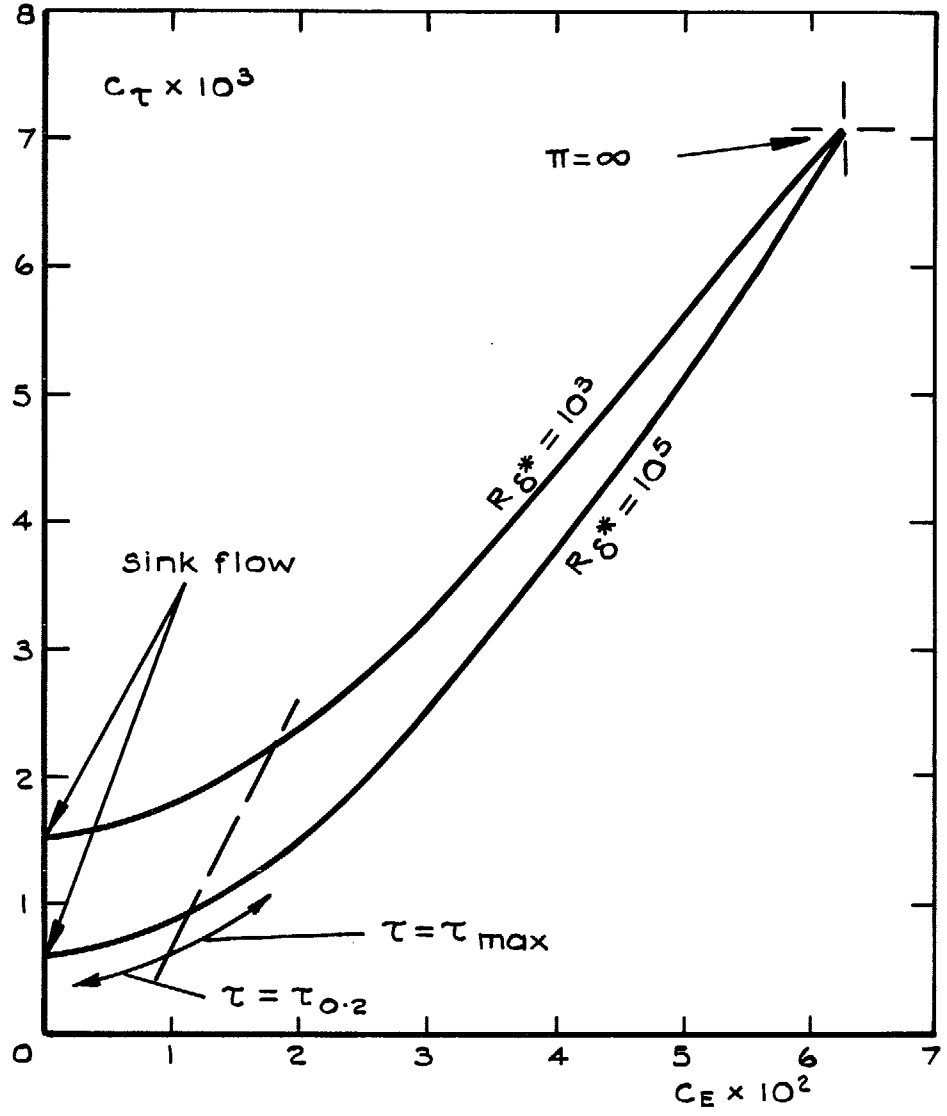

a. Values derived from Mellor and Gibson

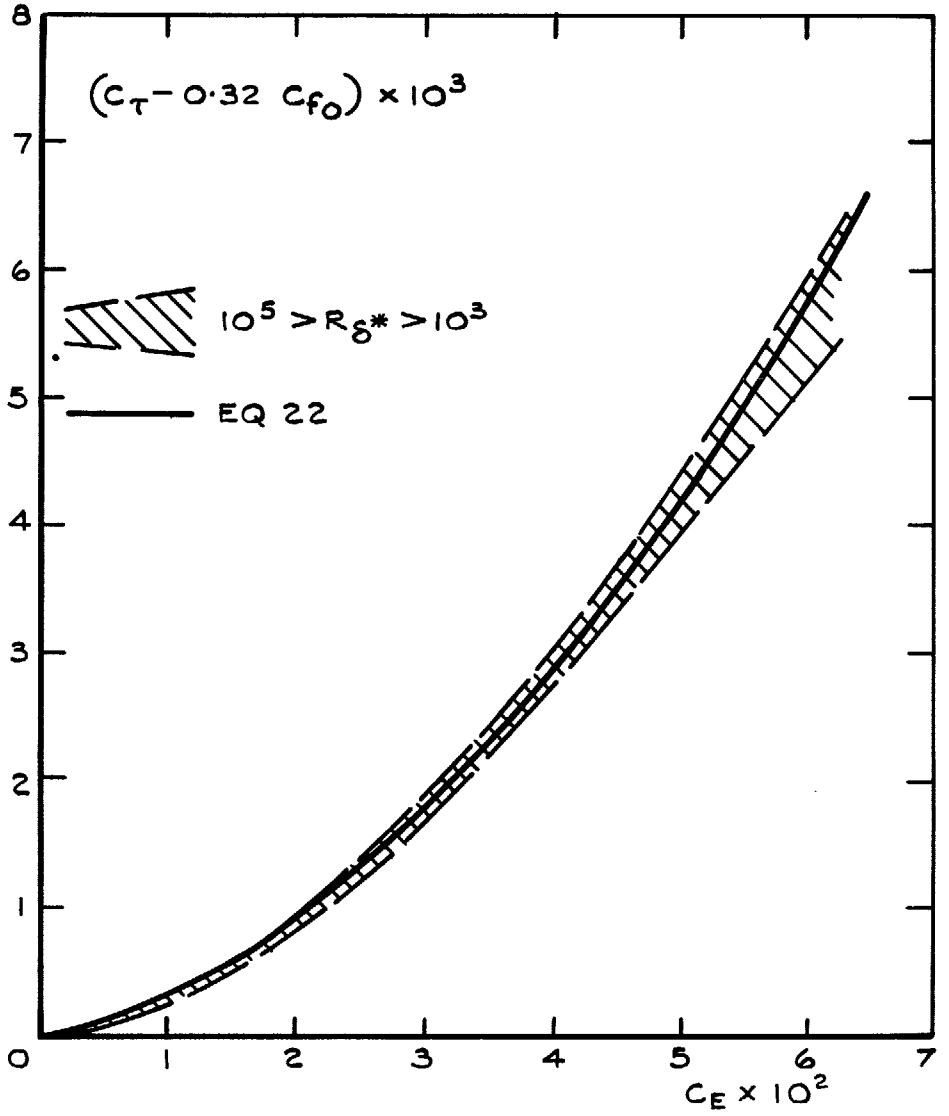

b. Analytic approximation

FIG. 3a. and b. Relation between C_E and C_τ in equilibrium flows.

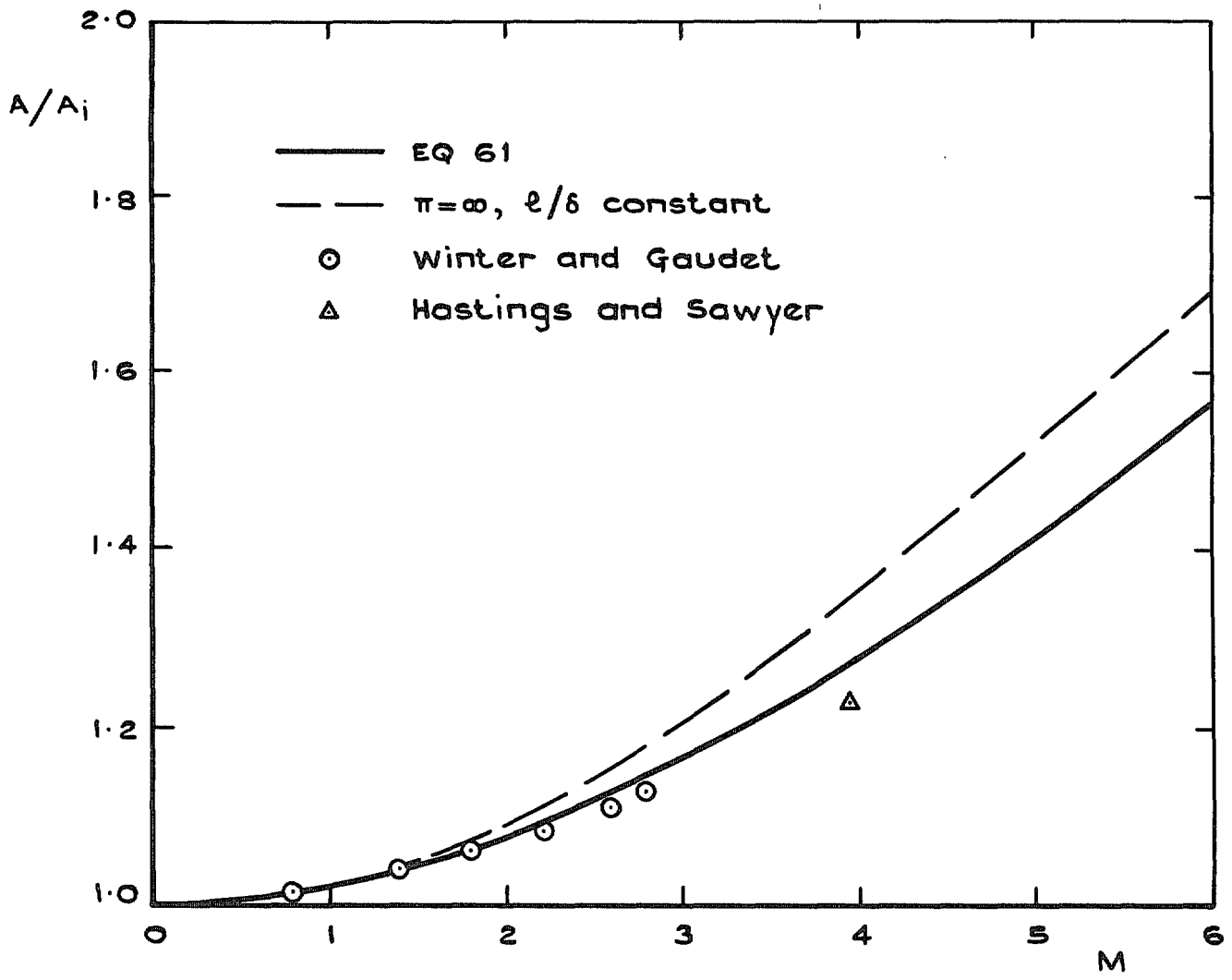

FIG. 4. Influence of Mach number on equilibrium locus.

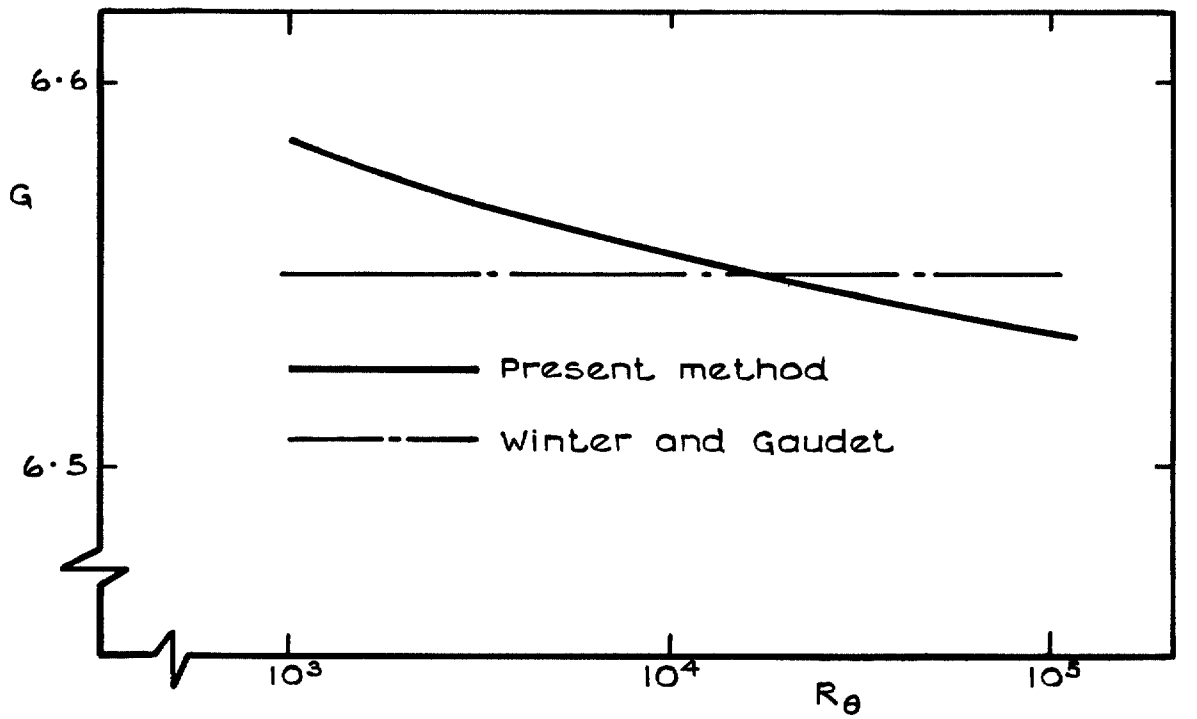

FIG. 5. Equilibrium flow in zero pressure gradient.

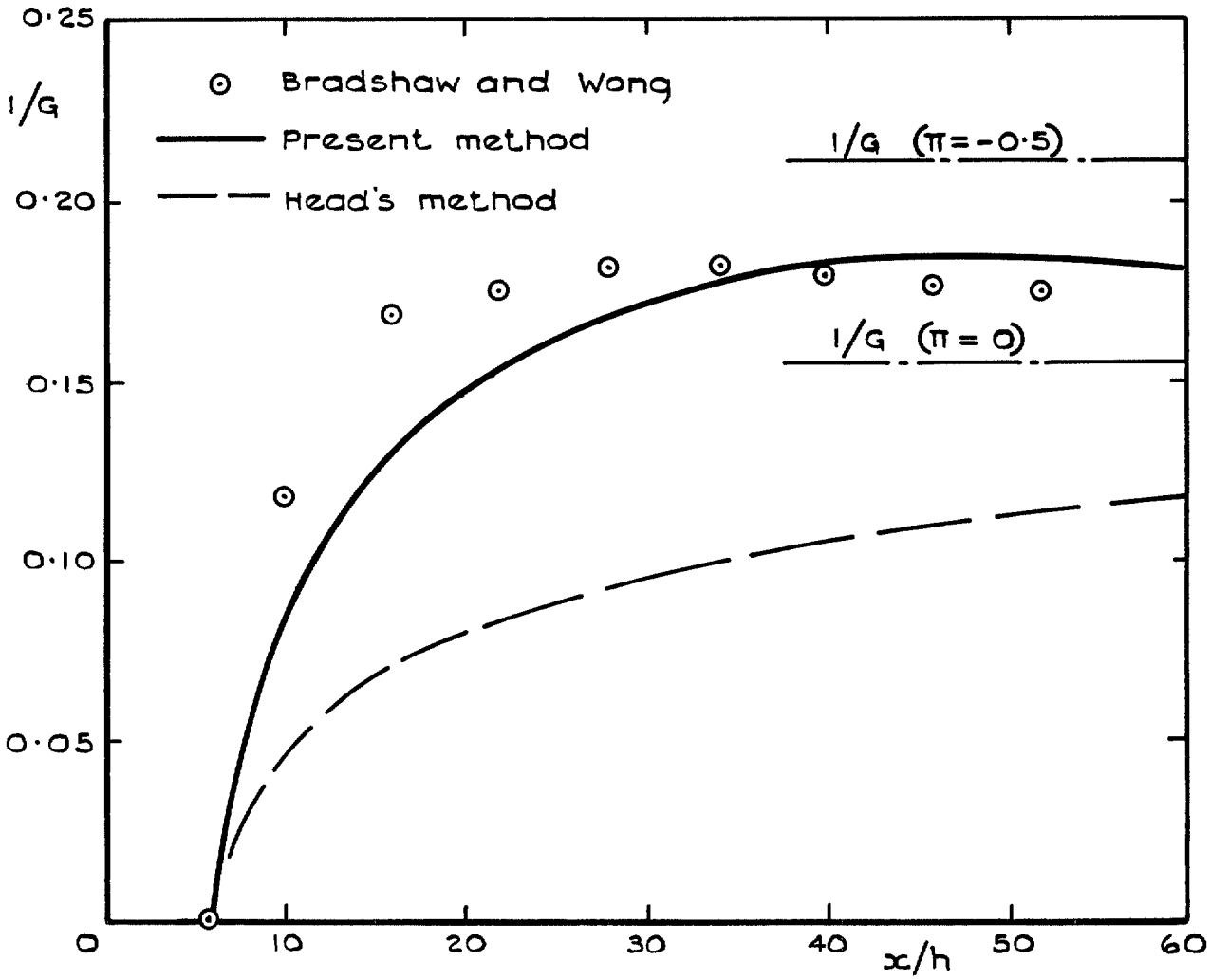

FIG. 6. Initially perturbed flow in zero pressure gradient.

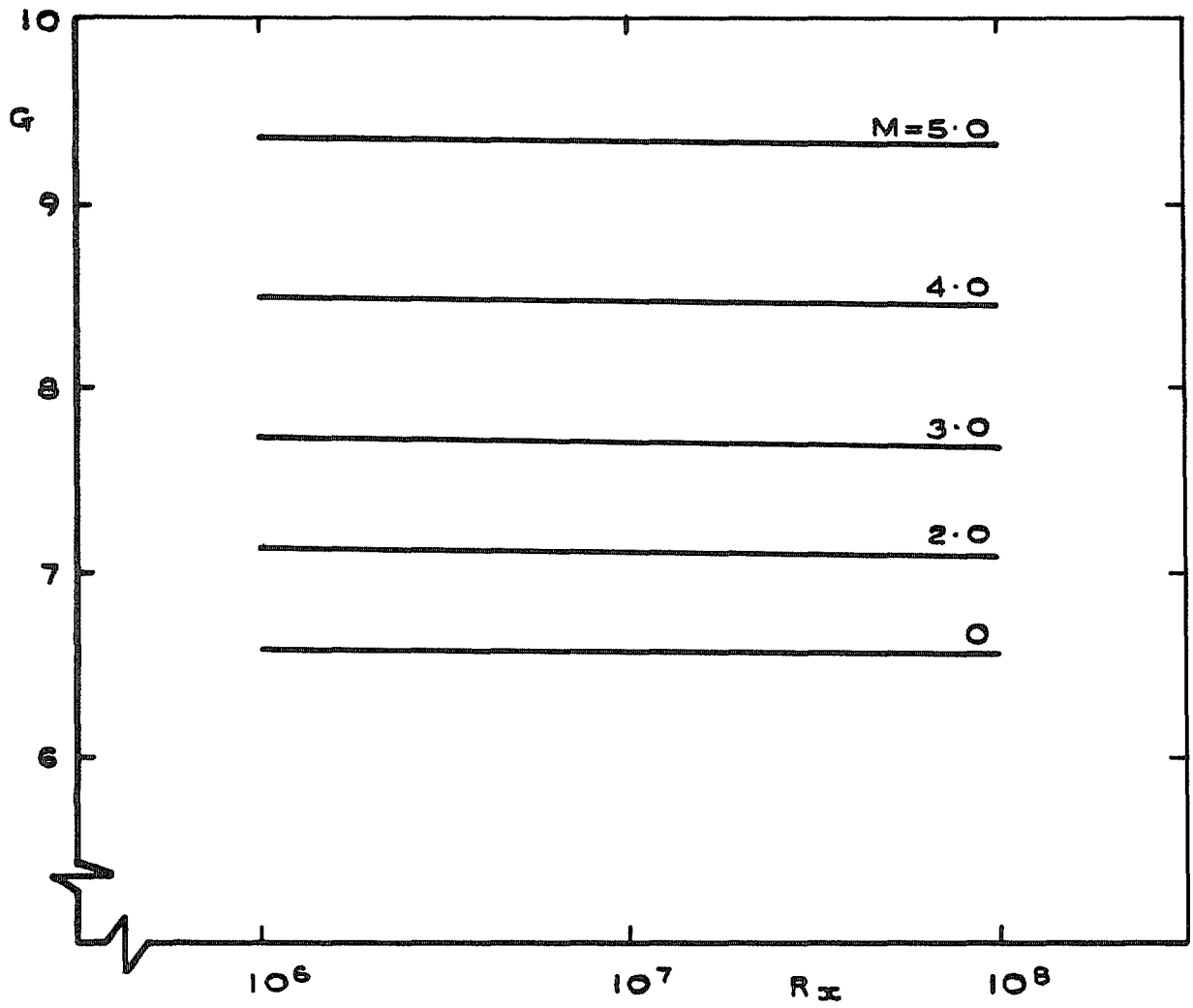

FIG. 7. Computed behaviour of G in compressible flow in zero pressure gradient.

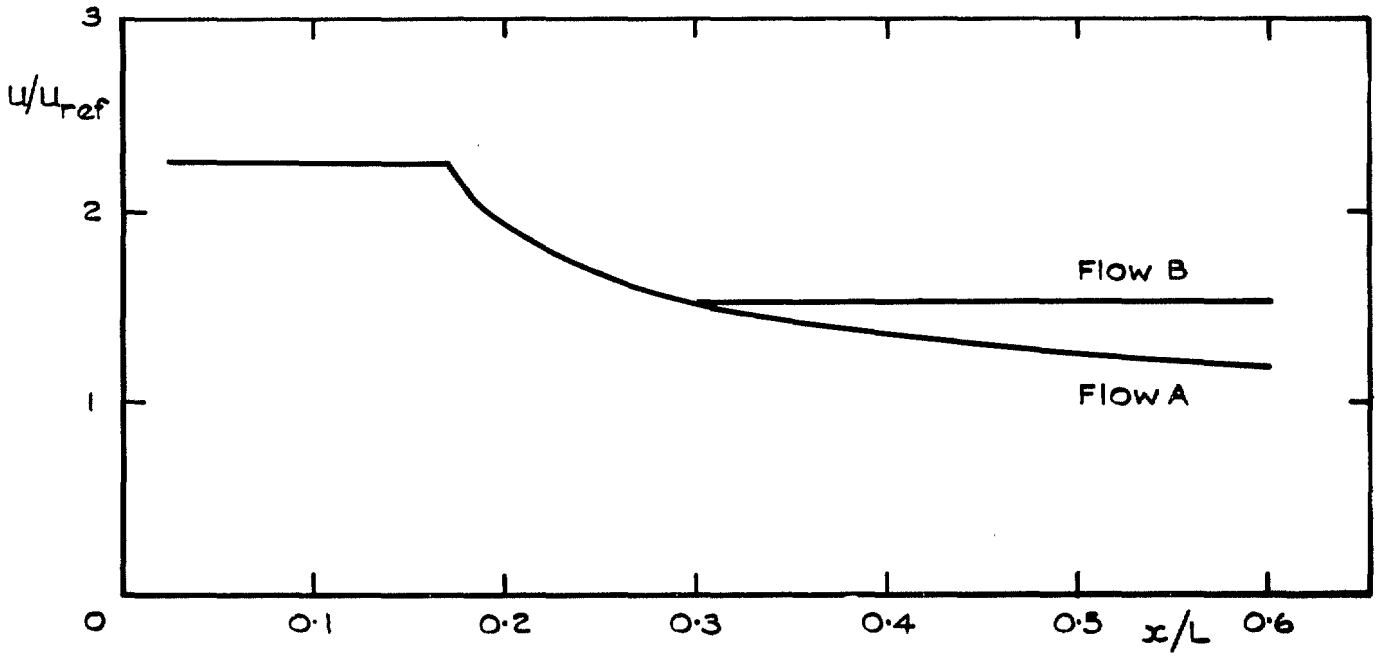

a. Velocity distribution

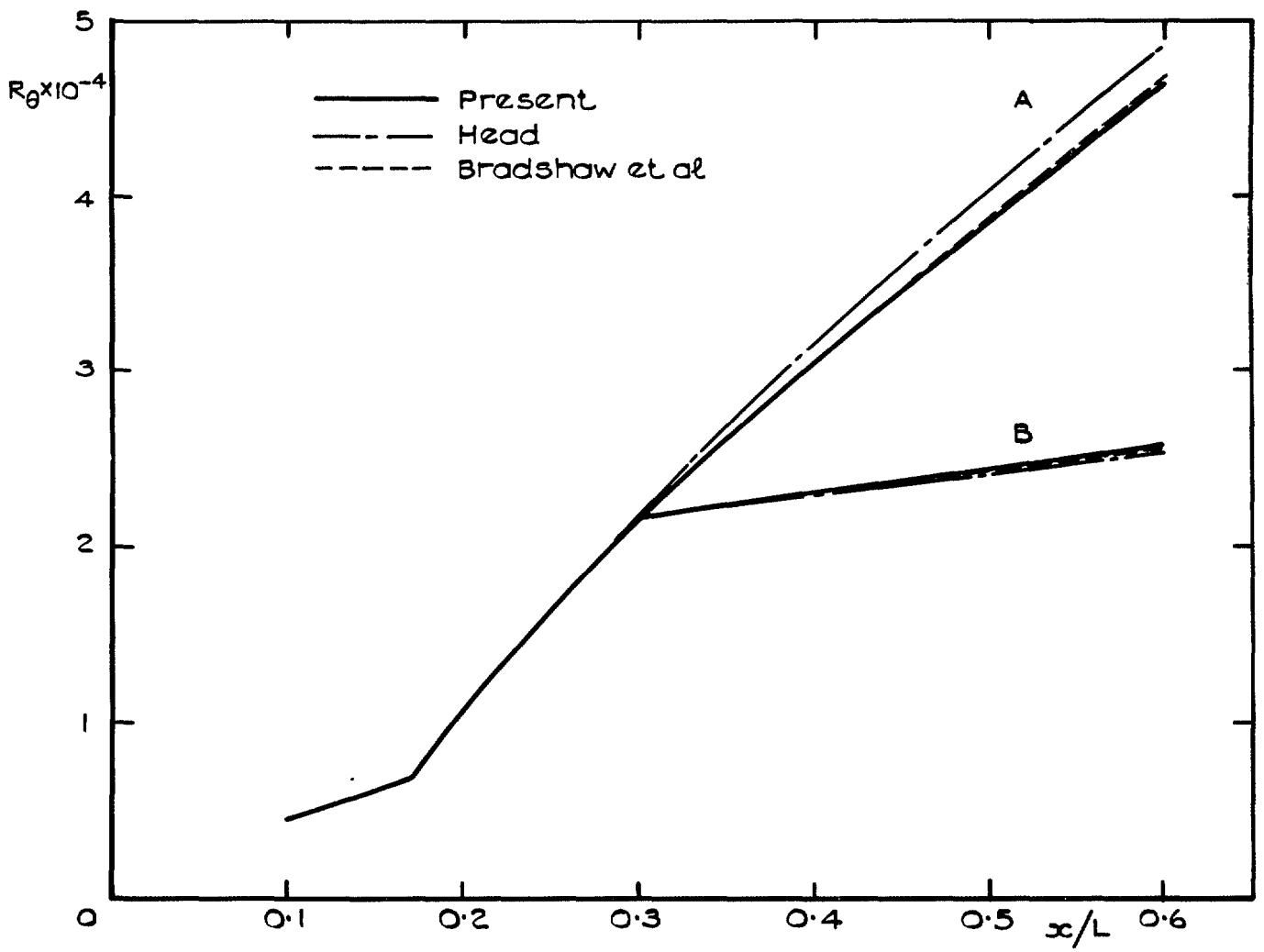

b. Reynolds number based on momentum thickness

FIG. 8. Comparison with methods of Head and Bradshaw *et al.* for two flows with rapid departures from equilibrium.

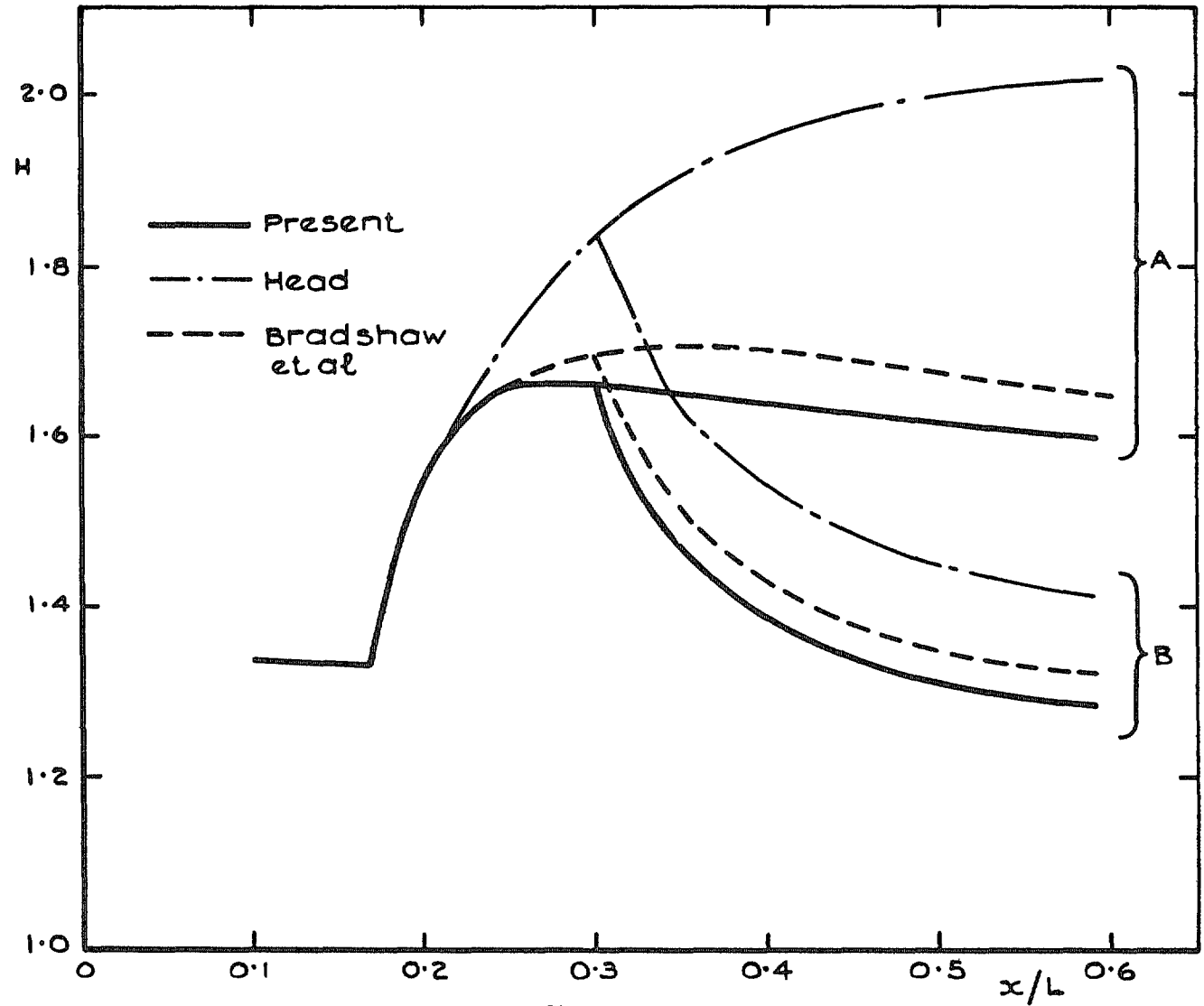

c. Shape parameter

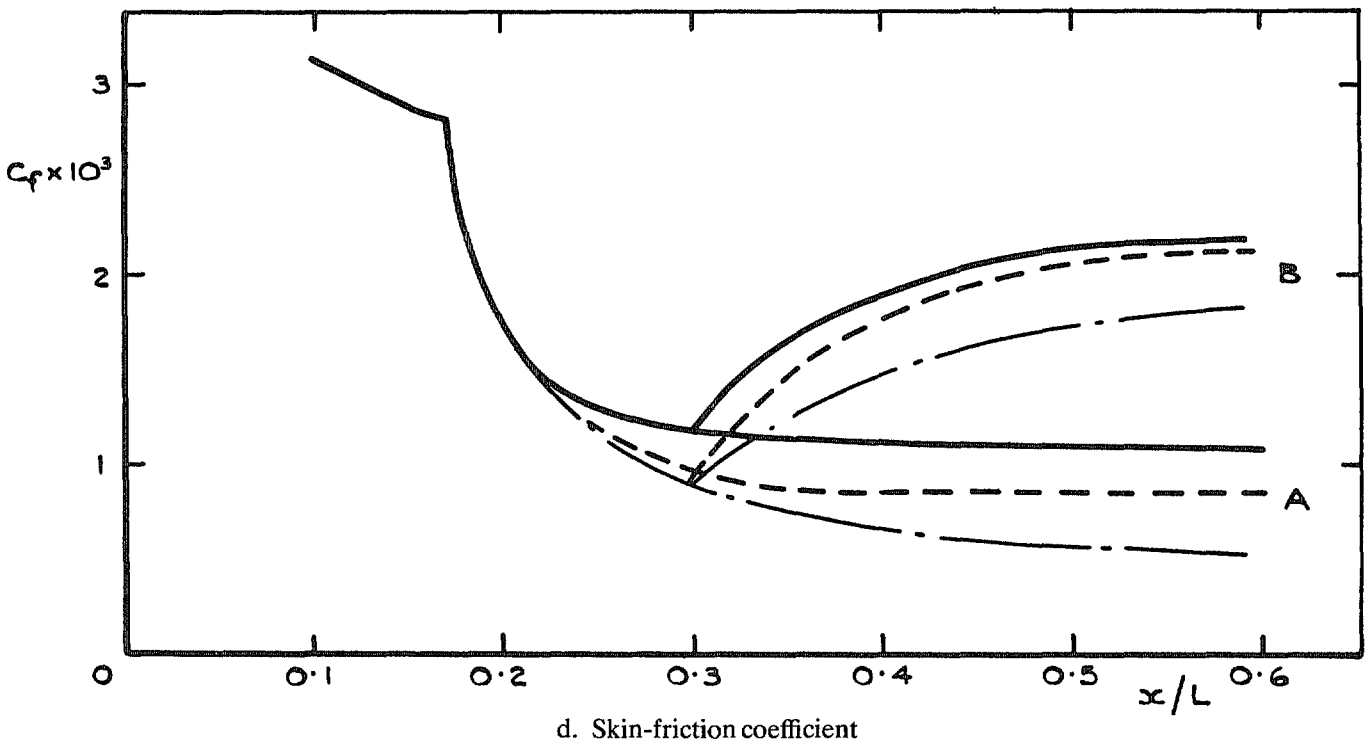

d. Skin-friction coefficient

FIG. 8, concld.

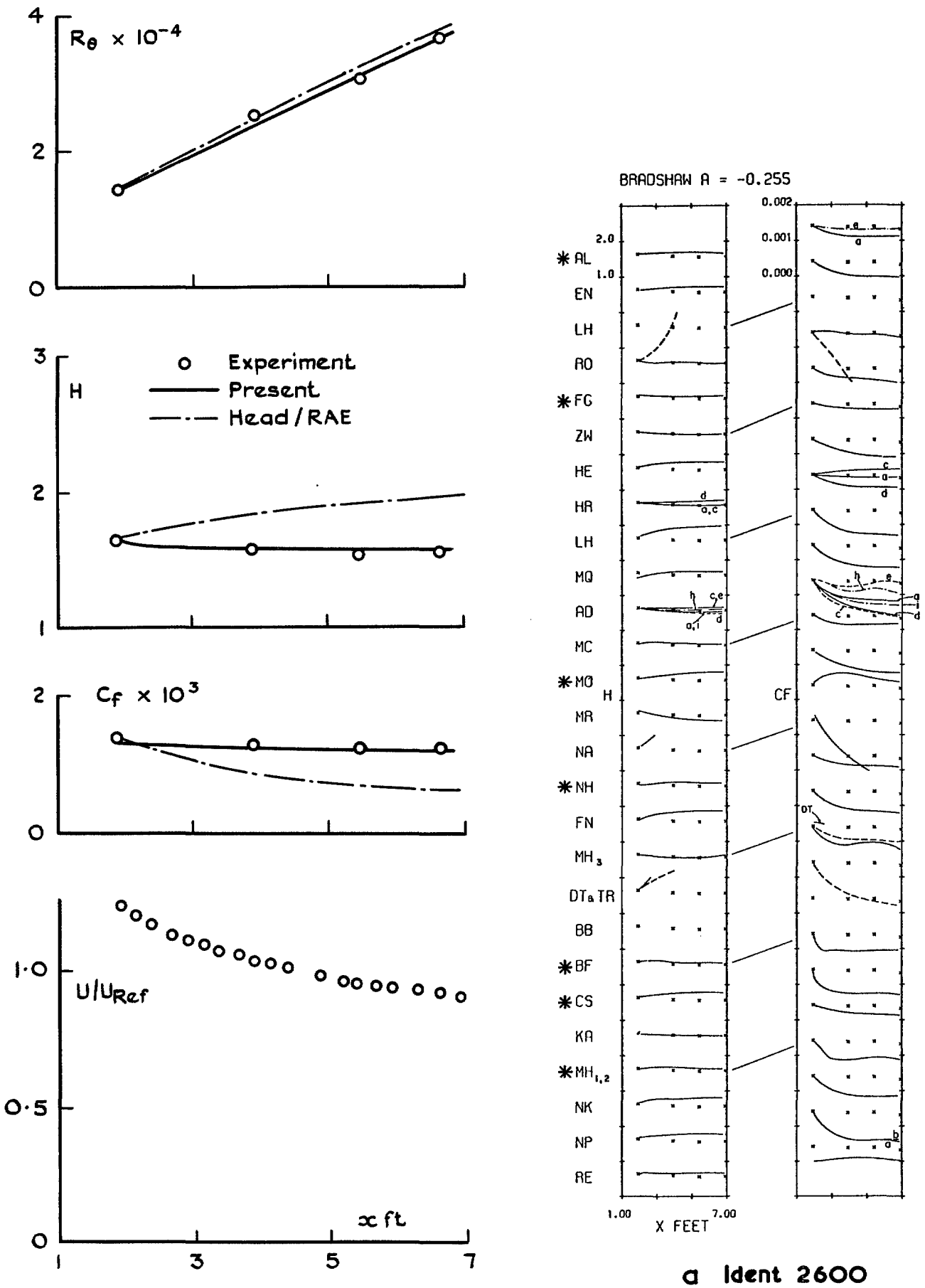

FIG. 9. Comparison with test cases from Stanford Conference.

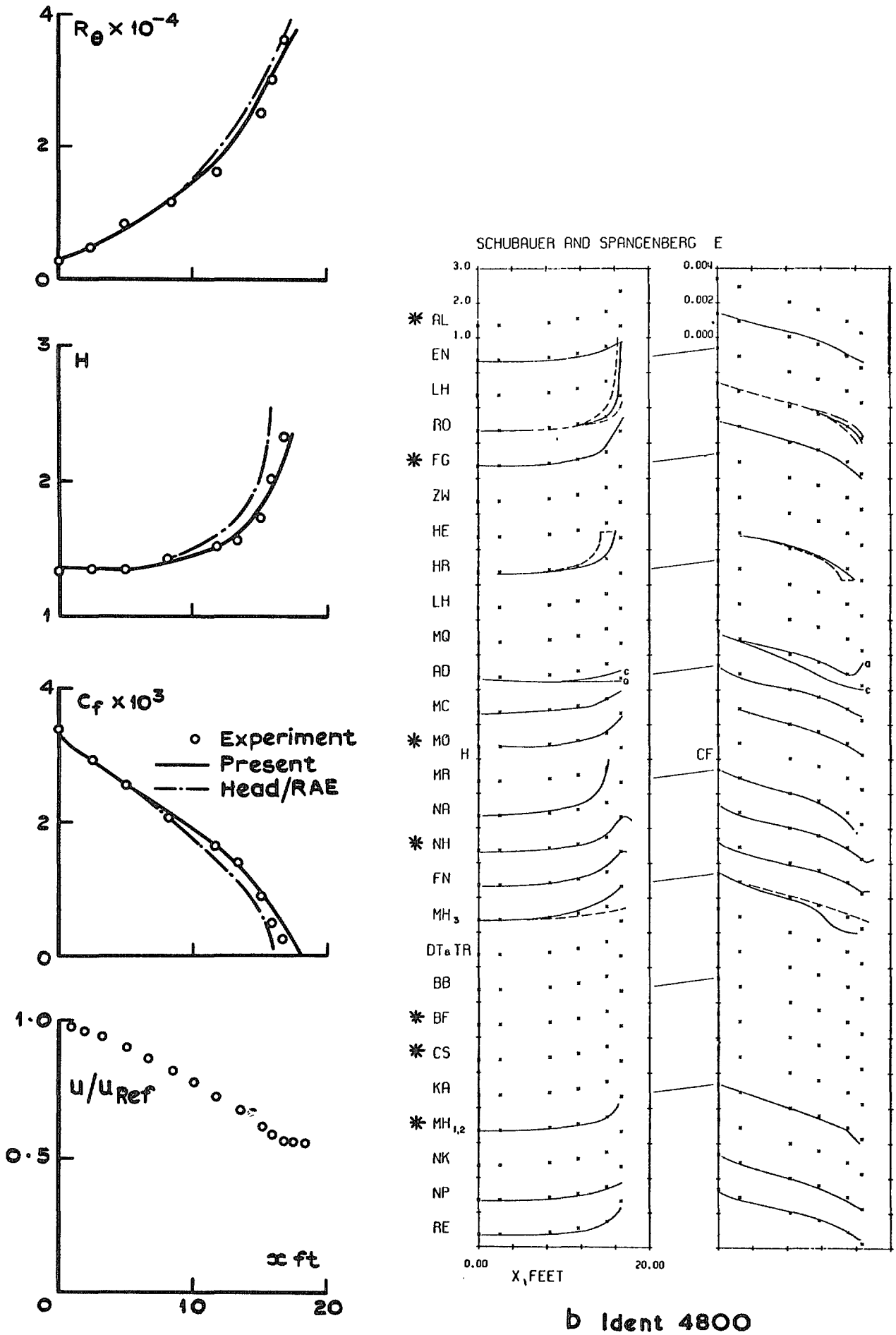
$R_\theta \times 10^{-4}$
H
$C_f \times 10^3$
Experiment
Present
Head/RAE
u/u_{Ref}
x ft
SCHUBAUER AND SPANGENBERG E
AL
EN
LH
RO
FG
ZW
HE
HR
LH
MQ
AD
MC
MO
MR
NA
NH
FN
MH_3
DT&TR
BB
BF
CS
KA
$MH_{1,2}$
NK
NP
RE
H
CF
X, FEET
b Ident 4800

FIG. 9, contd.

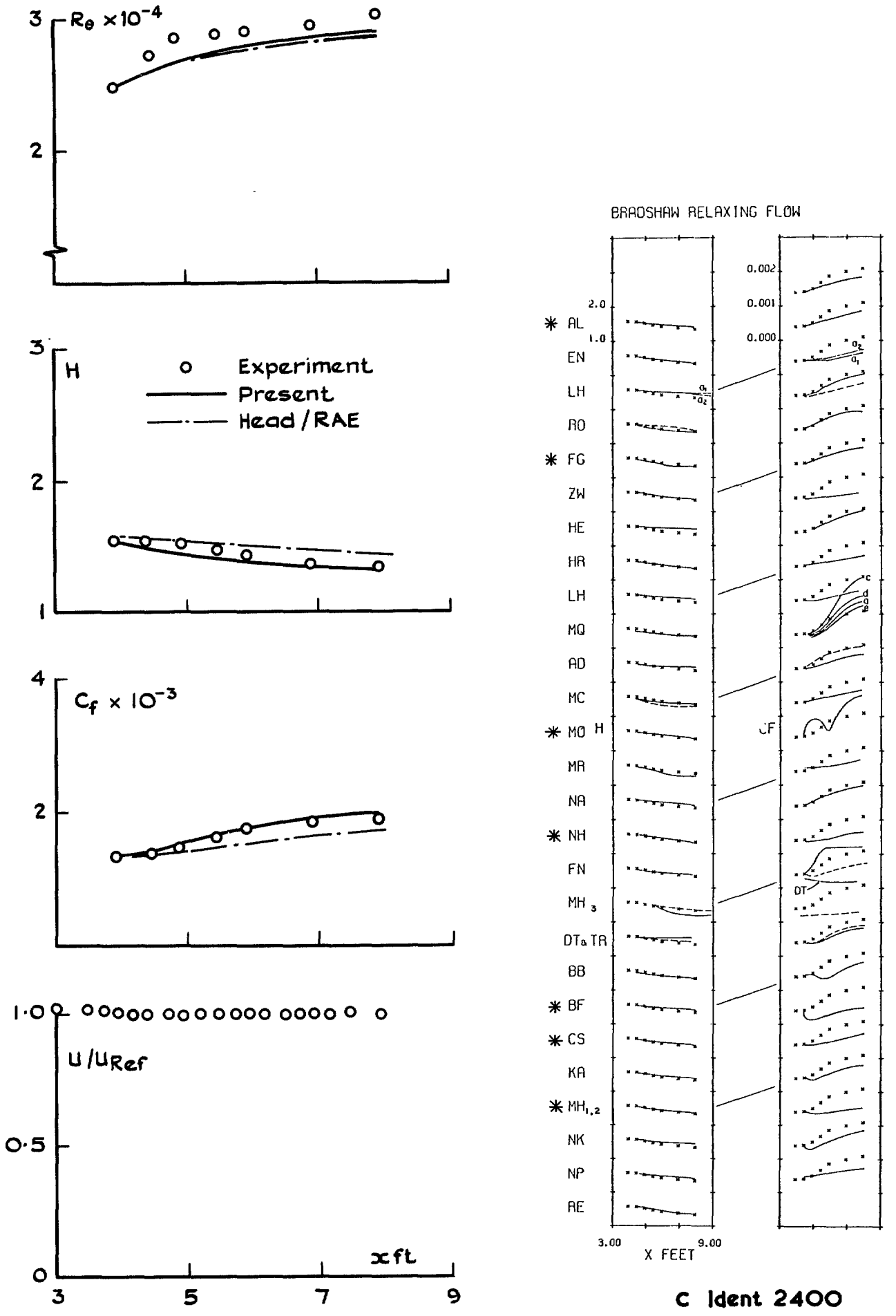
3
$R_\theta \times 10^{-4}$
2
3
H
Experiment
Present
Head / RAE
2
1
4
$C_f \times 10^{-3}$
2
1·0
U/U Ref
0·5
0
3
5
7
9
xft
BRADSHAW RELAXING FLOW
2.0
1.0
AL
EN
LH
RO
FG
ZW
HE
HR
LH
MQ
AD
MC
MO H
MR
NA
NH
FN
MH 3
DT& TR
BB
BF
CS
KA
MH 1,2
NK
NP
RE
0.002
0.001
0.000
CF
DT
3.00
9.00
X FEET
C Ident 2400

FIG. 9, contd.

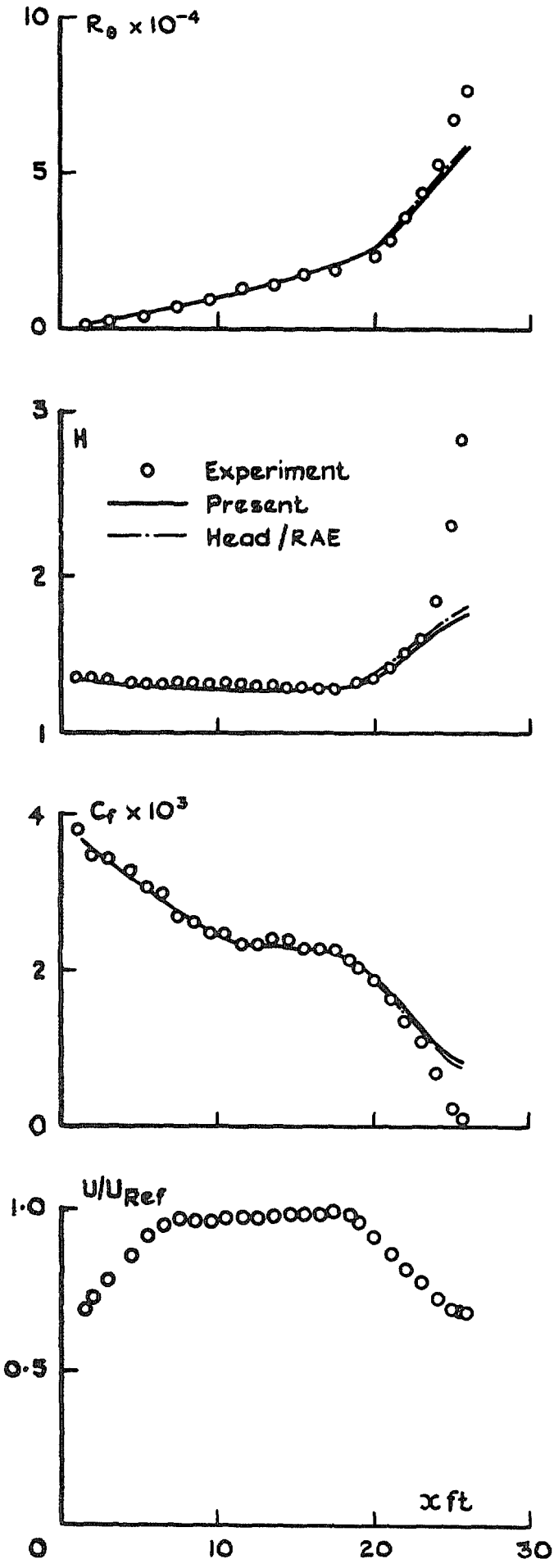

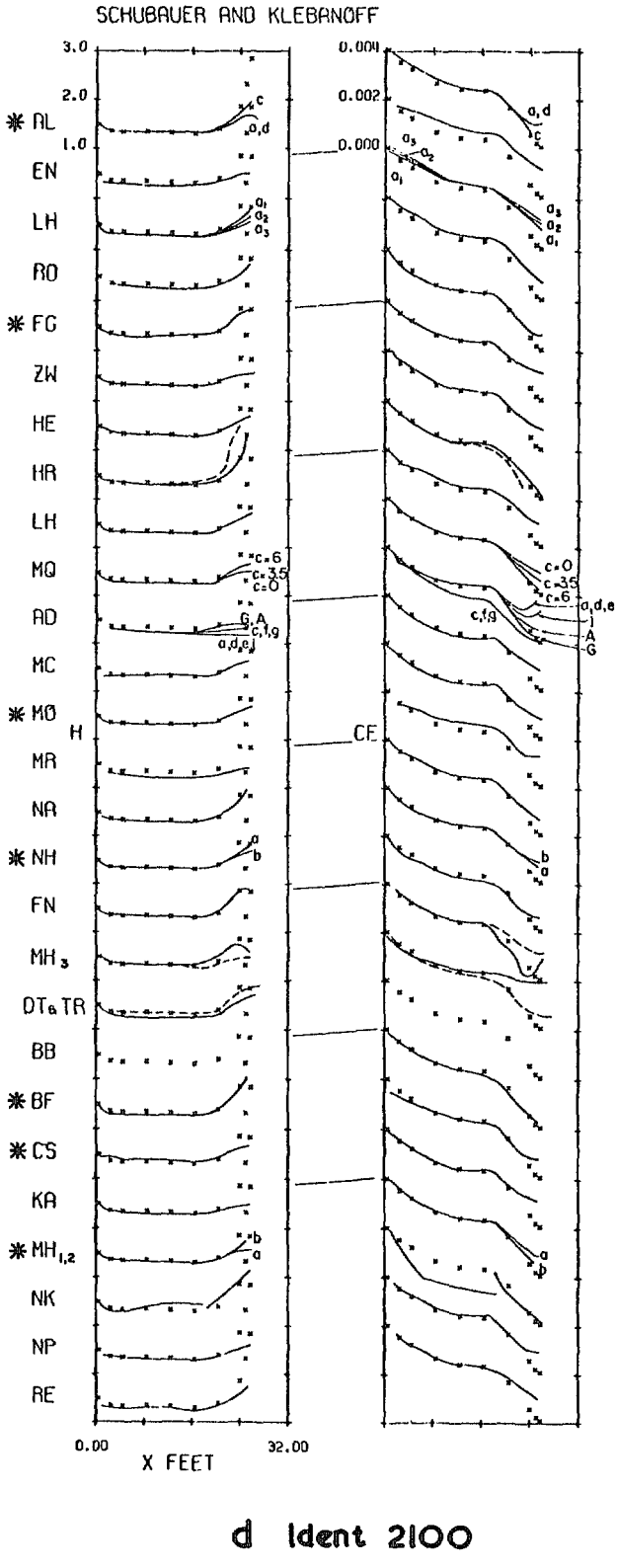

d Ident 2100

FIG. 9, contd.

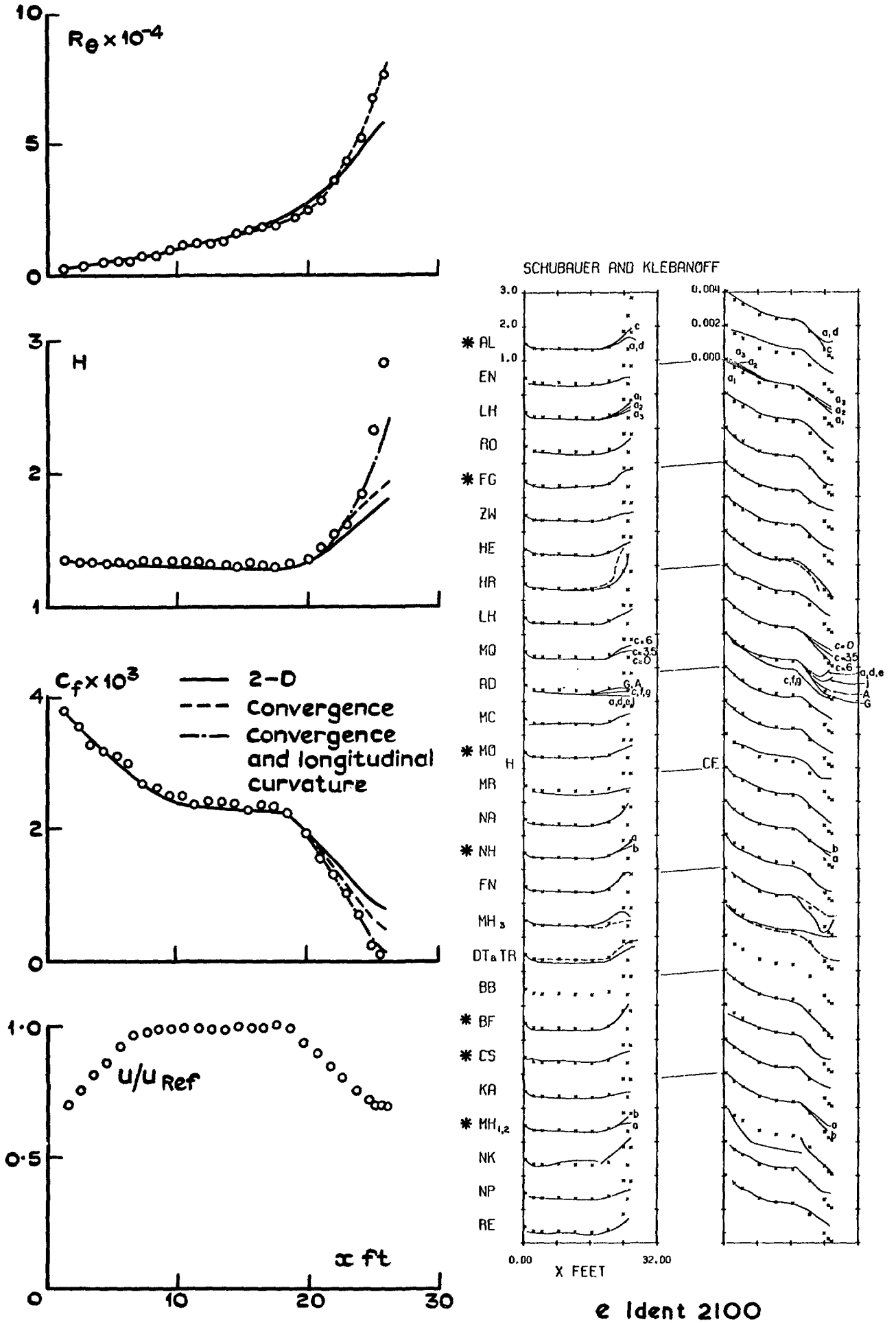
$R_\theta \times 10^{-4}$
H
$C_f \times 10^3$
2-D
Convergence
Convergence and longitudinal curvature
U/U Ref
x ft
SCHUBAUER AND KLEBANOFF
AL
EN
LH
RO
FG
ZW
HE
HR
LH
MQ
AD
MC
MO
MR
NA
NH
FN
MH_3
DT_aTR
BB
BF
CS
KA
$MH_{1,2}$
NK
NP
RE
H
CF
X FEET
e Ident 2100

FIG. 9, contd.

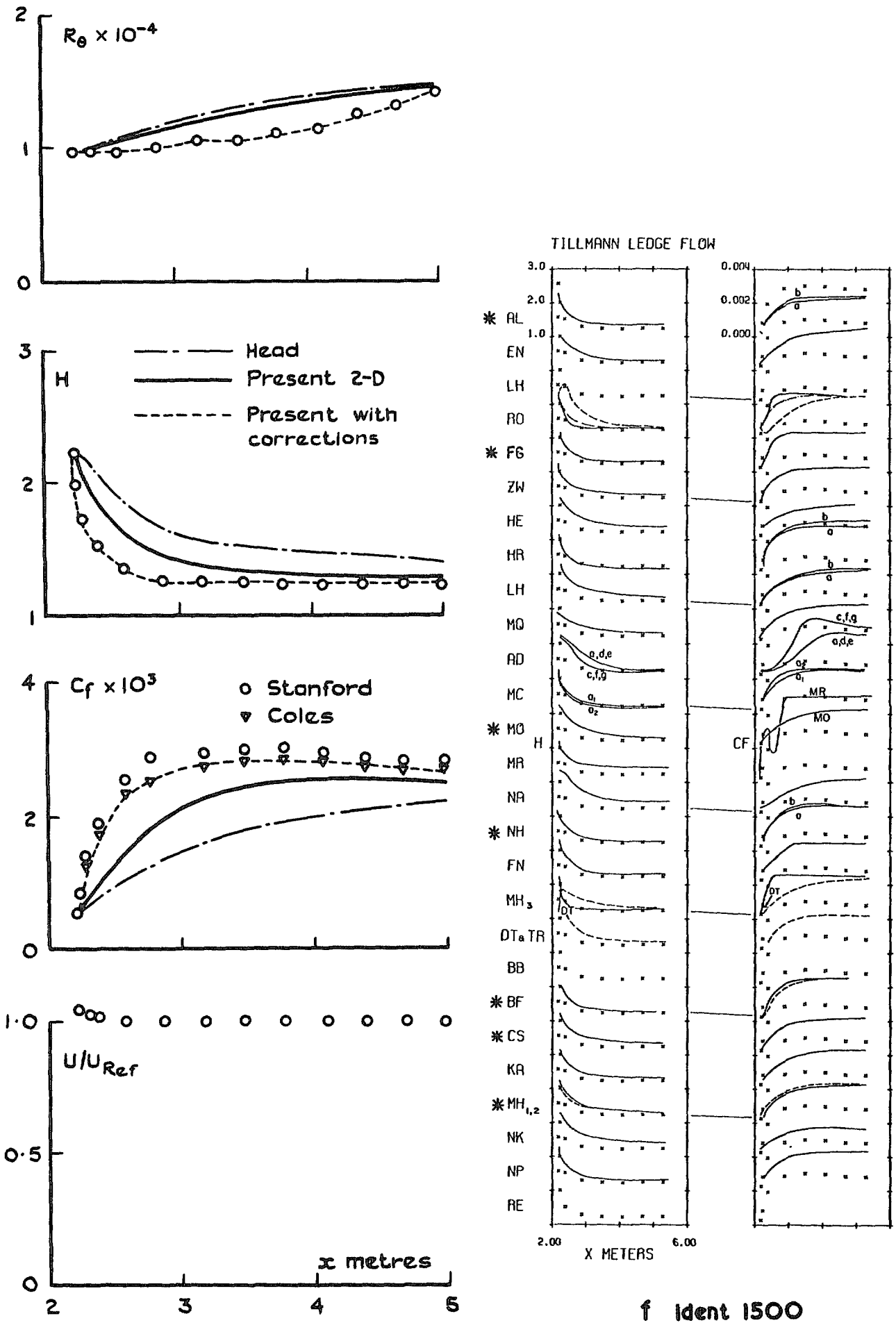
$R_\theta \times 10^{-4}$
H
Head
Present 2-D
Present with corrections
$C_f \times 10^3$
Stanford
Coles
U/U Ref
x metres
TILLMANN LEDGE FLOW
AL
EN
LH
RO
FG
ZW
HE
HR
LH
MQ
AD
MC
MO
MR
NA
NH
FN
MH_3
DT & TR
BB
BF
CS
KA
$MH_{1,2}$
NK
NP
RE
CF
X METERS
f Ident 1500

FIG. 9, contd.

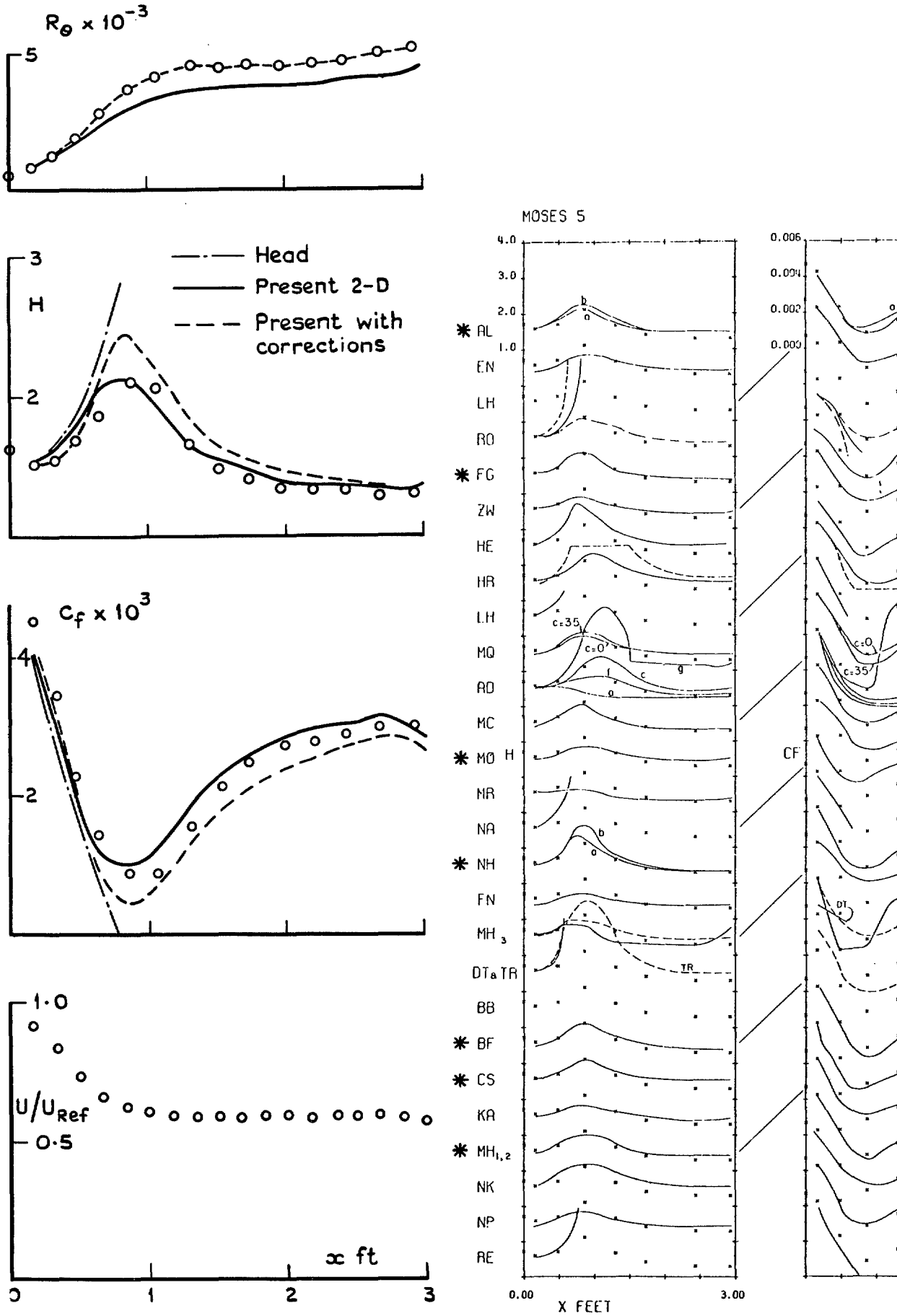
$R_\theta \times 10^{-3}$
5
3
H
2
Head
Present 2-D
Present with corrections
$C_f \times 10^3$
4
2
1·0
U/U_Ref
0·5
x ft
0
1
2
3
MOSES 5
4.0
3.0
2.0
1.0
AL
EN
LH
RO
FG
ZW
HE
HR
LH
MQ
AD
MC
MO H
NR
NA
NH
FN
MH 3
DT&TR
BB
BF
CS
KA
MH1,2
NK
NP
RE
c=35
c=0
TR
0.006
0.004
0.002
0.000
CF
DT
0.00
3.00
X FEET

FIG. 9, concld.

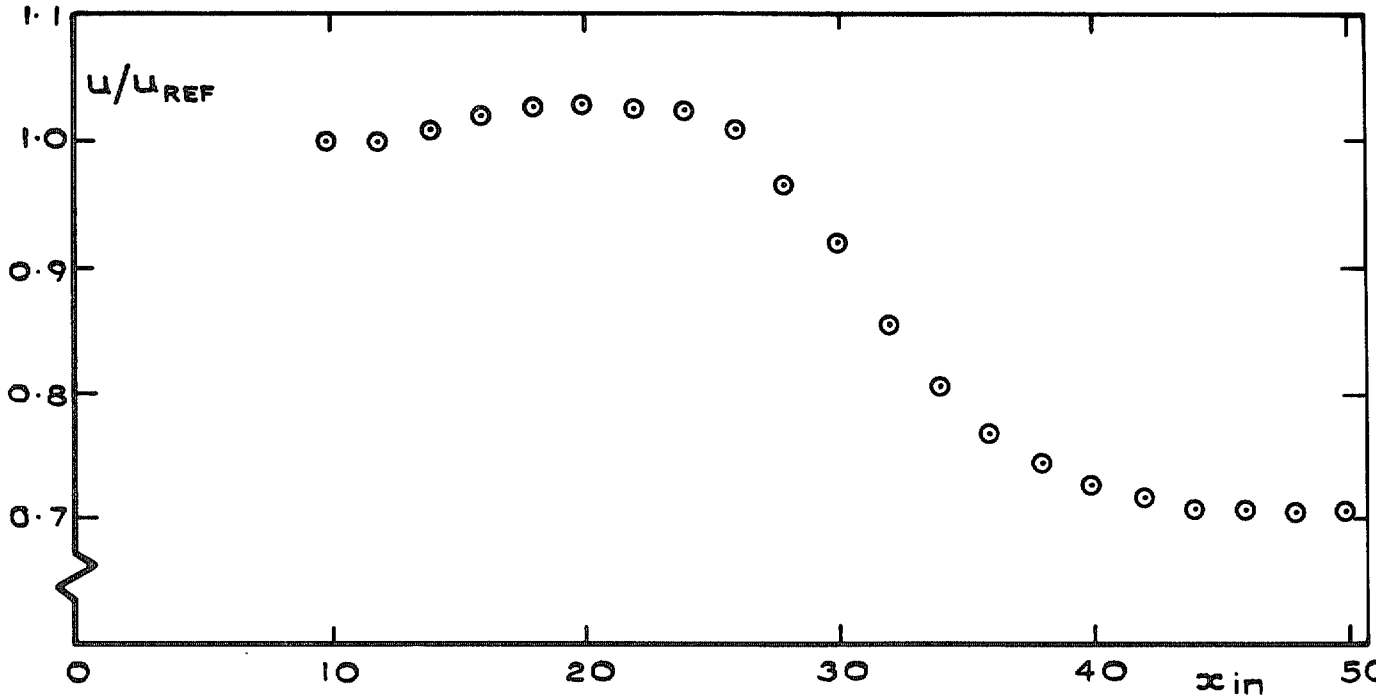

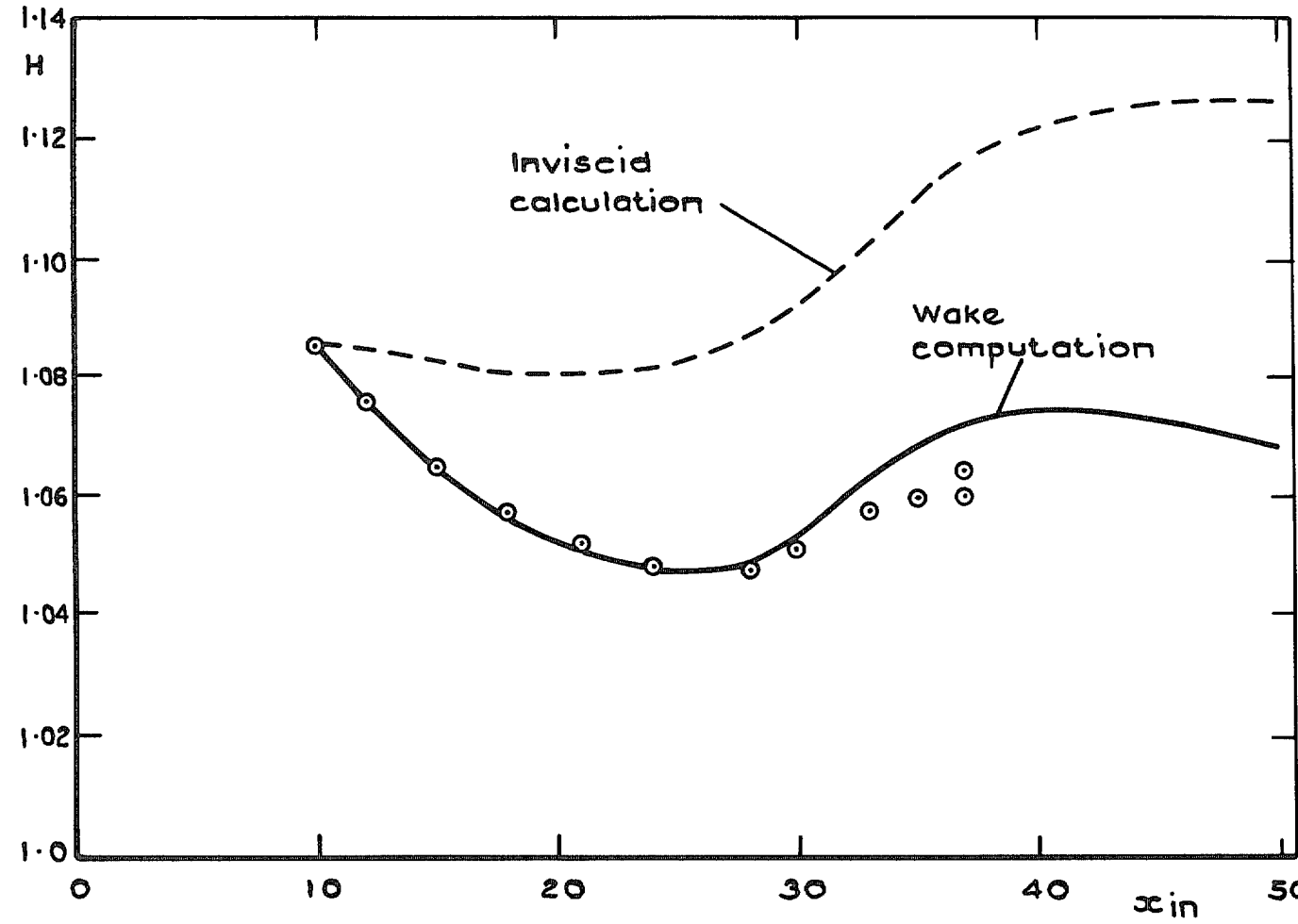

FIG. 10. Comparison with wake measurements by Prabhu and Narasimha case A1.

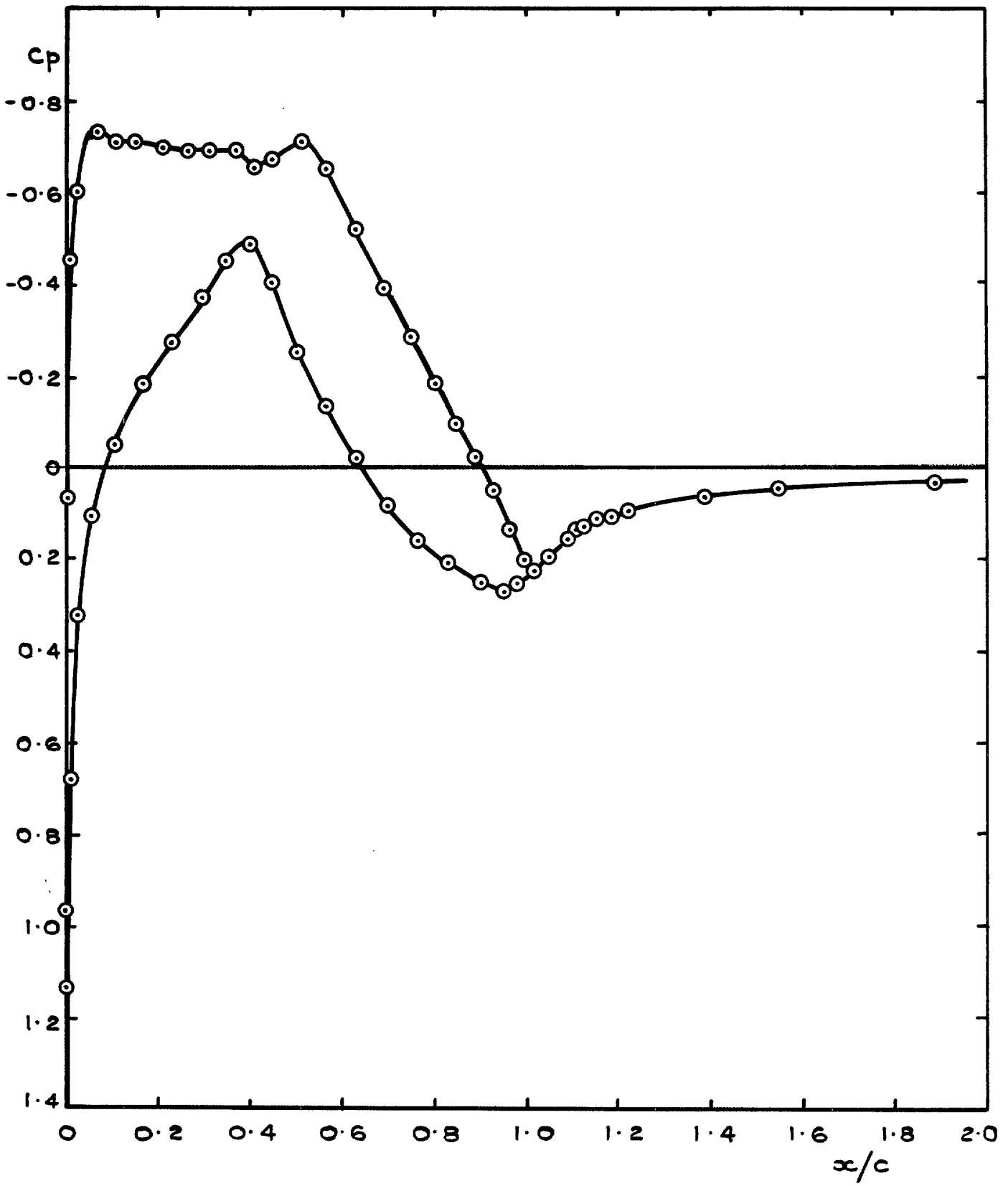

a. Measured pressure distribution

FIG. 11. Boundary layers and wake of two-dimensional aerofoil section (R.A.E. 2814) at $M = 0{\cdot}725$, $R_c = 15 \times 10^6$.

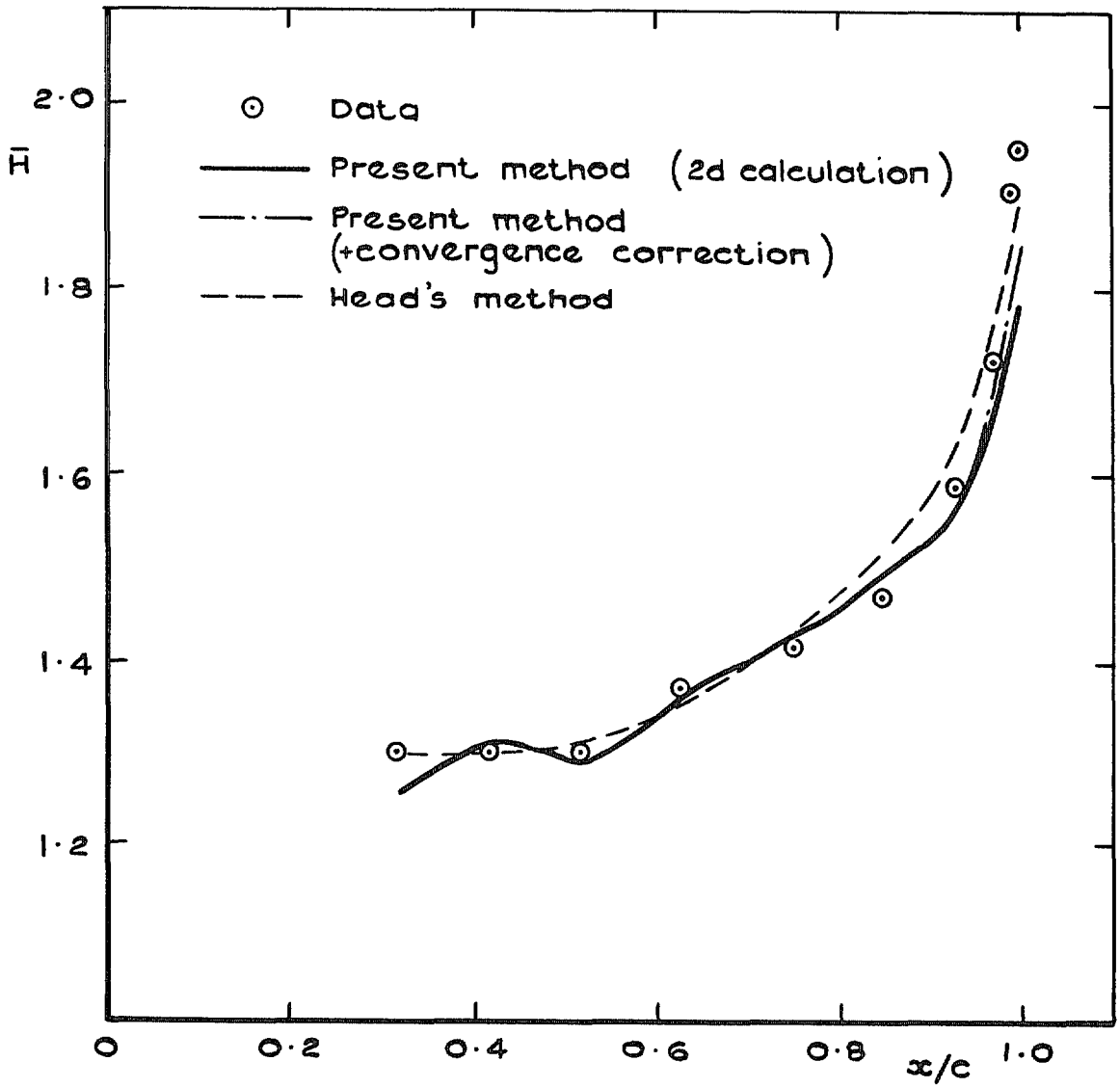

b. Shape parameter on upper surface

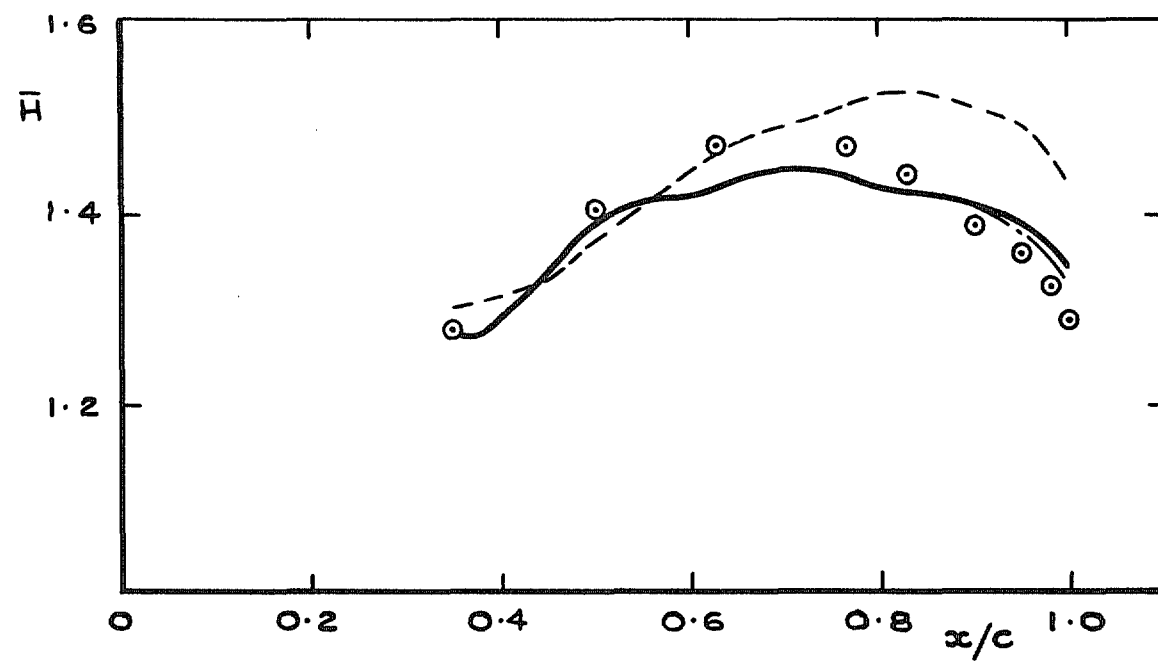

c. Shape parameter on lower surface

FIG. 11, contd.

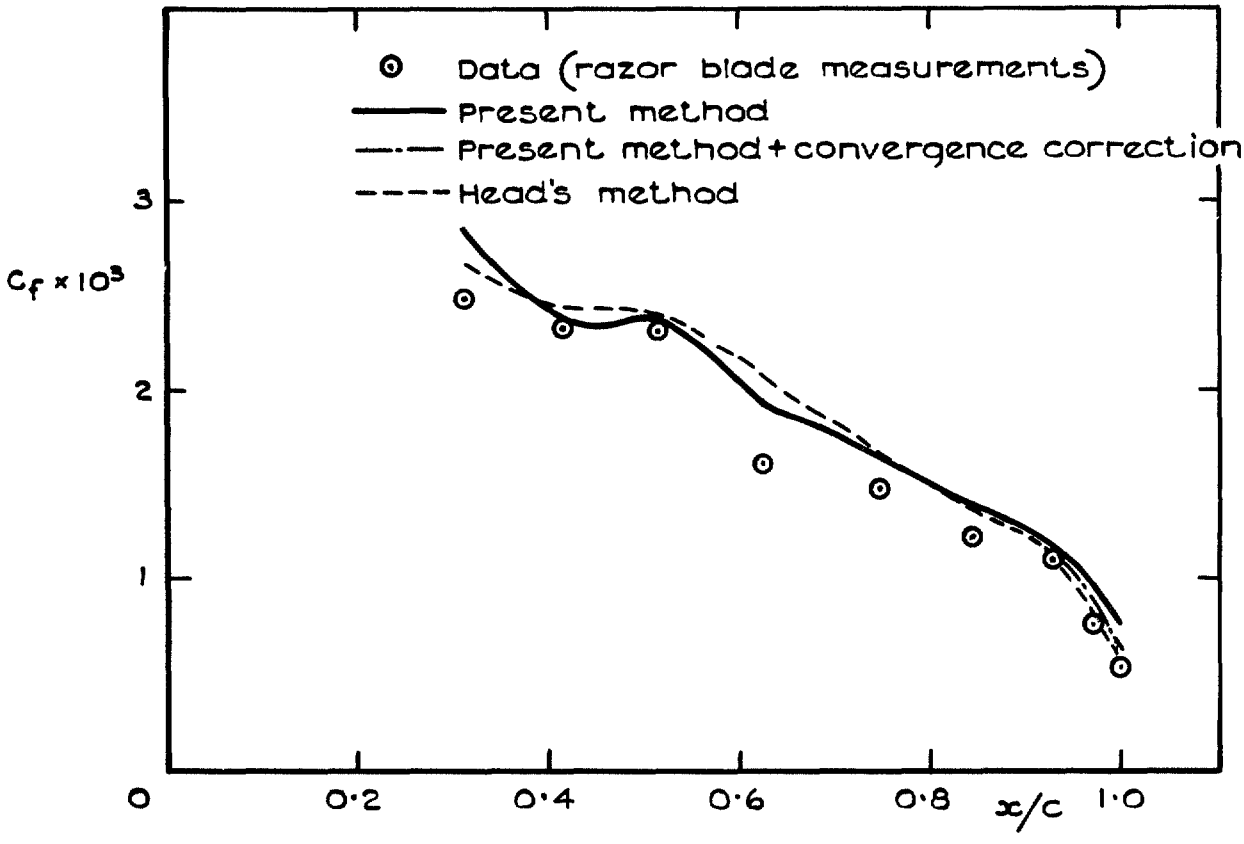

d. Skin friction on upper surface

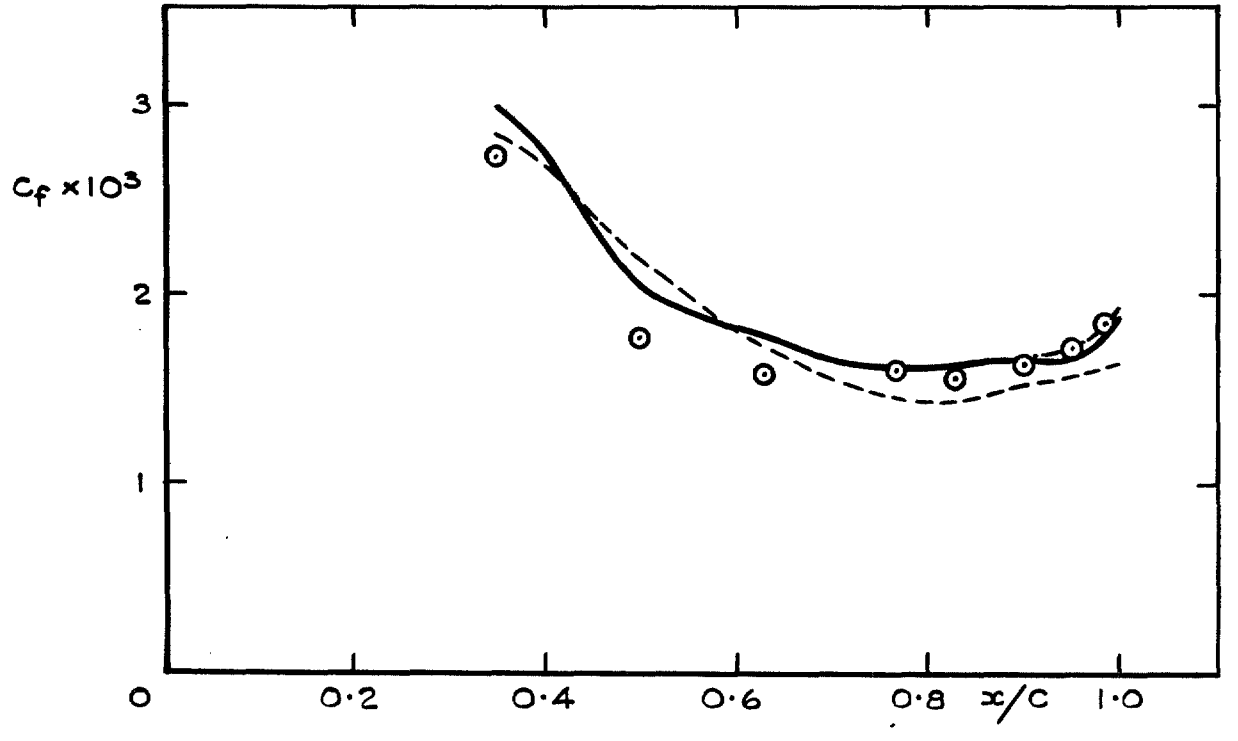

e. Skin friction on lower surface

FIG. 11, contd.

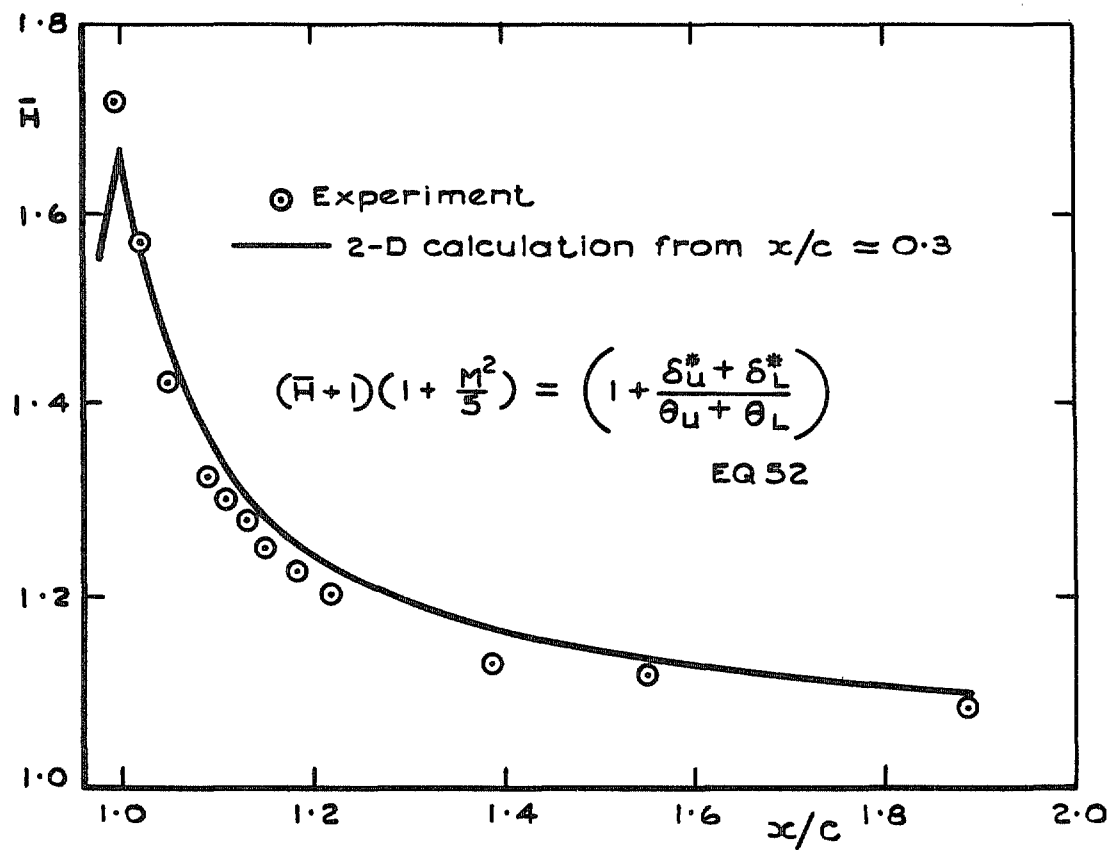

f. Shape parameter in wake

FIG. 11, concld.

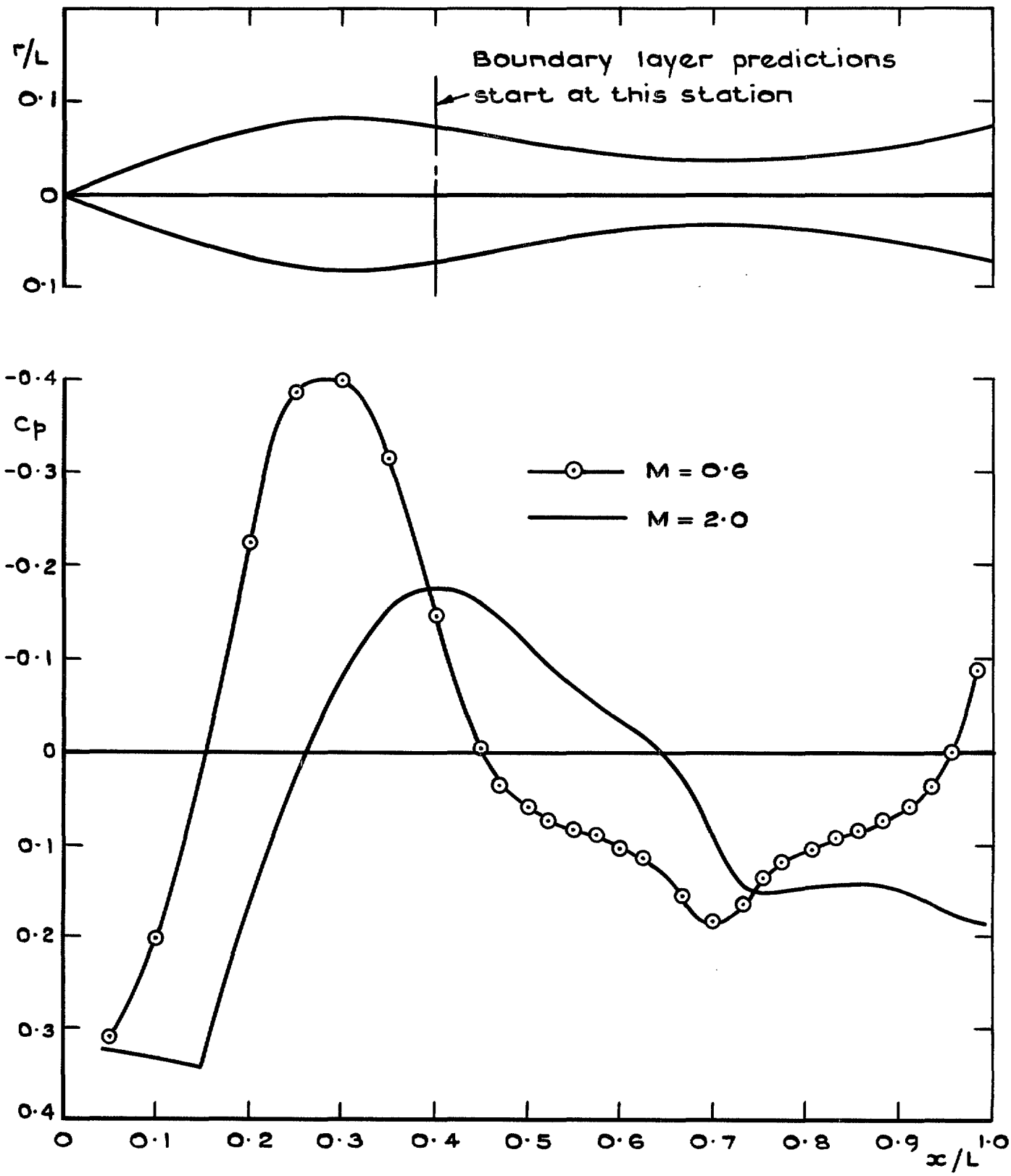

FIG. 12a. Geometry and pressure distributions for waisted body of revolution of Winter *et al.*

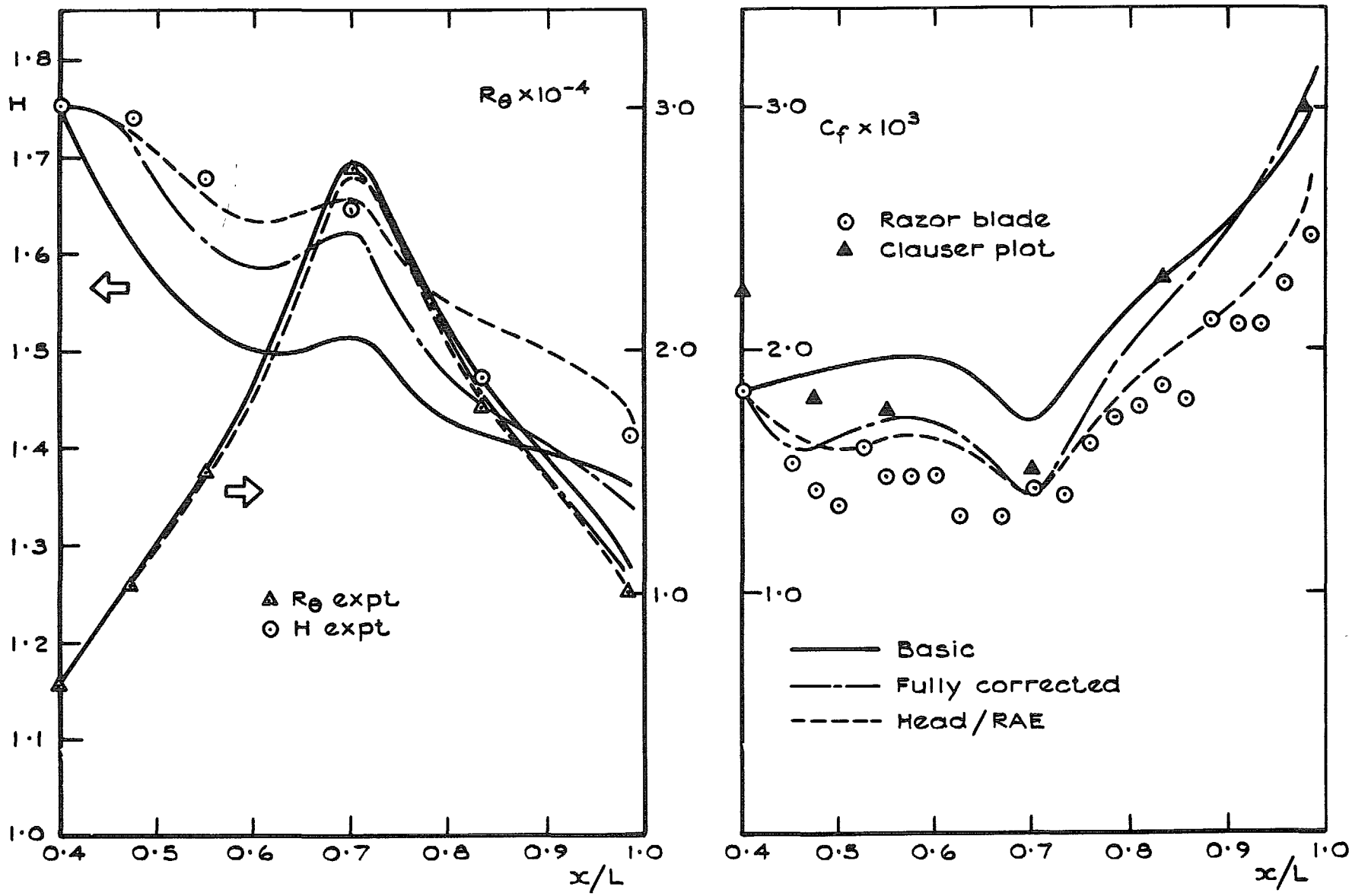

FIG. 12b. Waisted body of revolution at $M = 0{\cdot}6, R_L = 10^7$.

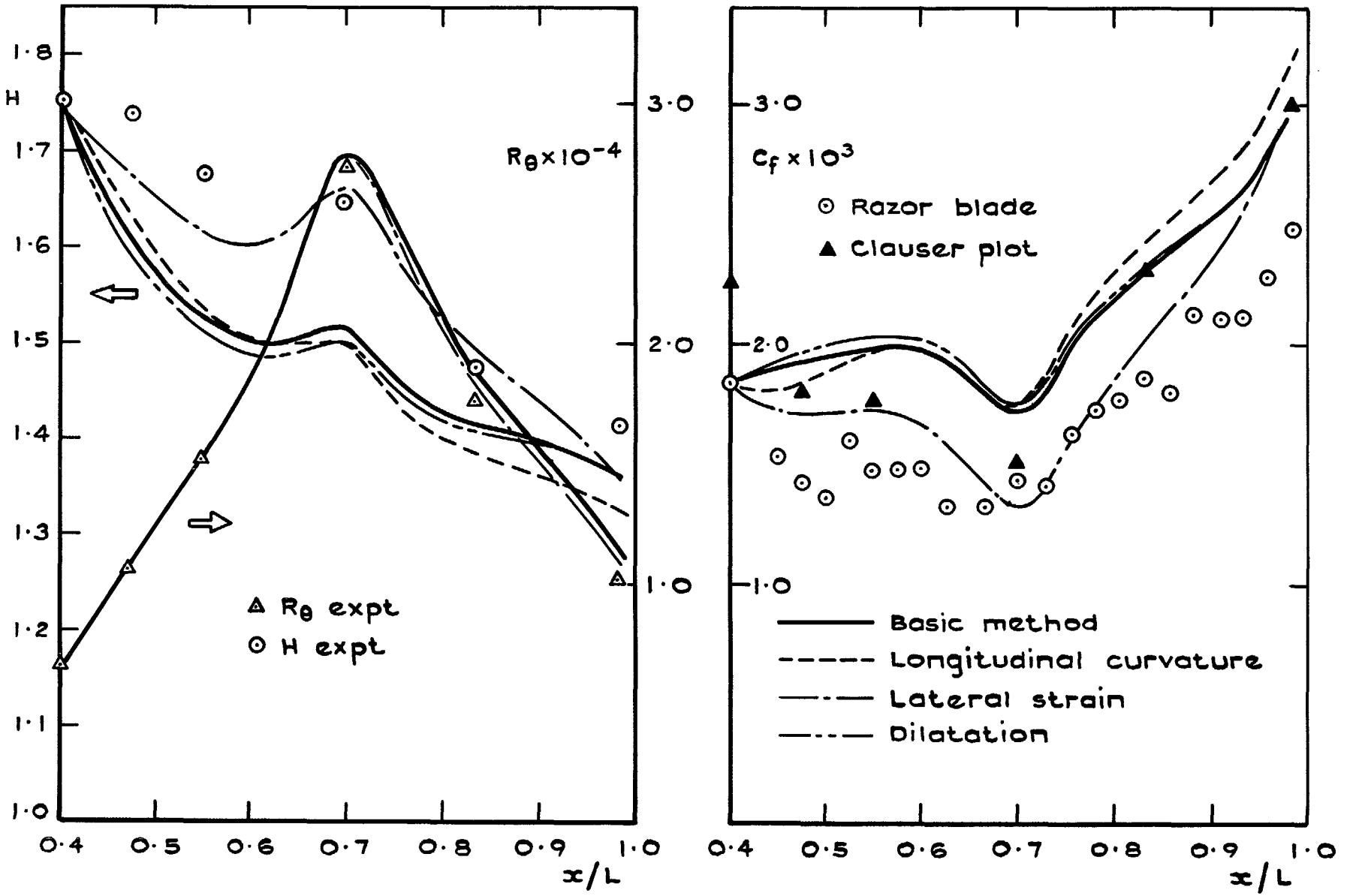

FIG. 12c. Waisted body of revolution at $M = 0{\cdot}6, R_L = 10^7$.

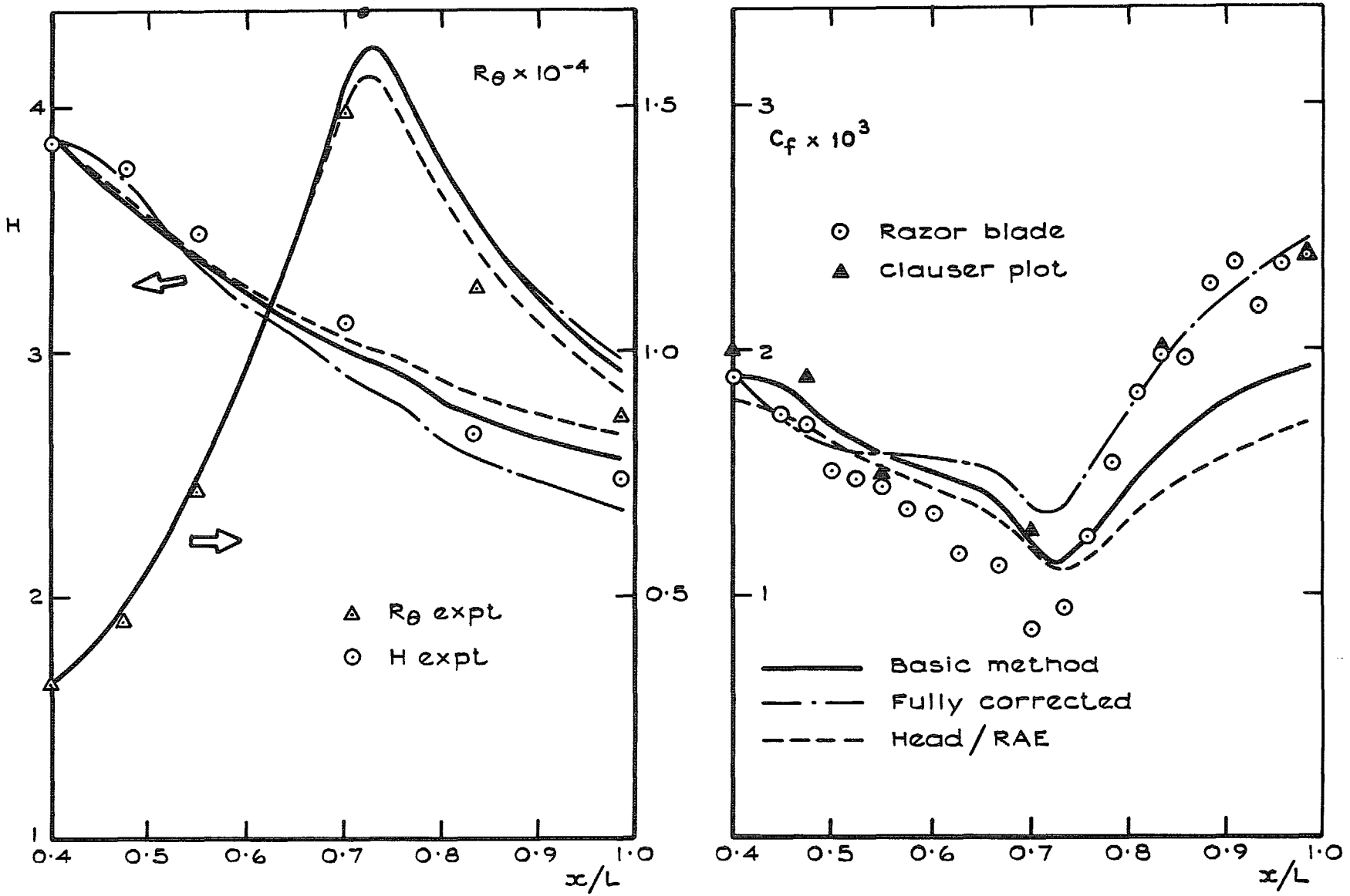

FIG. 12d. Waisted body of revolution at $M = 2{\cdot}0$, $R_L = 10^7$.

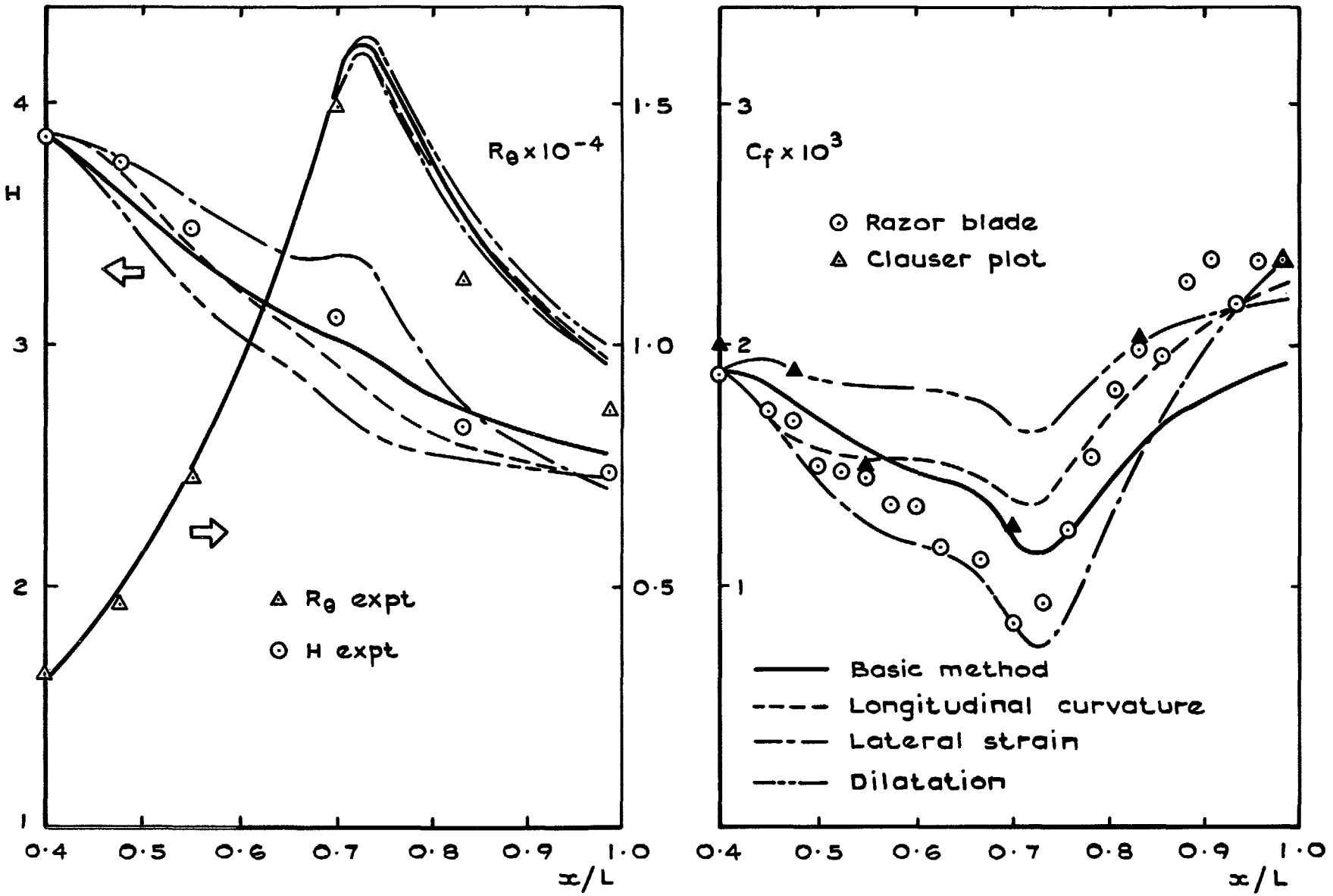

FIG. 12e. Waisted body of revolution at $M = 2{\cdot}0$, $R_L = 10^7$.

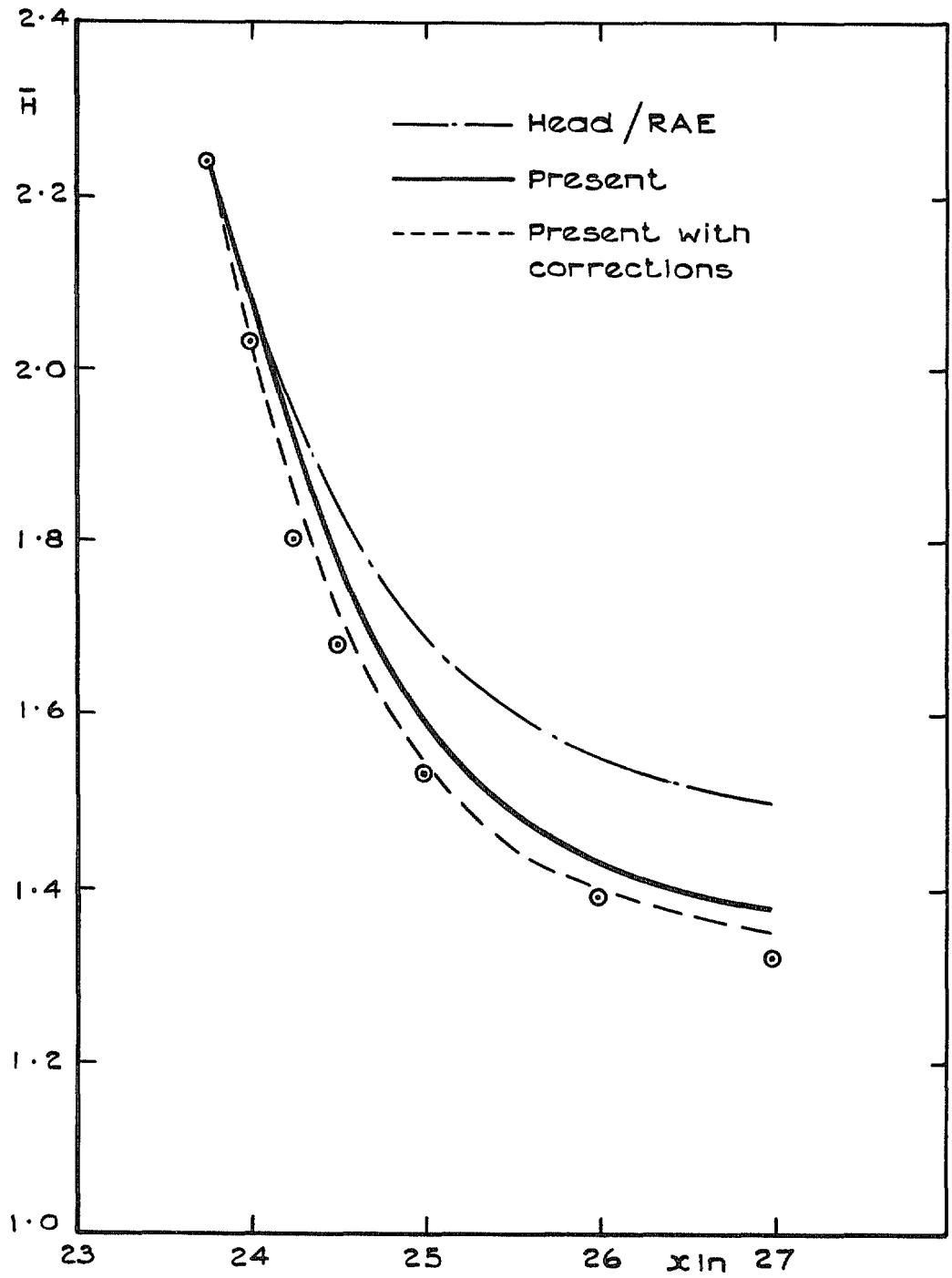

FIG. 13. Prediction of boundary layer recovery after interaction with an incident shock wave ($M \simeq 2$).

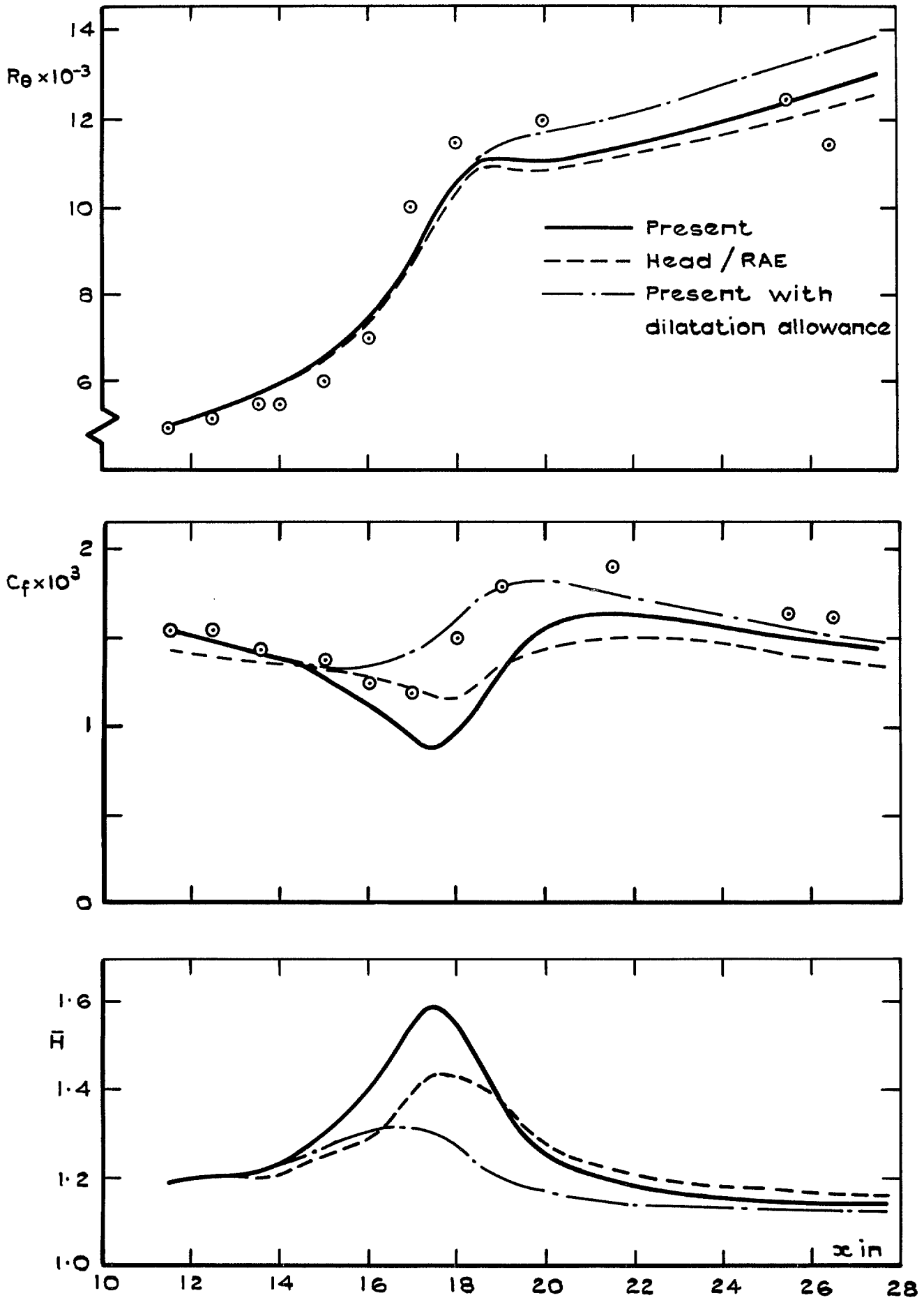

FIG. 14. Comparison with measurements by Lewis *et al.* in decelerating supersonic flow.

Printed in England for Her Majesty's Stationery Office by J. W. Arrowsmith Ltd., Bristol BS3 2NT
D. 289031 K.5. 3/77.

HER MAJESTY'S STATIONERY OFFICE

Government Bookshops

49 High Holborn, London WC1V 6HB
13a Castle Street, Edinburgh EH2 3AR
41 The Hayes, Cardiff CF1 1JW
Brazennose Street, Manchester M60 8AS
Southey House, Wine Street, Bristol BS1 2BQ
258 Broad Street, Birmingham B1 2HE
80 Chichester Street, Belfast BT1 4JY

Government publications are also available through booksellers

ISBN 0 11 470962 9